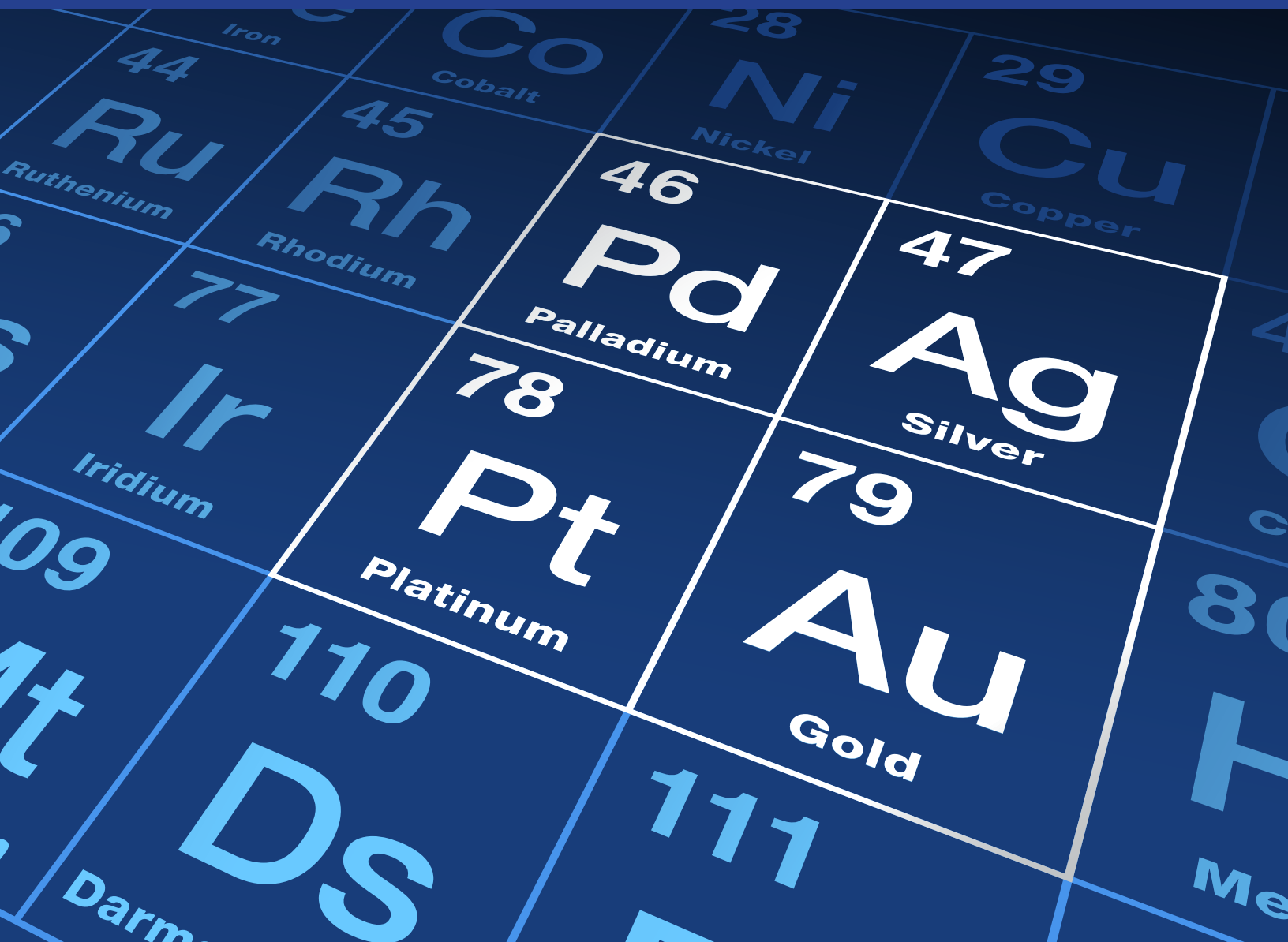


# The IPMI Journal



A Publication of the  
**International Precious Metals  
Educational and Scientific Foundation**



# Recover more Worry less

Recovering your **precious**  
metals since 1919.

 GANNON & SCOTT

[gannon-scott.com](http://gannon-scott.com)

800.556.7296



## FOREWARD

It is with great pleasure that we announce the availability of this fourth issue of the IPMI Journal, a publication of the International Precious Metals Educational and Scientific Foundation. This digital peer reviewed publication has been created as a vehicle for the sharing of technical information related to the science and technology of precious metals.

Since 1976, the International Precious Metals Institute has championed the exchange of information of critical importance to the precious metals scientific and commercial communities through its various communications vehicles. This has included instructional videos, annual conference symposia, special topic committee meetings, regional

seminars, and professional and student achievement awards. Due to the breadth of important topics related to all aspects of precious metals, it has been the vision of the IPMI to provide a publication available to the general public that would become a key source of pertinent topics containing high quality publications by experts in their fields of study.

Historically, the IPMI has attracted world renowned experts in many fields (including Nobel Laureates Henry Taube, Ei-ishi Negishi, Robert Grubs, Professor Ben Feringa, and David MacMillan) in the dissemination of discoveries, inventions, and industry proven practices. Such information has a total value greater than the sum of its parts as seemingly unrelated

innovations from distinct focus areas can be adapted to solve problems. Because of this important characteristic of information exchange, we have decided to create a digital journal, available to the general public, that will not only communicate state of the art discoveries and sound practices, but will also review historical communications from the IPMI's archives that have value and use even in today's environment.

On behalf of the members and leaders of the IPMI, we hope you will find value in this new publication.

Dr. Corby G. Anderson, co-editor  
Dr. Robert M. Ianniello, co-editor  
Mark Caffarey, co-editor



A large industrial ladle is shown pouring a thick, bright yellow-orange stream of molten metal into a mold. The metal is glowing with intense heat, and the background is dark, emphasizing the bright light of the molten metal. The ladle is tilted, and the metal is captured mid-pour, creating a dynamic sense of movement.

# Protecting our elements of life.

At **BASF Environmental Catalyst and Metal Solutions**, we empower our customers with the services they need to succeed in these volatile precious metal markets by offering access to:

- Global Trading & Hedging Services
- Trusted and transparent catalyst recycling and refining
- World-renowned, ISO17025 certified assay labs
- An extensive Precious Metal Chemicals portfolio
- Industry-leading technical experts in every region

Learn more and contact us here:  
[www.catalysts.basf.com/pgm](http://www.catalysts.basf.com/pgm)

Environmental Catalyst  
and Metal Solutions

 **BASF**  
We create chemistry





## The International Precious Metals Educational and Scientific Foundation

In 1976, the International Precious Metals Institute, Inc. ("IPMI") was founded to promote the development of precious metal science and technology. Over the past 47 years, the IPMI has provided its members with an extraordinary body of technical and educational work and an exceptional series of technical videos. The IPMI has also recognized leaders in the industry and academia and students through its long standing Awards Program. This recognition and financial support for continued dedication and research in the field of precious metals is a cornerstone of the IPMI and owes its support to generous sponsorships and endowments.

In 2019, the IPMI made a fundamental structural change by reorganizing IPMI into a trade association to focus on its membership and the needs of the precious metal industry. At the same time, IPMI preserved its scientific and educational roots by renaming its original

organization the International Precious Metals Educational and Scientific Foundation (the Foundation).

The Foundation will continue IPMI's charitable activities by focusing on its long-standing Student and Industry Awards Program and by continuing to promote the science and technology of precious metals as its primary mission. This Journal of the International Precious Metals Institute is a cornerstone project of the Foundation.

Another of the Foundation's primary goals will be to expand its fundraising activities to ensure the long term sustainability of its educational and scientific work, including new and expanded initiatives, such as the student internship program, designed to attract a new generation of trained professionals to the precious metals industry.

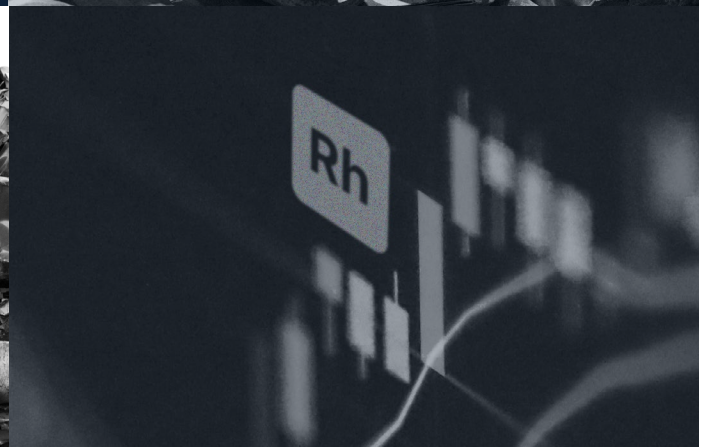
On behalf of both the IPMI and the Foundation, I want to personally thank our Board of Directors,

Awards Committee, corporate sponsors, donors, and the benefactors of our endowments for their continued hard work, support, and dedication to our mission.

I would also like to thank Dr. Corby Andersen, Dr. Bob Ianniello and Mark Caffarey, who are the co-editors of our Journal. Their research through our historical treasure trove of technical papers has produced an extremely important and relevant body of work. Special thanks to all the authors of the papers in this fourth issue. It is through work like yours that the industry has continued to grow and improve technologically. And lastly, thank you to the sponsors of this publication. Because of your generosity, the net proceeds of the Journal will go directly to the Foundation and help provide continued support for our programs.

Larry Drummond  
Executive Director

**IN THIS  
INDUSTRY,  
KNOWLEDGE  
IS POWER.**



Get valuable data and insights that help you take your nonferrous enterprise to the next level with PMR's Corporate Market Report.

**By downloading our report, you'll discover:**

- PGM recycling market growth from 2024 – 2030
- Supply & demand outlook for platinum, palladium, and rhodium
- The future for automotive manufacturers
- Catalytic converter recycling market growth from 2024 – 2030

**Your future begins with the insights you gain today.**



**Download  
Our Free Report**





**THE INTERNATIONAL PRECIOUS METALS  
EDUCATIONAL AND SCIENTIFIC FOUNDATION**  
Board of Directors

**Mark Caffarey**  
*President*

**Jonathan Butler**  
*Vice President*

**Simon Codrington**  
*Secretary*

**Dave Deuel**  
*Treasurer*

**Scott Schwartz**  
*Governance and Compliance Officer*

**John Dourerkas**  
*Digital Media and Marketing Officer*

**Regine Albrecht**  
*Director*

**Corby Anderson**  
*Director*

**Ron Davies**  
*Director*

**Bob Ianniello**  
*Director*

**Jonathan Jodry**  
*Director*



**SABIN** Metal Corporation

**ENABLING  
THE CIRCULAR  
ECONOMY**

**REFINING • PRECIOUS METALS • RECYCLING**

We recover and refine precious metal from spent process catalysts and by-products – transforming them back into valuable assets. With best-in-class techniques and over seven decades of experience, we deliver the highest possible metal returns for our customers.

Learn more about our services at [sabinmetal.com](http://sabinmetal.com)





TECHEMET®

www.techemet.com

Full Range Of

# Recycling And Metal Trading

Recycling catalytic converters for the recovery of Platinum, Palladium and Rhodium



CONVERTERS PURCHASING



RECOGNITION TRAINING



TOLL REFINING



PRECIOUS METAL TRADING



TECHEMET®  
www.techemet.com



## Upcoming 2024 IPMI Events



### Legislative and Regulatory Affairs Seminar

January 30-31, 2024

Army Navy Club, Washington.D.C.



### IPMI Winter Meetings

February 20-22, 2024

Hyatt Grand Cypress Resort, Orlando, Florida



### IPMI 48th Annual Conference

June 8-11, 2024

Hyatt Grand Cypress Resort, Orlando, Florida



# Rigaku

Applied Rigaku Technologies, Inc.

## Need a cost-effective solution for precious metals analysis?



Maximize time and productivity with Rigaku EDXRF analyzers featuring powerful and easy to use Matching Library software.

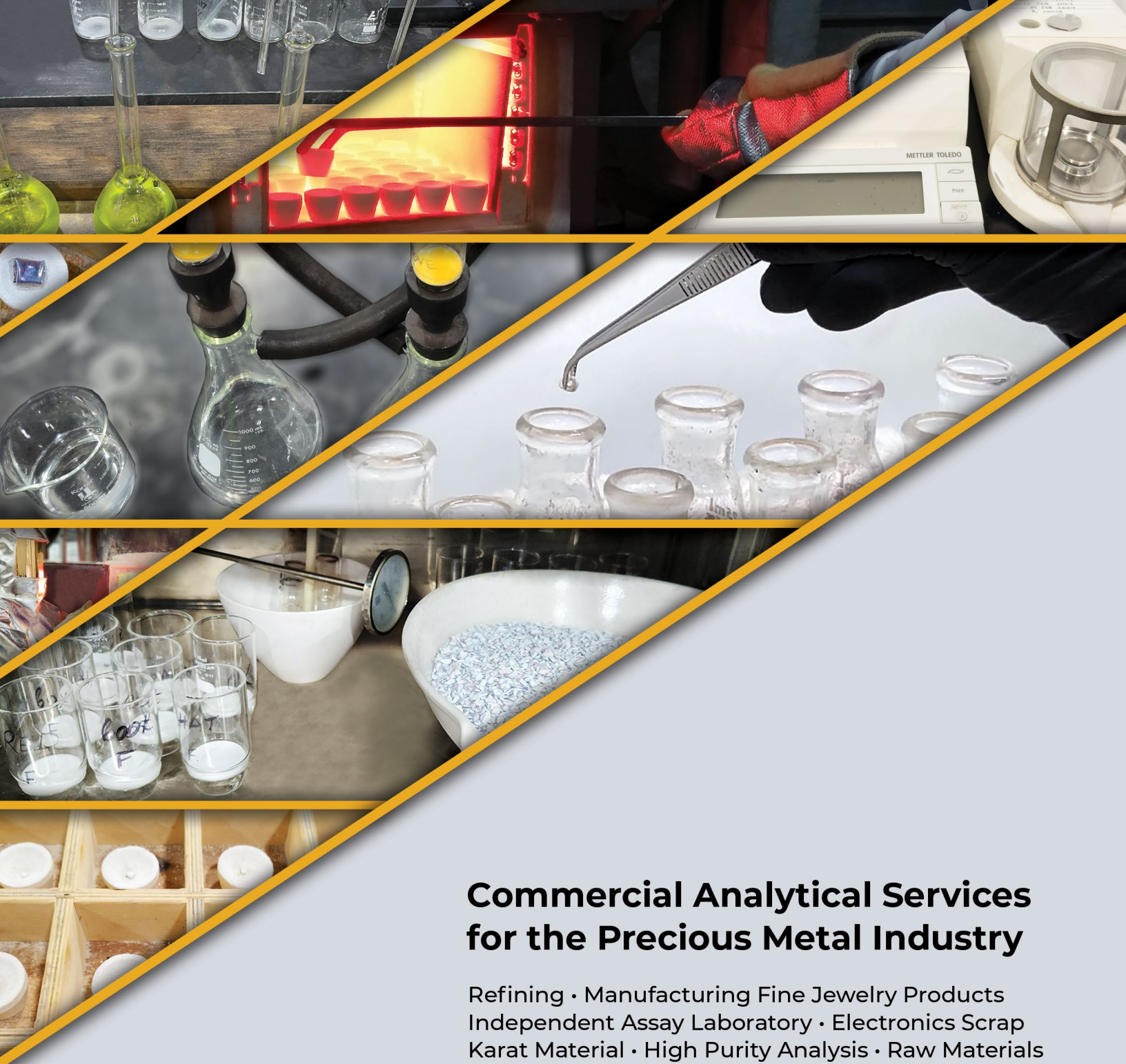
- ✓ Benchtop spectrometers for autocatalyst recycling
- ✓ Non-destructively analyze elements sodium to uranium
- ✓ Intuitive software allows for user-defined custom libraries
- ✓ Optional factory-installed Auto Cats starter library
- ✓ Exceptionally low detection limits
- ✓ Affordable with an unmatched price-to-performance ratio
- ✓ User-installed and minimal routine maintenance



[www.RigakuEDXRF.com](http://www.RigakuEDXRF.com)

+1-512-225-1796 | [info@RigakuEDXRF.com](mailto:info@RigakuEDXRF.com)





## Commercial Analytical Services for the Precious Metal Industry

Refining • Manufacturing Fine Jewelry Products  
Independent Assay Laboratory • Electronics Scrap  
Karat Material • High Purity Analysis • Raw Materials

### We Offer:

- Fire Assay
- Inductively Couple Plasma  
Optical Emission Spectrometry
- Gravimetric Analysis
- Wet Chemistry
- Turnkey/Combination Analysis

**UPMR**  
ANALYTICAL LLC

716.395.4444  
info@upmranalytical.com  
UPMRAnalytical.com



# 2023

## IPMI JOURNAL

Foreword

P. 3 >>

The International Precious Metals Educational & Scientific Foundation

P. 5 >>

Foundation Board of Directors

P. 7 >>

RECOVERY OF GOLD FROM ARSENICAL ORES

*Mahesh C. Jha and Marcy J. Kramer ... P. 12 >>*

PALLADIUM(II) COMPLEXES AS CATALYSTS FOR ORGANIC REACTIONS

*Natalia V. Karninskaia and Nenad M. Kostic ... P. 39 >>*

THE USE OF DESIGN OF EXPERIMENTATION SOFTWARE  
IN APPLIED COPPER GOLD ORE FLOTATION TESTING

*Dr. Corby G. Anderson, PE; Mr. Todd S. Fayram, QP; Dr. Larry G. Twidwell ... P. 61 >>*

FIRE ASSAY TIN COLLECTION: A PRACTICAL TOOL  
FOR ASSAYING COMPLEX REFINERY SWEEPS

*John Whitney, Chemist ... P. 71 >>*

PLATINUM GROUP METALS: HIGHLY SELECTIVE SEPARATIONS BY MRT™  
(MOLECULAR RECOGNITION TECHNOLOGY™)

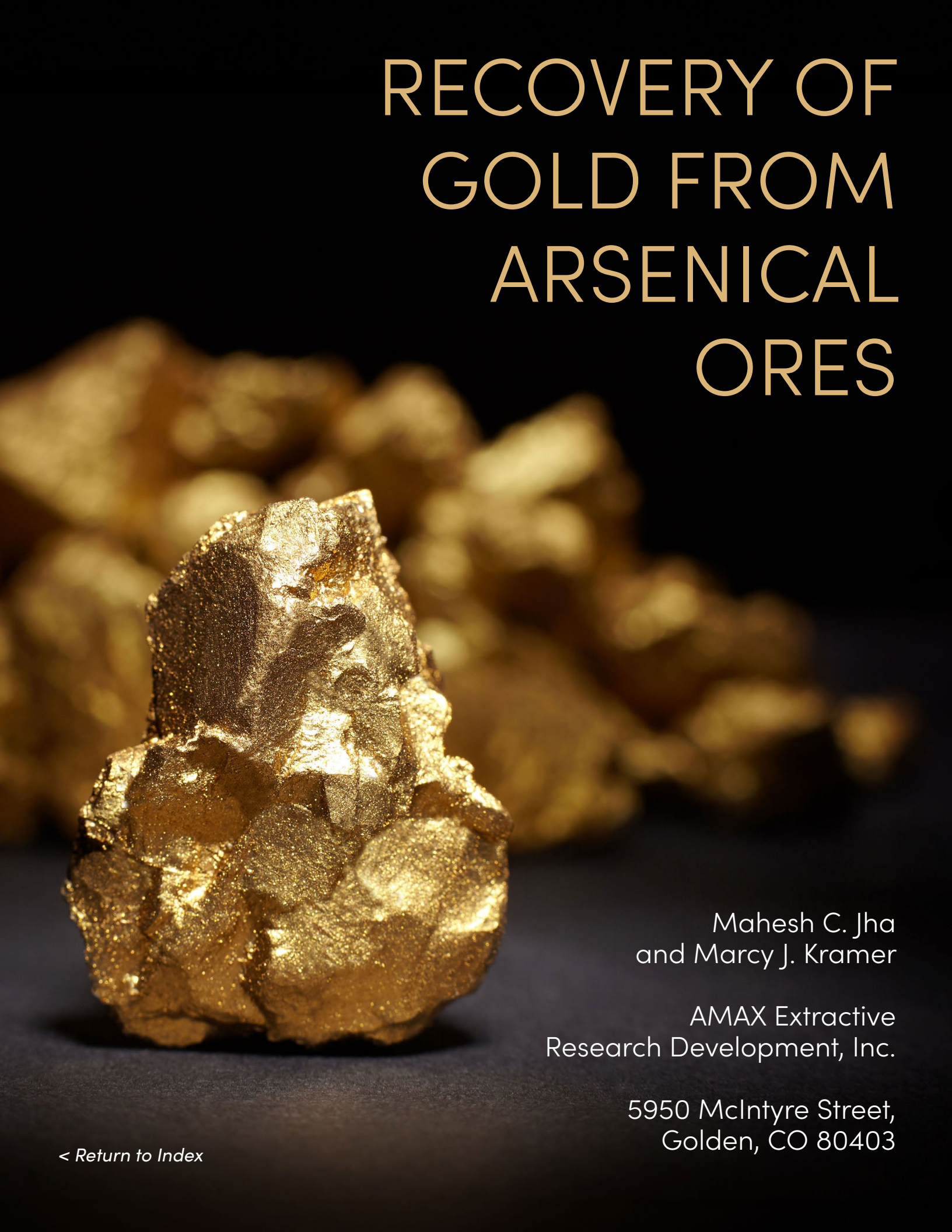
*S.R. Izatt, R.M. Izatt, R.L. Bruening, K.E. Krakowiak, L. Navarro ... P. 78 >>*

*Thank you to our sponsors*

---



# RECOVERY OF GOLD FROM ARSENICAL ORES



Mahesh C. Jha  
and Marcy J. Kramer

AMAX Extractive  
Research Development, Inc.

5950 McIntyre Street,  
Golden, CO 80403

[< Return to Index](#)



## ABSTRACT

Arsenical gold ores occur in many parts of the world, including numerous mines in Canada and the western United States. Free gold is often finely disseminated in the grains of sulfide minerals, arsenopyrite, pyrite, orpiment and realgar. Generally, a sulfide concentrate is produced by flotation. Arsenical ores or concentrates are not amenable to direct cyanidation and therefore are considered refractory. A wide variety of roasting equipment and conditions have been used by the mills to remove arsenic and sulfur from these concentrates. The resulting calcine is easy to cyanide and gold is recovered from the cyanide solution by zinc dust cementation. Room-temperature potential-pH diagrams and high-temperature phase-stability diagrams are presented to discuss the chemistry of the gold cyanidation, cementation, and roasting steps in the presence of arsenic. The environmental aspects of arsenic discharge are also included.

## INTRODUCTION

In several parts of the world, gold has been found in association with arsenic. This association is common in the sulfide gold deposits of Canada and the western United States. It was found early in the milling of these gold ores that a significant fraction of gold, probably closely associated with arsenic, was not recovered by amalgamation, gravity separation, or direct cyanidation. The normal practice was to subject the residue from the amalgamation or cyanidation step to a notation treatment and ship the resulting concentrate to a smelter.

Around 1920, it was realized that a more economically attractive alternative was to produce an arsenical sulfide flotation concentrate, roast the concentrate, and cyanide the resulting calcine. While the value of the byproduct arsenic fluctuated considerably, the value of the extra gold recovered at the mill was generally more than that received from the smelter after paying for the transportation and smelting charges. Over the next three to four decades, single and multiple-hearth roasters were replaced by fluidized-bed roasters, which provided better control of roasting parameters and enhanced gold recovery. During the 1970s, as environmental regulations regarding arsenic emissions were formulated and enforced, the emphasis has shifted toward better emission control systems.

As new arsenical gold ore deposits are still being discovered or found underlying free-milling gold deposits, metallurgists face the challenge of developing an efficient process for recovery of gold from these arsenical ores while meeting environmental safeguards. A necessary first step in that direction is to have a comprehensive knowledge of the basic problems associated with the treatment of arsenical ores and the evolution of the present treatment methods as well as their limitations. This paper aims at providing such information.

First, the world-wide occurrence of arsenical gold ores is briefly described along with the mineralogy of such ores. Next, the operating practice and experience of several gold mills and the laboratory test results published in the past are discussed in light of the current knowledge of the chemistry of the process as affected by the presence of arsenic. To this end, room-temperature potential-pH diagrams

and high-temperature phase-stability diagrams are presented to illustrate the thermodynamics of the cyanidation, cementation, and roasting steps. Finally, the environmental aspects of arsenic emissions are briefly discussed.

## OCCURRENCE OF ARSENICAL ORES

Because of its noble or unreactive nature, gold occurs in nature mostly in metallic form, either by itself or alloyed with silver as electrum. The only other important gold minerals found in nature are gold or gold-silver tellurides. However, there are numerous sulfide deposits around the world in which finely disseminated gold is found in association with pyrite and arsenopyrite or other arsenic sulfides.

An excellent review published by Schwartz (1) in 1944 refers to numerous gold deposits in which gold was associated with arsenopyrite. Out of the 115 districts reviewed, 45 reportedly had a direct relationship between gold and arsenopyrite, i.e., the gold occurred in or on arsenopyrite. In several of the remaining districts, arsenopyrite was present in the ore but no direct relationship was described. The review briefly describes several arsenical ore deposits and, in most cases, refers to other published articles for details. A more recent review published by Henley (2) in 1975 lists some additional deposits. Canada has the most arsenical ore deposits. In fact, in a recent monograph on cyanidation of gold and silver ores (3), the three plants, described to exemplify the roasting of arsenical sulfide gold ores prior to cyanidation, were all located in Canada: the Campbell Red Lake Mines, the Giant Yellowknife Mines, and the Kerr Addison Mines. The combined capacity of these three operations was about 3,400 tons of ore per day. Other arsenical gold deposits include the Cortez., Getchell, Carlin, Bald Mountain, Jardine, and Mercur mines in the United States, Darasun, Mindyak, and Kazakhstan mines in the USSR, Barberton, Eastern Transvaal, and Witwatersrand regions in South Africa and scattered properties in Sweden, France, Brazil, Fiji, and Australia. While this list does not include every arsenical gold deposit, it does point out the wide-spread nature of gold-arsenic association.

## MINERALOGY OF ARSENICAL GOLD ORES

Of the three sulfides of arsenic,  $As_2S_2$ ,  $As_2S_3$ , and  $As_2S_5$ , only two, realgar\* ( $As_2S_2$ ) and orpiment ( $As_2S_3$ ) occur naturally. These two minerals constitute the major host minerals for gold in Getchell Mine in Nevada (4). However, in most of the go sulfide ores, arsenic is present as the mineral arsenopyrite ( $FeAsS$ ). Other arsenic-containing minerals such as cobaltite ( $CoAsS$ ), enargite ( $Cu_3AsS_4$ ), tennantite ( $(Cu, Fe)_{12}As_4S_{13}$ ), proustite ( $Ag_3AsS_3$ ), and argentiferous tennantite ( $(Cu, Ag, Fe)_{12}As_4S_{13}$ ) are found mostly in silver-bearing complex sulfide deposits.

Microscopic examination of polished specimens has been the most common experimental technique used for study of the association of gold and arsenic in the sulfide ores. Numerous such studies were reviewed by Schwartz (1) in 1944. and by Henley (2) in 1975. Both papers contain some excellent photomicrographs illustrating the association of gold and arsenopyrite. In most of the ores, gold is disseminated in pyrite and arsenopyrite crystals. A major limitation of the microscopic examination is that in many cases gold particles are too small to be seen under the microscope. This limitation has been largely overcome using the electron microscope and electron microprobe in recent years.

---

\* While standard mineralogy texts use  $AsS$  to describe realgar,  $As_2s_2$  has been more commonly used in the process chemistry publications referred to in this paper.



Wells and Mullens (5) have used the electron microprobe to study gold-bearing arsenical pyrites from the Cortez and Carlin gold mines in Nevada. They conclude that in the unoxidized sulfide ore, gold is concentrated along with arsenic in tiny ( $\leq 0.005$  mm) pyrite grains and in the rims of larger pyrite grains. Gold is also concentrated in arsenopyrite which is sparsely distributed in the Cortez ore. Little, if any, gold or arsenic is contained in quartz, carbonate, clay, and carbonaceous material, which are the main constituents of the gangue.

Because of the fine nature of the gold particles and their dissemination in pyrite and arsenopyrite crystals, it is generally impractical to grind the ore fine enough to liberate all the gold for amalgamation or cyanidation. This was realized by the early gold operations such as the Jardine Mine in Montana (6), Beattie Mines in Quebec (7) and Cochenour Willans Mines in Ontario (8). These mines could recover only about 50 to 70 percent of the gold during amalgamation or cyanidation. The common practice was to ship the residue, as such or after concentration, to a smelter. The high shipping cost, however, persuaded all these gold mills to develop alternative methods to increase gold recovery at the mill site.

## MINERAL BENEFICIATION

Due to the finely disseminated nature of gold and the relatively coarse grind (30 to 50 percent plus 200 mesh) required to avoid dust losses in the roasting step, it is not possible to concentrate gold with respect to pyrite and arsenopyrite. While gravity separation methods have been used occasionally,

$$* \text{ Gold Upgrading Ratio} = \frac{\text{Gold Assay of Concentrate}}{\text{Gold Assay of Feed}}$$

flotation has been the most widely used method for beneficiation.

A review of published information about four commercial flotation operations involving arsenical gold ores ( $9^{12}$ ) indicates a typical gold recovery of about 90 percent. Since pyrite is the main mineral to be floated, soda ash, xanthate and pine oil are the common reagents used. The flotation of arsenopyrite is somewhat slower than that of pyrite and copper sulfate has been used as an activator (10). Reported reagent consumptions were about 0.3 lb/ton xanthate, 0.2 to 0.4 lb/ton copper sulfate, 0.2 to 1.5 lb/ton soda ash and 0 to 0.15 lb/ton pine oil. Mechanical-type notation cells have been the standard equipment. In general, the grade and recovery have an inverse relationship, i.e., recovery can be increased at the expense of grade and vice versa. The published data indicate that the gold upgrading ratio\* has varied from about 5 to about 9.

The rejection of gangue, which increases the concentration of gold and sulfur, results in a corresponding decrease in the size of the roasting and cyanidation plants. The increase in sulfur and arsenic contents enables the roasting process to be autogenous or at least decreases the external energy requirement. Elimination of gangue may also help in avoiding sintering or other undesired side reactions in the roaster.

In this context it is interesting to note that one operation, the Getchell Mine in Nevada, does not use flotation to upgrade the ore before roasting, but rather roasts the ore directly after grinding (13). In the case of Getchell, orpiment ( $\text{As}_2\text{S}_3$ ) and realgar ( $\text{As}_2\text{S}_2$ ) are the host minerals of gold.

## CYANIDATION OF CONCENTRATES

As discussed in the Introduction, a significant amount of the gold present in arsenical ores and concentrates is not extracted by direct cyanidation. Additionally, lime and cyanide consumption increase considerably. This behavior classifies arsenical ores as refractory. In the following paragraphs an attempt is made to explain this refractory behavior in terms of the physical chemistry of the gold cyanidation process in the presence of arsenic sulfide minerals.

### Laboratory Investigations

In 1952, Hedley and Tabachnick of the American Cyanamid Company presented the results of their systematic investigation into the behavior of arsenic sulfides during the cyanidation of gold (14). They concluded that arsenopyrite ( $\text{FeAsS}$ ) had no adverse effect on gold dissolution at pH 10, 11 or 12. Realgar ( $\text{As}_2\text{S}_2$ ) had no adverse effect on gold dissolution at pH 10 or 11, but at pH 12 the retarding effect was appreciable. Orpiment ( $\text{As}_2\text{S}_3$ ) was detrimental to gold dissolution, and the retardation became more pronounced as the pH was increased. The gold extractions after 48 hours at pH 10, 11, and 12 were 73, 44, and 19 percent, respectively, as compared to 95 percent in the case of control tests where no arsenic minerals were added to the ore.

About the same time, Carter and Samis (15) published their work indicating that the presence of arsenopyrite had a definite detrimental effect on gold extraction during cyanidation. Only 20 to 30 percent gold extraction was achieved. On the other hand, recent work completed at U.S. Bureau of Mines, Reno, claims over 95 percent gold extraction by direct cyanidation of an arsenopyrite concentrate produced by gravity separation at a small operation in California (16).

These apparently conflicting conclusions may be attributed to different leaching conditions or to vast differences in the gold, sulfur, and arsenic contents of the concentrates used in these three studies. Table 1 presents relevant information from the three publications to develop a better understanding of the chemistry of gold dissolution during cyanidation of arsenical concentrates. It is seen that of the three arsenical sulfides, orpiment with a higher sulfur to arsenic ratio is the most detrimental for gold dissolution. Arsenopyrite appears more harmful when the arsenic content is high. The U.S. Bureau of Mines (13) sample is unusually high in gold at 21.8 oz/ton. At 95 percent gold extraction, the residue will still contain about 1 oz/ton gold which is higher than the gold content of the feed sample used by Hedley and Tabachnik (14) and close to that of the sample used by Carter and Samis (15).

The difference in the effect of arsenopyrite on the extraction of gold observed by Hedley and Tabachnik (14) and the other investigators (15, 16) may also be attributed to the different nature of



**Table 1. Results of Laboratory Studies on Direct Cyanidation  
of Gold-Bearing Arsenical Sulfide Concentrates**

Investigators	Hedley and Tabachnik			Carter and Samis	Heinen et al
Reference	(14)			(15)	(16)
Feed	Synthetic Gold Ore*			Flotation Concentrate	Table Concentrate
Arsenic Sulfide Mineral	As <sub>2</sub> S <sub>3</sub>	As <sub>2</sub> S <sub>2</sub>	FeAsS	FeAsS	FeAsS
<u>Feed Analysis</u>					
Gold, oz/ton	0.27	0.27	0.27	1.63	21.8
Sulfur, %	*	*	*	33	24
Arsenic, %	0.25	0.25	0.25	17	3.7
Iron, %	*	*	*	34	33
<u>Cyanidation Conditions</u>					
Pulp Density, % solids	25	25	25	17	25
CN <sup>-</sup> Concentration, % NaCN	0.05	0.05	0.05	0.1	0.5
pH	11	11	11	—	11
<u>Gold Extraction, percent</u>					
6 hours	10	54	61		
24 hours	35	93	85	21 or 31**	85
48 hours	44	97	96		95
72 hours					96
96 hours					97

\* Synthetic ore consisted of quartz with gold-bearing quartz crystals and arsenic minerals added to it in required amounts.

\*\* 21 percent from as-received concentrate and 31 percent from concentrate ground for 1 hour.

The difference in the effect of arsenopyrite on the extraction of gold observed by Hedley and Tabachnik (14) and the other investigators (15, 16) may also be attributed to the different nature of the occurrence of arsenopyrite. In the former study, the sample was a synthetic ore, which consisted of gold-bearing quartz crystals to which arsenic minerals were added. Any effect that the arsenic

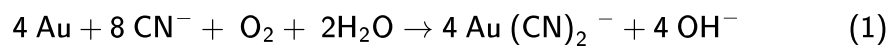
the occurrence of arsenopyrite. In the former study, the sample was a synthetic ore, which consisted of gold-bearing quartz crystals to which arsenic minerals were added. Any effect that the arsenic minerals had on gold extraction were only chemical in nature, as gold was not entrapped in them. In this case, chemical inertness of arsenopyrite in cyanide would not adversely affect gold extraction. On the other hand, the other investigators used naturally occurring gold ores which contained arsenic minerals. In these cases, it is likely that at least some of the gold was physically entrapped in arsenopyrite particles. This entrapped gold was not exposed to cyanide and thus, the gold extraction was lower, due to physical reasons.

The results presented in Table 1 also show that the kinetics of leaching gold from arsenical concentrates is slow, requiring 48 hours or more to attain 95 percent gold extraction. In a continuous operation, such as normally practiced on a commercial scale, the required residence time would be about twice as long, on the order of 100 hours. As a comparison, most gold operations provide a residence time of 24 to 48 hours for free-milling gold ores (17).

## Eh-pH Requirements for Gold Dissolution

An important variable that has not been listed in Table 1, but which significantly affects the dissolution of gold, is the redox potential of the solution. It has long been known that aeration is essential during cyanidation of gold (18). As a noble metal, gold remains unattacked by most aqueous solutions. In the presence of cyanide ions, gold can be dissolved as the complex ion,  $\text{Au}(\text{CN})_2^-$ , but this requires oxidizing conditions, under which water is oxidized to hydroxyl ions. Although there is some uncertainty regarding the mechanism of the reaction, particularly the importance of  $\text{H}_2\text{O}_2$  formation as an intermediate (18,19), the overall reaction can be expressed by

The chemical requirements for this reaction may be represented by an Eh pH diagram. Finkelstein (19) has discussed this aspect in detail, and a simplified version of his potential-pH diagram for the  $\text{Au-H}_2\text{O-CN}^-$  system is shown in Figure 1. It is seen that the gold dissolution line is always above hydrogen line, i.e., the Eh must always be higher than that corresponding to the reduction of water to



hydrogen. On the other hand, the oxygen line (Eh potential at which water can be oxidized to oxygen), is always above the gold dissolution line, so that air can be successfully used to oxidize metallic gold. Because hydrocyanic acid is a very weak acid, the concentration of free cyanide ions increases with increasing pH. This results in lower reduction potentials, which in turn favors the leaching of metallic gold. At pH levels above 9, almost all the cyanide is present as free ions and the reduction potential becomes insensitive to pH.

To avoid the formation of poisonous HCN and to have maximum concentration of free cyanide ions, while minimum sodium cyanide or lime requirements, commercial leaching operations are generally performed at pH 10 to 12. It can be seen from Figure 1 that at this pH, the redox potential should be higher than -400 mV (vs. the standard hydrogen electrode) for gold to dissolve. The thermodynamics of gold dissolution become more favorable as the potential increases.

### Effect of Arsenic Sulfides

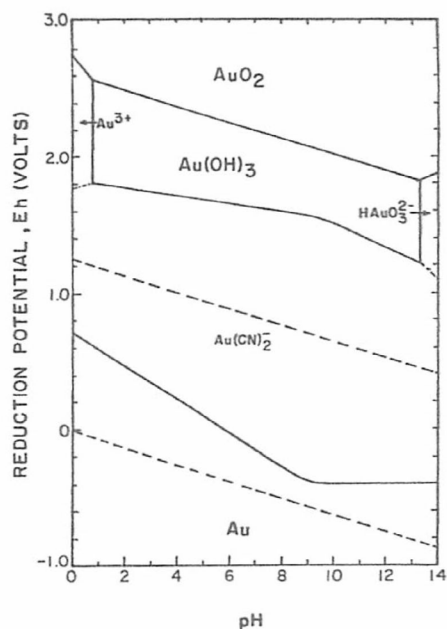


Figure 1. Potential-pH equilibrium diagram for the system  $\text{Au-H}_2\text{O-CN}^-$  at  $25^\circ\text{C}$  (Reference 19).



The previously mentioned work of Hedley and Tabachnick (14) demonstrated that orpiment ( $\text{As}_2\text{S}_3$ ) and realgar ( $\text{As}_2\text{S}_2$ ) decompose and introduce sulfide ions in cyanide solution. The extent of decomposition was higher for orpiment and increased with increasing pH. Similar conclusions can be reached from the potential-pH diagram for the As-S- $\text{H}_2\text{O}$  system presented in Figure 2, based on the work of Tsuchizawa and Nishimura (20). It can be seen from Figure 2, that any arsenic sulfide (no data could be found for arsenopyrite at high concentrations) dissolved in the alkaline solution at pH 11 or so will be present as  $\text{As}_3\text{S}_6^{2-}$  ions and that the Eh will be about -500 mV. This potential is lower than that required for dissolution of gold (-400 mV or above). Thus it is mandatory to oxidize any  $\text{As}_3\text{S}_6^{2-}$  ions to  $\text{AsO}_2^-$  ions and probably to  $\text{AsO}_4^{3-}$  ions, so that the Eh is raised to a point where gold can dissolve. Calcium arsenate may precipitate at this point.

The adverse effect of sulfide minerals during cyanidation of gold has long been known (18). Generally, it was explained in terms of increased oxygen demand to oxidize the sulfide ion to sulfate ion and increased lime demand to maintain the desired pH. The interpretation presented by the potential-pH diagram, such as Figure 2, is another way to look at the same problem. The advantage is that such diagrams provide a quantitative basis for measuring and controlling the Eh, in addition to pH, at which gold will dissolve.

Besides the thermodynamics, the kinetics of gold dissolution is also affected by the presence of arsenic sulfides. Physical entrapment of finely disseminated gold within the sulfide particles increases the diffusion path for cyanide ions. Thus, fine grinding is expected to improve the rate of gold dissolution (15). In addition, the presence of sulfide minerals may also cause electrochemical passivation of gold according to the recent work of Filmer (21) on partially roasted pyrite concentrates.

In conclusion, it can be said that direct cyanidation of gold from arsenical sulfide ores is difficult due

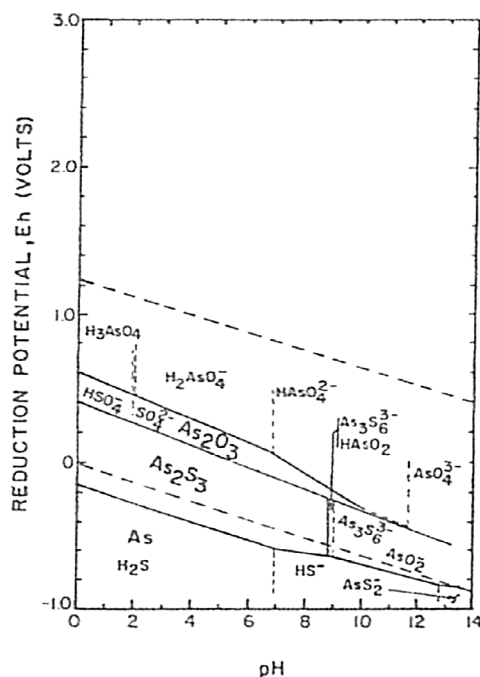


Figure 2. Potential-pH equilibrium diagram for the system As-S- $\text{H}_2\text{O}$  at 25°C (Reference 20).

to both physical and chemical factors. While it may be possible to use oxidants such as chlorine or oxygen to oxidize the arsenic and sulfur in an aqueous system, and thereby improve gold leaching, traditionally, it has been found more convenient to oxidize the concentrate at high temperature by roasting and remove most of the arsenic and sulfur altogether prior to cyanidation.

## ROASTING OF CONCENTRATES

The main objectives of roasting the arsenical sulfide concentrates are to oxidize and remove arsenic and sulfur, while producing a porous calcine from which gold can be leached by cyanidation. Both the physical and chemical characteristics of the calcine are important for high gold extraction during cyanidation of the calcine. Porosity and particle size are the important physical characteristics requiring that roasting be performed under conditions that do not cause fusion and sintering of particles. As for the chemical factors, it is important to eliminate sulfide sulfur which affects the redox potential and the passivation of gold during cyanidation. Further, it has been suggested that if arsenic is oxidized to nonvolatile  $As_2O_5$  instead of volatile  $As_2O_3$ , iron or calcium arsenates are formed which adversely affect the extraction of gold and silver (9).

The objective of roasting plant operators has been to select the temperature and excess of air such that most of the arsenic and sulfur are oxidized without causing sintering or fusion. In practice the desired performance has been difficult to achieve, more so in the case of arsenical concentrates than for straight pyrite concentrates.

During the last 50 years or so, the design of roasters has changed considerably from single-hearth Edwards type (10, 22, 23) to multiple-hearth McDougall and Wedge type (6, 7, 9) and, finally, to the fluidized-bed Dorree FluoSolids type (11, 12, 13). A parallel effort continued in the laboratories to develop a better understanding of the chemistry of the roasting process and its influence on gold recovery during the subsequent cyanidation step (15, 22, 24-27).

The optimum roasting conditions recommended in these publications differ significantly. For example, the recommended temperature varies from about 400°C to about 700°C. This is partly because of the vastly different compositions of the concentrates used and partly because of the type of equipment used in the laboratory and commercial-scale roasting operations. An attempt has been made in the following pages to present a comprehensive picture of the roasting process - first by discussing laboratory investigations, then the evolution of the roasting practice, and finally by presenting the chemistry of the roasting reactions.

### Laboratory Investigations

There are several papers that describe laboratory investigations of the roasting of arsenical concentrates to optimize gold recovery from the calcines (15, 22, 24, 25). However, these laboratory tests were performed in a muffle furnace with occasional rabbling of the charge. There is considerable uncertainty about the actual temperature and gas composition, as a function of time.



Moreover, agglomeration is very likely wider these conditions. Thus it is not surprising that many of the conclusions derived from these investigations, regarding temperature and excess air, became irrelevant when fluidized-bed roasters came into operation.

Two papers describing laboratory testing of fluidized-bed roasting of Russian gold-arsenic concentrates also appear in the literature (26, 27). Both studies suggest optimum roasting conditions for removal of arsenic and sulfur, but neither correlates their roasting conditions with gold extraction during subsequent cyanidation.

## **Evolution of Roasting Practice**

Table 2 summarizes the roasting practices of six United States and Canadian plants. All three major types of roasters, single-hearth, multiple hearth, and fluosolids are represented. The arsenic content of the roaster feed covers the range of 2 to 38 percent. It can be seen that the roasting conditions (temperature and throughput rate), varied considerably and so did the results in terms of gold extraction by cyanidation of the calcine.

The Jardine mine in Montana (6) was one of the first gold mines to roast arsenical concentrates. The concentrate was extremely high in arsenic content, 38 percent, and the significant increase in arsenic price, after World War I, helped in the decision to install roasters and arsenic kettles. The gold recovery was unsatisfactory, less than 60 percent, even after roasting the concentrate, and the calcine was still shipped to a smelter. However, the substantial weight loss during roasting, due to the removal of arsenic and sulfur, resulted in considerable savings in the shipping costs. A multiple-hearth McDougall roaster was used at Jardine, which under certain conditions operated autogenously.

A slightly different version, a Wedge-type multiple-hearth roaster was used at Beattie Mines in Quebec. The roasting plant was built in 1937. Prior to that, the flotation concentrate was shipped to a smelter. Archibald has published several papers on the Beattie operation; a paper published in 1949 presents excellent coverage of all the plant and laboratory work done to develop the so called "Beattie Roasting Process" for treating arsenical gold ores (9). An important feature of this roasting practice was to eliminate almost all the arsenic at a low temperature, below 482°C. This, however, was probably possible only because of the very low arsenic content of about 2 percent.

Another type of roaster, a single-hearth Edwards type was preferred by many operators because of the convenience of single-floor operation. It has been used in Australia (22), South Airica (23) and Canada (10). The Canadian operation at MacLeod-Cockshutt (10) has been included in Table 2. Because of the very high sulfur content of this concentrate, 35 to 38 percent, it was possible to operate the roaster autogenously most of the time.

While the long, horizontal single-hearth type and tall vertical multiple- hearth type roasters had their relative advantages and disadvantages, it was apparent to most operators that there was non-uniformity in temperature and gas composition in both types of roasters, and that these important variables were difficult to control. Poor control not only affected the chemical analysis of the calcine,

but more importantly its physical properties - the extent of agglomeration and the porosity.

Table 2. Details of Roasting Practice of Various Gold Mills  
Treating Arsenical Ores

Mill	Jardine	Beattie	MacLeod- Cockshutt	Cochenour- Willans	Giant Yellowknife	Getchell
Reference	(6)	(9)	(10)	(11)	(12)	(13)
Roaster Type	Multiple hearth (6) (McDou- gall)	Multiple hearth (13) (Wedge- type)	Single- hearth (Edwards) 139'x15'	FluoSolids (Dorrco)	FluoSolids two-stage	FluoSolids oil-fired
Diameter, ft	16	25		6.7	Stage 1: 16 Stage 2: 14	16
Throughput, tons/day	20-40	100-125	50	8-15	200	1500-1800
Temperature, °C	550-600	470-704	538-650	593	Stage 1: 496 Stage 2: 468	593 to 650
<u>Feed Analysis</u>						
Gold, oz/ton		0.9	1.1	6.0	4.1	0.25
Arsenic, %	38	2.3	3-5	5.3	9.3	2.9
Sulfur, %	20	16	35-38	16.6	20.1	3.6
<u>Calcine Analysis</u>						
Gold, oz/ton	3.5	1.1	1.5	6.3	5.0	0.3 (est.)
Arsenic, %	1.1	0.3	0.4	—	1.35	—
Total Sulfur, %	—	1.6	1.2	4.3	3.8	0.2
<u>Gold Extraction by Calcine</u>						
Cyanidation, %	60 (prelim.)	92	75*	92	94	75-80 (est.)

\* Part of the gold is recovered by gravity concentration, prior to cyanidation.

The development of fluidized-bed roasters during the 1940s solved most of the control problems by providing a reactor with uniform temperature and gas composition. The Dorr company pioneered the development and installation of these under their trade name Dorrco FluoSolids reactors, commonly known as fluosolids reactors now. One of the first installations was at Cochenour-Willans (11). This relatively small unit demonstrated that arsenical concentrates can be roasted at one temperature to attain the desired porous calcine. A temperature of about 600°C was found optimum and the gold recovery during cyanidation of the calcine was 92 percent. It should be noted, however, that the calcine was very rich in gold content, above 6 oz/ton.

The operators of the Giant Yellowknife Gold Mine, also in Canada, decided in the late 1950s to replace



its Edwards-type roaster with a large fluosolids roaster (12). Two-stage roasting was developed for the highly arsenical sulfide concentrate (9% As). In the first stage, almost all of the arsenic and about half of the sulfur are eliminated at a low temperature, under 500°C, and very low free oxygen content of the gas, 0.25 to 0.5 percent. Most of the remaining sulfur is oxidized in the second stage, at a still lower temperature. The entire operation is autogenous. Excellent gold extraction, about 94 percent, is obtained by cyanidation of the calcine containing about 5 oz/ton gold.

A novel feature of the fluosolids roaster installed at the Getchell Mine in Nevada in the early 1960s is that it is oil-fired and roasts the ore rather than a concentrate (13). The arsenic and sulfur contents of the feed are only about 3 percent each and its gold content is only about 0.25 oz/ton. It is not surprising that the gold extraction during cyanidation of the low-grade calcine is only 75 to 80 percent. The operation uses a higher roasting temperature, in spite of lower arsenic and sulfur contents, in comparison to Giant Yellowknife operation, but is able to cut down the residence time considerably and achieve a much larger throughput rate for a single roaster of the same size (16-ft diameter).

Fluosolids roasters continue to be the choice for roasting of gold-bearing pyritic and arsenopyritic concentrates. They are in use at the three Canadian plants, Campbell Red Lake Mine, Giant Yellowknife Mine and Kerr Addison Mines, illustrated in a monograph on cyanidation (3).

### **Chemistry of Roasting**

Most of the papers presenting details of roasting practice propose theories regarding the effect of roasting temperature on the subsequent cyanidation of the calcine. Djinghenzian (25) presented a state-of-the-art review in 1952 and listed several possible reactions, but no thermodynamic data were presented.

An attempt is made in the following paragraphs to discuss the chemistry of roasting of arsenic and iron sulfides under conditions of commercial roasting, about 450 to 650°C and from near zero concentration of free oxygen to about 10 percent oxygen. Three temperatures, 500, 700, and 900°K, (227, 427, and 627°C) have been selected to present the relevant data. First, the volatilization and decomposition of various compounds are discussed to show how temperature affects the removal of arsenic and sulfur from the concentrates into the vapor phase. Then the stability diagrams are presented to show the effect of temperature and oxygen partial pressure not only on oxidation of sulfur and arsenic to SO<sub>2</sub> and As<sub>2</sub>O<sub>3</sub> gases, but also on the stability of various oxides and sulfates in the solid phase. Finally, the findings on the chemistry of the roasting process are discussed in terms of their application to roasting practice.

It should be mentioned here that some standard thermodynamic data books such as JANAF Tables (28) have no information on arsenic or its compounds. In many cases, the data estimated long ago (29) have not been verified. However, a recent publication by the U.S. Bureau of Mines (30) has summarized and critically reviewed most of the published thermodynamic data on arsenic.

**Volatilization and Decomposition of Compounds:** Arsenic, sulfur, and many of their compounds have significant vapor pressures at the temperatures encountered during the roasting of arsenical concentrates, 450 to 650°C. The pyrite and arsenic sulfides present in the concentrate or in the vapor phase decompose at these high temperatures to yield elemental arsenic and sulfur vapors which are easily oxidized by air. The two oxidation products,  $As_2O_3$  and  $SO_2$ , leave the roaster as off-gas along with nitrogen and any unused oxygen.

Strathdee and Pidgeon (31) measured the vapor pressure of arsenic over elemental arsenic as well as arsenopyrite. Their results are presented in Table 3, which also lists vapor pressure of some other compounds of interest. Their measurements for elemental arsenic agree fairly well with the data tabulated in an ASM compilation (32). This provides credibility to their measurements of arsenic vapor pressure over arsenopyrite. Their data suggest that arsenopyrite will decompose easily at about 700 to 800°K to arsenic vapor and pyrrhotite, (FeS).

As for the two arsenic sulfides, realgar,  $As_4S_4$ , and orpiment,  $As_2S_3$ , a book on the thermodynamics

Table 3. Vapor Pressure of Certain Species of Interest  
in Roasting of Arsenical Sulfide Concentrates

<u>Species in Vapor Phase</u>	<u>Condensed Phase</u>	<u>Equilibrium Vapor Pressure (mm Hg)</u>			<u>Reference</u>
		<u>500°K</u>	<u>700°K</u>	<u>900°K</u>	
Sulfur*	Sulfur	5	14	b.p. 718°K	32
Arsenic*	Arsenic	0.0002	5.6	s.p 876°K	32
Arsenic	Arsenopyrite	0.0002	1.3	158	31
$As_4S_4$	Realgar	0.62	77.3	—	31
**	Orpiment	—	10.7	248.5	33

\* Includes all polymers

\*\* Includes arsenic, sulfur and combined sulfides

of sulfides by Mills (33), lists vapor pressure data at elevated temperatures. However, according to Barton's work on the Fe-As-S system (34), the two sulfides are not stable above about 580 and 588°K, and melt into an arsenic-sulfur liquid phase. Thus, any vapor pressure measurements made above these temperatures may not be definitive because of the presence of  $S_2$ ,  $As_4$  and combined arsenic sulfides such as  $As_2S_2$  and  $As_2S_3$  in the vapor phase.

Figure 3 is a simplified version of Barton's presentation of a sulfur activity temperature diagram for the Fe-As-S system. Because of the relatively lower arsenic contents in gold concentrates, in comparison to iron and sulfur contents, iron arsenides have been deleted. It should be noted that Barton has considered only  $S_2$  gas in the vapor phase and not other sulfur species. Thus at 718°K, sulfur's boiling point, the vapor pressure of  $S_2$  is only about 0.03 atmosphere.

It can be seen from Figure 3 that even at relatively low temperatures, about 300°C, any orpiment



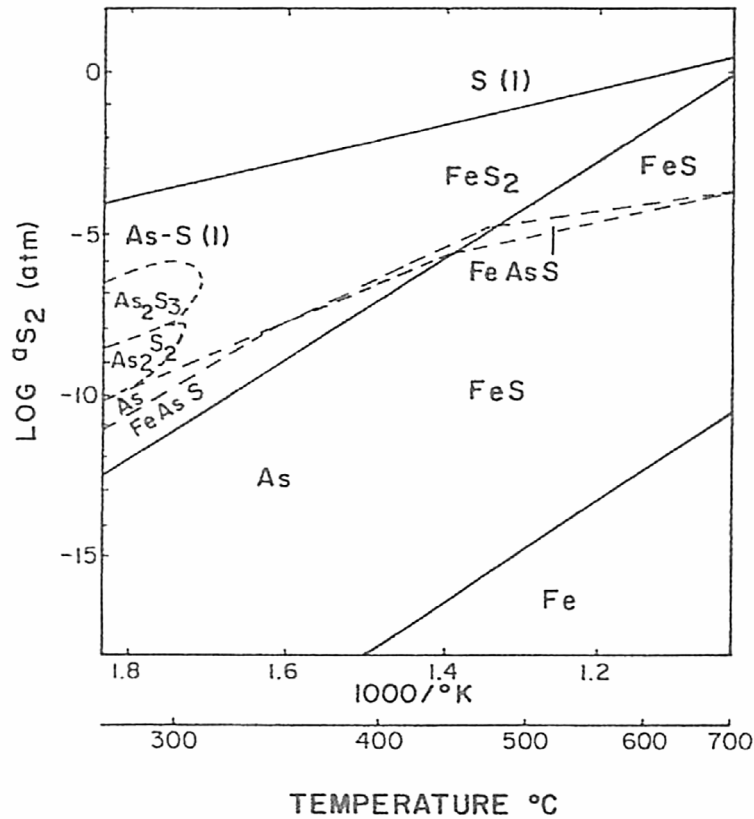


Figure 3. Temperature-activity of  $S_2$  projection for the Fe-As-S system (Reference 34).

( $As_2S_3$ ) and realgar ( $As_2S_2$ ) present in the concentrate will decompose to sulfur vapor (equilibrium pressure of about  $10^{-7}$  to  $10^{-9}$  atm) and an arsenic-sulfur liquid phase. As the temperature increases, the equilibrium sulfur vapor pressure also increases. Thus, at about  $600^\circ C$ , the sulfur pressure can range from 1 to  $10^{-4}$  atm, depending upon whether the arsenic-sulfur liquid phase is rich or poor in sulfur.

However, in most of the gold concentrates, arsenopyrite ( $FeAsS$ ) rather than orpiment or realgar, is present. It can be seen from Figure 3 that the equilibrium sulfur pressure is lower by an order of magnitude. As for the decomposition of pyrite ( $FeS_2$ ) to pyrrhotite ( $FeS$ ) the equilibrium sulfur pressure is lower than that for arsenic sulfides at temperatures below about  $400^\circ C$ , but is higher at temperatures above about  $500^\circ C$ .

In summary, it can be said that heating of arsenical sulfide concentrates leads to their decomposition into lower sulfides and sulfur and arsenic vapors. The equilibrium vapor pressures of arsenic and sulfur increase with increasing temperature and become significant, 0.01 to 0.1 atm, in the 500 to  $600^\circ C$  temperature range, commonly used for roasting. Only pyrrhotite remains behind as a stable solid sulfide phase under these conditions.

### Phase-Stability Diagrams

The discussion of the previous section assumed that elemental sulfur and arsenic vapors are emitted from the concentrates into a static and inert atmosphere. In roasters, however, air is continuously introduced, causing oxidation of arsenic and sulfur to  $\text{As}_2\text{O}_3$  and  $\text{SO}_2$ , which then leaves as off-gas. Availability of oxygen more than that required to oxidize arsenic and sulfur oxidizes pyrrhotite ( $\text{FeS}$ ) to magnetite ( $\text{Fe}_3\text{O}_4$ ) and to hematite ( $\text{Fe}_2\text{O}_3$ ).

The extents to which oxidation occurs will depend mostly upon the temperature and oxygen partial pressure, which vary considerably as cold sulfide particles enter the roaster and are converted to hot oxide particles exiting the roaster. A convenient means of presenting the thermodynamics of these reactions, at varying temperature and oxygen partial pressure, is to construct phase-stability diagrams at several temperatures of interest.

Thermodynamic data from various sources (28–30, 34) have been used to calculate the equilibrium constants of various reactions at 500, 700, and 900°K. These equilibrium constants were then used to construct the phase stability diagrams for the As–S–O and Fe–S–O systems presented in Figures 4, 5, and 6.

Figure 4 shows the As–S–O system at 500°K. This temperature is typical of the early stages of roasting, either in the upper hearths of multiple-hearth roasters, or near the surface of freshly fed concentrate particles in the fluidized-bed reactor. As seen in the previous section the equilibrium partial pressure of sulfur and arsenic will be about  $10^{-5}$  to  $10^{-10}$  atm, depending mostly upon whether  $\text{As}_2\text{S}_3$ ,  $\text{As}_2\text{S}_2$ , or  $\text{FeAsS}$  is present in the feed. It can be seen from Figure 4 that there is a strong driving force for both sulfur and arsenic to be oxidized to  $\text{SO}_2$  and  $\text{As}_2\text{O}_3$ . According to Wicks and Block (29),  $\text{As}_2\text{O}_3$  melts at 586°K and boils at 730°K. Thus the vapor pressure of  $\text{As}_2\text{O}_3$  is significant even at 500°K and it leaves with the off-gas.

It is important that most of the arsenic be removed as  $\text{As}_2\text{S}_3$  at low oxygen pressures and low temperature. Nonvolatile  $\text{As}_2\text{O}_5$  may form at higher oxygen pressure, above about  $10^{-15}$  atm at 500°K (see Figure 4). Also, if the temperature is increased to a high level, without complete arsenic elimination,  $\text{FeS}$  may oxidize and form iron arsenite, which is soluble in water and will consume oxygen and lime during cyanidation.

Figures 5 and 6 show the phase-stability diagrams for Fe–S–O systems at 700 and 900°K, respectively. As noted before in Table 2, commercial roasters have operated in the temperature range of 460 to 650°C (733 to 923°K). The As–S–O diagram at 700°K has been superimposed in Figure 5 using dashed lines. At low  $\text{O}_2$  and high  $\text{S}_2$  pressures, while the  $\text{FeS}_2$  is being converted to  $\text{FeS}$ , sulfur and arsenic will be oxidizing to  $\text{SO}_2$  and  $\text{As}_2\text{O}_3$ , respectively, both of which will leave the roaster as off-gas. The  $\text{SO}_2$  partial pressure will probably be in the range of  $10^{-1}$  to  $10^{-2}$  atm, nitrogen being the main diluent.  $\text{As}_2\text{O}_3$  vapor pressure will depend upon the arsenic content of the concentrate but should be an order of magnitude lower. As sulfur is eliminated and oxygen partial pressure is increased during the later stages of roasting,  $\text{FeS}$  will be oxidized to  $\text{Fe}_3\text{O}_4$ ,  $\text{Fe}_2\text{O}_3$ , or  $\text{Fe}_2(\text{SO}_4)_3$  depending upon the oxygen partial pressure,  $\text{SO}_2$  partial pressure, and temperature (see Figures 5 and 6). While the presence

of magnetite has been considered desirable by some operations (9), hematite is the usual product. As a comparison of Figures 5 and 6 will show, sulfate formation is more likely at lower temperature. It should be mentioned here that the arsenic lines in Figure 5 are based on solid arsenic metal and  $As_2O_3$ , whereas in real situations, at  $700^\circ K$ , both will be present as vapors in significant quantities.

### Application to Roasting Practice

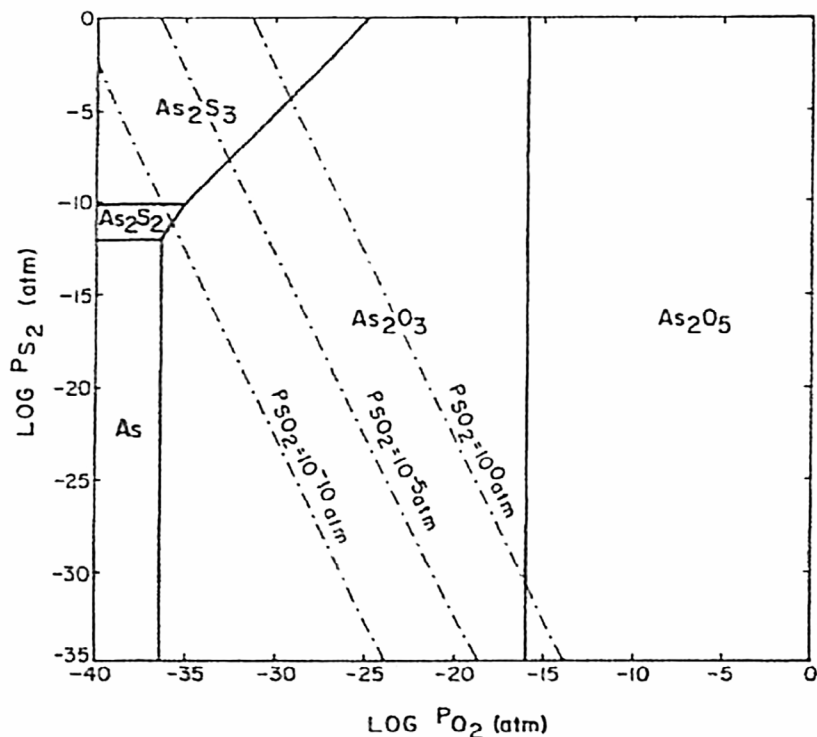


Figure 4. Phase-stability diagram for As-S-O system at  $500^\circ K$ .

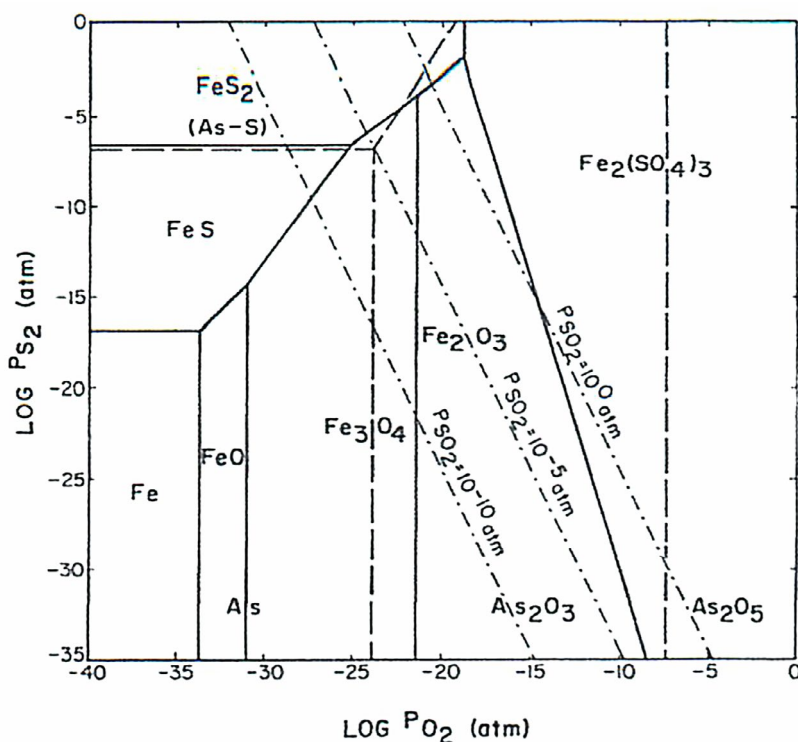


Figure 5. Phase-stability diagram for As-Fe-S-O system at  $700^\circ K$ .



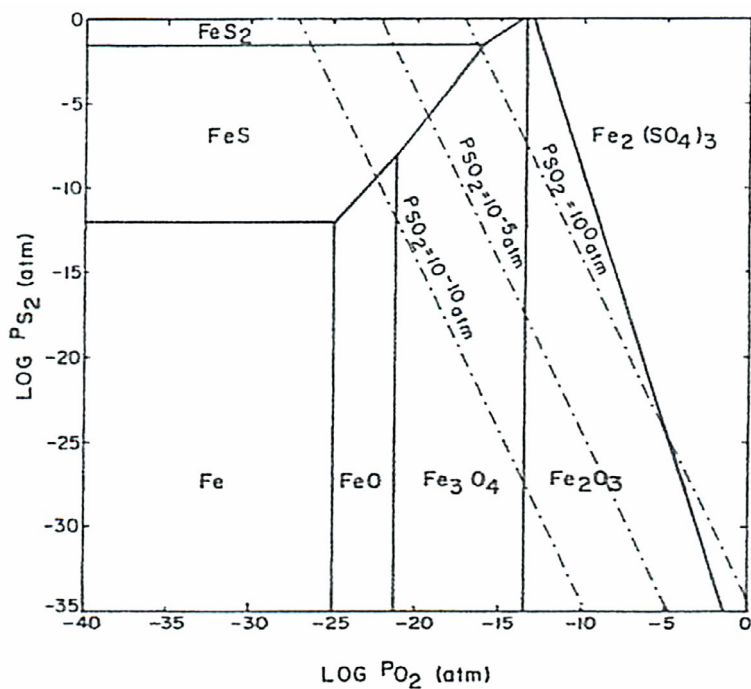


Figure 6. Phase-stability diagram for Fe-S-O system at 900°K.

The thermodynamic data presented and discussed in the last two sections can be applied to commercial roasting practice to provide a better understanding and thereby better control of the process.

As mentioned before, the roasting temperature has been varied from 470 to 700°C (see Table 2). Of two plants which both used multiple-hearth roasters, Jardine operated at a higher initial roasting temperature (550°C) than Beattie (470°C). The reason for the temperature difference is the significantly higher arsenic content of Jardine concentrate, 38 percent in comparison to about 2 to 3 percent in Beattie concentrate. Higher temperature results in higher equilibrium sulfur and arsenic vapor pressures (see Table 3 and Figure 3) and thereby increases the rate of arsenic and sulfur removal. On the other hand, the final roasting temperature was higher for Beattie, 100°C, than for Jardine, 600°C, probably because of the higher iron content of the Beattie concentrate. The single-hearth McLeod-Cockshutt roaster used temperatures intermediate to those mentioned above. This seems logical in view of the intermediate arsenic content of this concentrate and the desire to operate the roaster autogenously, using the very high sulfur content of the concentrate.

The fluosolids roasters were developed to avoid localized oxidation and superheating of solids to minimize agglomeration. Despite a high temperature, 593°C, and low throughput rate, 0.2 to 0.4 ton per day per ft<sup>2</sup>, the sulfur elimination was not very good at Cochenour Willans. This is probably because a low air flow rate was used in this single stage fluosolids reactor, which would result in low partial pressure of oxygen but high partial pressure of SO<sub>2</sub>. Under these conditions, arsenic will be eliminated, even from intermediate level concentrates, 5.3 percent arsenic, but a considerable

amount of sulfation will occur (see Figure 6).

The use of two-stage roasting at Giant Yellowknife permitted treatment of concentrates relatively high in arsenic, 9.3 percent, at very low temperatures, 496 and 468°C (see Table 2). The throughput rates for the two stages were about 1 and 1.3 tons per day per ft<sup>2</sup>. Almost all the arsenic and about half of the sulfur were removed in the first stage, which operated at low oxygen and high so<sub>2</sub> partial pressure, at 496°C. An even lower temperature, 468°C, in the second stage of roasting is responsible for a high sulfate level of the calcine which necessitated washing prior to cyanidation (12).

The oil-fired roaster at Getchell is a different case because it treated an ore rather than a concentrate. A high temperature, 593 to 650°C, coupled with low arsenic and sulfur contents, about 3 percent each, permitted throughput rates as high as 7 to 8 tons; per day per ft<sup>2</sup>.

## WASHING AND CYANIDATION OF CALCINE

As was noted in the previous section, the calcines produced by various roasters still contain some arsenic and sulfur (see Table 2). The arsenic is generally present as oxide, arsenites, or arsenates, the former being somewhat soluble in water. The sulfur is present partly as sulfide and partly as sulfate. The amounts of sulfate formation and arsenic retention increase with a decrease in roasting temperature as discussed in the previous section.

The presence of significant amounts of arsenic and sulfur in the calcine cause increased cyanide and lime consumption during cyanidation. They also cause problems in extraction of gold due to increased oxygen demand, and possibly in cementation of gold from "foul" solutions.

To overcome these ill effects, the Giant Yellowknife Mine incorporated an elaborate water washing circuit prior to cyanidation of calcine (12). The washing removes soluble arsenites as well as metal sulfates which are cyanicides. At Giant Yellowknife, incorporation of washing steps resulted in a significant decrease in cyanide consumption, from about 1.8 pounds per ton of calcine to about 0.8 pound per ton of calcine. Washing prior to cyanidation of calcine was also practiced at MacLeod-Cockshutt (10) and Getchell (13). On the other hand, Cochenour--Willans (11) discontinued water washing practice because of the difficulties encountered in the settling of fine calcine particles and the resultant loss of gold present in these particles that were discarded as thickener overflow.

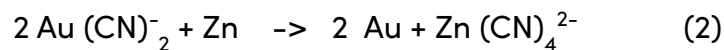
It may be advantageous in certain cases to aerate the calcine slurry in the presence of lime so as to remove some of the alkali- and oxygen-consuming substances prior to cyanidation (17). Washing or lime treatment of calcines becomes even more important if the barren solution from the gold precipitation step is recycled to the plant, so that the cyanicides do not build up to a very high concentration level.

Generally speaking, cyanidation of calcine is a straightforward process and no major problems are encountered. Gold extractions as high as 92 to 94 percent are obtained. The kinetics is generally

faster than with non-calcined, oxide ores. In one case, it was reported that 50 percent of the gold can be extracted within 1 minute in a percolation test (12). The cyanide and lime consumptions are reported in the range of 0.75 to 25 pounds per ton of calcine (10-13). The composition of the calcine and its washing are the governing factors. Agitated tanks and thickeners are the standard equipment used. In some cases, ball mills are also used.

## RECOVERY OF GOLD FROM SOLUTION

At almost all the plants described in the roasting and cyanidation sections, gold was recovered from the cyanide solution by a standard zinc dust cementation technique. The most common variation of this technique is known as the Merrill Crowe process. Finkelstein (19) has reviewed the chemistry of this cementation process and the potential-pH diagram presented in Figure 7 is taken from his paper. As the diagram indicates, metallic zinc easily reduces the  $\text{Au}(\text{CN})_2^-$  ions to metallic gold according to the reaction



The cemented gold is fire refined to remove zinc and other metallic impurities, before being marketed.

Little information is available on the gold recovery efficiency at the plants described in this report. It is mentioned in the literature (19) that the presence of arsenic, even at concentrations of only a few parts per million, adversely affects the gold cementation process. Serious problems may be encountered at about the 15-parts-per-million concentration level. Arsenic is a relatively noble metal and will be cemented along with the gold, requiring its removal in the fire-refining step.

Another problem relates to safety. Under the strongly reducing conditions present during zinc dust cementation (an Eh of -1000 mV or less, see Figure 7), the dangerous gas arsine ( $\text{AsH}_3$ ) may form.

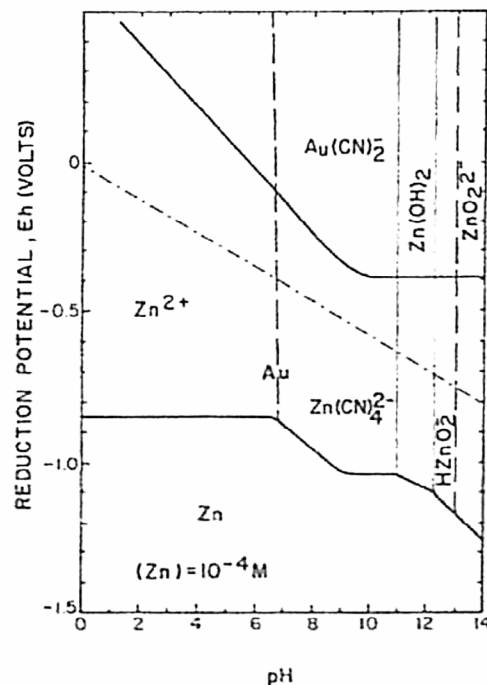


Figure 7. Potential-pH equilibrium diagram for the system Zn-Au-H<sub>2</sub>O-CN<sup>-</sup> at 25°C (Reference 19).



Special safety precautions, such as venting of the workplace, are required under these conditions, adding to the cost of operation.

In view of the above-mentioned problems, an alternate technique, that of adsorption of gold on activated carbon has been suggested for arsenic-bearing solutions. Excellent results have been obtained on a laboratory scale at the U.S. Bureau of Mines, Reno (16). On a commercial scale, this method has been used for arsenic-rich gold-bearing dusts collected from the electrostatic precipitators at Campbell Red Lake Mine (35). A major advantage of this method is that carbon absorption may be carried out directly from the cyanidation pulp, eliminating the need for an expensive continuous countercurrent decantation system. The loaded carbon is screened out. While the gold can be stripped and the activated carbon recycled for reloading of gold, Campbell Red Lake, due to the small size of its operation, prefers to sell the gold-loaded carbon to a smelter.

## ENVIRONMENTAL ASPECTS

Arsenic and most of its compounds are toxic. In the past, little attention was paid to environmental pollution caused by arsenic emissions leaving the stacks of roasters or discharged with the barren solution. This was partly because of the location of the mills in sparsely populated, remote areas. The practice continued until the early 1970s (35).

However, in recent years the governments in several countries have passed regulations to protect the environment. The United States Environmental Protection Agency has set guidelines for arsenic emissions in air and water streams (36, 37). For air emissions, the average arsenic content should be less than 0.5 mg/m<sup>3</sup> (STP). For domestic water, the arsenic limit is at 0.05 mg/L while for other waters the limit is 1 mg/L.

The atmospheric emission of arsenic consists of As<sub>2</sub>O<sub>3</sub>, both as particulate matter and as vapor present in equilibrium with air. Thus, it is important to install not only an efficient condensation system but also a particulate collection system. The facilities installed at Campbell Red Lake Mines are considered not only adequate but exemplary (38). Here, the overall efficiency for the control of particulate emissions using a combination of a hot electrostatic precipitator, an air quench in a mixer-cooler, and a cold baghouse exceeded 99.9 percent. Collection of particulate arsenic in the baghouse was greater than 99.95 percent; however, overall arsenic collection efficiency in the baghouse was slightly less due to the passage of some As<sub>2</sub>O<sub>3</sub> as vapor.

According to Behrens and Rosenblatt (39), the vapor pressure of As<sub>2</sub>O<sub>3</sub> is given as in the temperature range of 94 to 156°C. Thus, at the temperature of the condenser at Campbell Red Lake, 107°C, the equilibrium As<sub>2</sub>O<sub>3</sub> vapor pressure is 7 x 10<sup>-4</sup> mm Hg, which would indicate a

$$\log p(\text{atm}) = \frac{-6067}{T} + 9.905$$

vapor phase arsenic content of about  $8 \text{ Mg/m}^3$  (STP) or in terms of arsenic,  $5$  to  $8 \text{ mg/m}^3$  (STP). This compares with total arsenic emission of  $11 \text{ mg/m}^3$  (STP) measured during the observation campaign (38). In order to reach an arsenic content of  $0.5 \text{ mg/m}^3$  (STP), the equilibrium vapor pressure has to be an order or magnitude smaller which means that the condenser temperature has to be about  $84^\circ\text{C}$  based on extrapolation of the above equation. This, of course, will enormously increase the requirement of cold air to be mixed in. It should be further noted that this cooling by mixing air is not suitable where  $\text{SO}_2$  has to be recovered as sulfuric acid.

With regards to the arsenic discharge in gold mine and mill water, Laguitton (40) has presented an excellent analysis of the most efficient method, the lime addition method. Figure 8, taken from his paper, shows that residual arsenic levels of  $1 \text{ mg/L}$  or less can be obtained by this method. It is important to oxidize arsenic to the pentavalent state, particularly if the barren solution from the zinc-dust cementation step is to be treated. While air can be used for this purpose, addition of chlorine or sodium hypochlorite is more expedient. Since arsenic acid,  $\text{H}_3\text{AsO}_4$ , is a weak acid, a high pH of 12 or so should be maintained.

The arsenic level in water can be further reduced below  $0.5 \text{ mg/L}$  by adding a small amount of phosphate ions (40). Otherwise, ion exchange or other techniques must be used to meet the standards

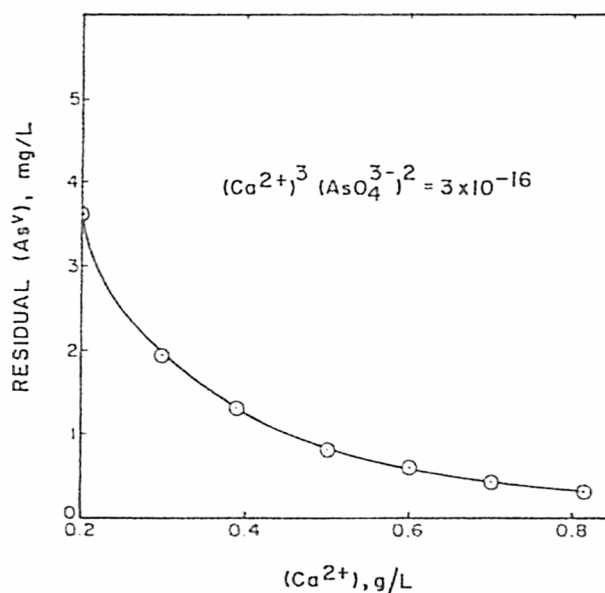


Figure 8. Variation of the residual As(V) concentration in equilibrium with  $\text{Ca}^{2+}$  ions in solution (Reference 40).

of drinking water.

As for the arsenic containing solids, the  $\text{As}_2\text{O}_3$  condensate can be purified and sold. The two major consumers are the alloy manufacturing industry and the agricultural chemical industry (41). In those cases, where market conditions do not permit this, the arsenic oxide, or other arsenic compounds such as calcium or iron arsenate or cyanidation tailings, have to be stored at the plant site in sealed spaces.

## SUMMARY AND CONCLUSIONS

The major conclusions regarding recovery of gold from arsenical ores are summarized below.

### 1. Occurrence of Arsenical Ores

Arsenical gold ore deposits occur in almost all parts of the world. Several large mines containing arsenical gold ore have operated or are operating in Canada and the western United States.

### 2. Mineralogy

Arsenopyrite ( $\text{FeAsS}$ ) is the most commonly occurring arsenic mineral, often in association with pyrite ( $\text{FeS}$ ). At the Getchell Mine in Nevada, orpiment ( $\text{As}_2\text{S}_3$ ) and realgar ( $\text{As}_2\text{S}_2$ ) are the major arsenic minerals. Generally, very fine particles of free gold are disseminated in the grains of sulfide minerals.

### 3. Mineral Beneficiation

Because of the nature of gold distribution, fine grinding of the ore may not increase the liberation of gold for cyanidation. Rather, gravity separation and, more commonly, flotation has been used to prepare a sulfide concentrate containing most of the gold (87 to 95 percent recovery). The concentrates contained from 2 to 38 percent arsenic, 16 to 38 percent sulfur, 17 to 38 percent iron and 1 to 6 oz/ton gold. At the Getchell Mine, where the beneficiation step was not included, the ore containing about 3 percent each of arsenic and sulfur, and about 0.25 oz/ton gold, was fed directly to the roaster.

### 4. Cyanidation of Concentrate

It has long been known that the presence of arsenic sulfide minerals adversely affects the gold extraction during cyanidation. This is why arsenical ores are considered refractory. Both physical and chemical factors are responsible for this behavior. Finely disseminated gold particles inside arsenopyrite grains require extremely fine grinding and unduly long residence time for cyanide ( $\text{CN}^-$ ) ions to reach the gold. On the chemical side, dissolution of gold as  $\text{Au}(\text{CN})_2^-$  ions requires oxidizing conditions, an Eh of  $-400$  mV (vs. standard hydrogen electrode) or above. The presence of arsenic sulfides tends to lower the Eh to  $-500$  mV and below. This necessitates excessive aeration or the use of stronger oxidants. There are also suggestions that the presence of sulfide grains in contact with gold causes an electrochemical passivation of gold.

### 5. Roasting of Concentrates

To overcome the above-mentioned problems, arsenical concentrates are roasted to remove most of the arsenic and sulfur as  $\text{As}_2\text{O}_3$  and  $\text{SO}_2$ , while producing a porous oxide calcine suitable for



cyanidation. The roasting practices of six United States and Canadian plants show how roasting technology has evolved from the early 1920s to the 1960s. The single-hearth and multiple-hearth roasters of the earlier plants have been replaced by fluidized-bed roasters. The optimum roasting temperature has ranged from about 470 to 700°C, depending upon the roaster design, arsenic, and sulfur contents of the calcine and throughput rate.

Available thermodynamic data have been used to describe the chemistry of the roasting process and its bearing on roasting practice. The vapor pressures of arsenic and sulfur over arsenic sulfide minerals are considerably higher than that of sulfur over pyrite. Also, the driving force for the oxidation of arsenic to  $\text{As}_2\text{O}_3$  vapor is comparable to that for the sulfur to  $\text{SO}_2$  gas. As a result, during the early stages of roasting while  $\text{FeS}_2$  is converted to  $\text{FeS}$ , most of the arsenic and about half of the sulfur are removed in the vapor phase as  $\text{As}_2\text{O}_3$  and  $\text{SO}_2$ . Higher temperature increases the rate of arsenic removal, and has been used to either increase the throughput rate or to treat feed materials with higher arsenic contents. It is important to remove most of the arsenic this way, otherwise during later stages of roasting when  $\text{FeS}$  is converted to  $\text{Fe}_2\text{O}_3$  under stronger oxidizing conditions, non-volatile  $\text{As}_2\text{O}_5$  will be formed and may combine with iron oxides to form iron arsenite or arsenate. The presence of soluble arsenic oxide compounds adversely affect the cyanidation of the calcine.

## 6. Washing and Cyanidation of Calcine

The calcines, particularly those produced at low temperature, are washed prior to cyanidation to remove soluble sulfates and arsenites to reduce oxygen, lime, and cyanide requirements during cyanidation. Generally, cyanidation of calcine presents no major problems and gold extractions of up to 94 percent have been obtained using standard equipment; agitated tanks followed by a series of thickeners.

## 7. Gold Recovery from Solution

Zinc dust cementation is the standard technique used. When treating arsenic-bearing solutions, there is a possibility of forming dangerous arsine gas ( $\text{AsH}_3$ ) due to strongly reducing conditions present during zinc cementation (an Eh of -1000 mV or so). For safety, the workplace has to be vented. It is also reported that the presence of arsenic in cyanide solutions, even at the 5 to 10 parts-per-million level, adversely affects gold recovery. For such situations, absorption of gold on activated carbon provides a better alternative.

## 8. Environmental Aspects

Atmospheric pollution can be minimized by installation of proper dust collecting equipment and designing  $\text{As}_2\text{O}_3$  condenser to operate at a low temperature, about 100°C. For aqueous streams, oxidation of arsenic to the As (V) state and addition of lime to the saturation level can bring down the arsenic level to less than 1 mg/L, which is the EPA limit for non-domestic water. As for the solids, arsenic oxide or calcium arsenate can be purified and sold to the alloy manufacturing or the agricultural chemical industries. Otherwise, a sealed space should be used to store the arsenic compounds.

## ACKNOWLEDGEMENT

The authors would like to thank AMAX management for permission to publish this paper.

## REFERENCES

1. G.M. Schwartz, "The Host Minerals of Native Gold", Economic Geology, Vol. 39, No. 6, September-October 1944, pp. 371-411.
2. K.J. Henley, "Gold-ore Mineralogy and its Relation to Metallurgical Treatment", Minerals Science Engineering, Vol. 7, No. 4, October 1975, pp. 289-312.
3. F.W. McQuiston, Jr. and R.S. Shoemaker, Gold and Silver Cyanidation Practice, SME-AIME, New York, 1975.
4. P. Joralemon, "The Occurrence of Gold at Getchell Mine, Nevada", Economic Geology, Vol. 46, 1951, pp. 267-310.
5. J.D. Wells and T.E. Mullens, "Gold-Bearing Arsenian-Pyrite Determined by Microprobe Analysis, Cortez and Carlin Gold Mines, Nevada", Economic Geology, Vol. 68, 1973, pp. 187-201.
6. E.H. Robie, "Producing Gold and Arsenic at Jardine, Montana", Engineering and Mining Journal Press, November 14, 1925, pp. 765-772.
7. W.G. Huber and F.J. Martin, "Ore Treatment at Beattie Gold Mines Limited", AIME Transactions, Vol. 112, 1934, pp. 690-703.
8. O. Matthews, "Cochénour- Willans Mill", Engineering and Mining Journal, March 1942, pp. 45-47.
9. P.R. Archibald, "Roasting Arsenical Gold Ores and Concentrates", The Canadian Mining and Metallurgical Bulletin, March 1949, pp. 129-139.
10. R.C. Gegg, "Milling and Roasting at MacLeod-Cockshutt", The Canadian Mining and Metallurgical Bulletin, December 1949, pp. 659-665.
11. O. Matthews, "Fluo-Solids Roasting of Arsenopyrite Concentrates at Cochénour Willans", The Canadian Mining and Metallurgical Bulletin, April 1949, pp. 178-187.
12. R.J.C. Tait, "Recent Progress in Milling and Gold Extraction at Giant Yellowknife Gold Mines Limited", The Canadian Mining and Metallurgical Bulletin, April 1961, pp. 302-314.

13. J.B. Hutti, "Getchell Mine Resumes Gold Production", Engineering and Mining Journal, January 1963, pp. 70-73.
14. N. Hedley and B. Tabachnik, "Arsenic and Antimony Sulfide Minerals in Cyanidation", Recent Developments in Mineral Dressing, Institution of Mining and Metallurgy, London, 1953. (Reproduced in reference 18)
15. R. Carter and C.S. Samis, "The Influence of Roasting Temperature Upon Gold Extraction by Cyanidation from Refractory Gold Ores", The Canadian Mining and Metallurgical Bulletin, March 1952, pp. 160-166.
16. H.J. Heinen, G.E. McClelland, and R.E. Lindstrom, "Recovery of Gold from Arsenopyrite Concentrates by Cyanidation-Carbon Adsorption", South African Mining and Engineering Journal, August 1981, pp. 109-115. Also U.S. Bureau of Mines Report of Investigations No. 8458, 1980.
17. J.V.N. Dorr and F.L. Bosqui, Cyanidation and Concentration of Gold and Silver Ores, McGraw-Hill Book Company, Inc., New York, 1950.
18. N. Hedley and H. Tabachnik, "Chemistry of Cyanidation", Mineral Dressing Notes, Number 23, American Cyanamid Company, Wayne, New Jersey, December 1968.
19. N.P. Finkelstein, "The Chemistry of the Extraction of Gold from its Ores", Chapter 10 in Gold Metallurgy in South Africa, R.J. Adamson (editor), Chamber of Commerce of South Africa, Johannesburg, 1972, pp. 284-351.
20. K. Tsuchizawa and T. Nishimura, "Electric Potential-pH Diagrams of Arsenic-Sulfur-Water Systems", Tohoku Dagaku Senko Seiren Kenkyusho 340D, 1978, pp. 74-79.
21. A.O. Filmer, "The Dissolution of Gold from Roasted Pyrite Concentrates", Journal of the South African Institute of Mining and Metallurgy, March 1982, pp. 90-94.
22. A.F.B. Norwood, "Roasting and Treatment of Auriferous Flotation Concentrates", Proceedings Australian Institute of Mining and Metallurgy, No. 116, 1939, pp. 391-412.
23. P.G. Mekusic and J.E. Laschings, "Refractory Gold Ores. Report on Investigations into Roasting of Gold Concentrates in the Edwards Roaster of the Fairview and the New Consort Reduction Plants", Report No. 211, National Institute for Metallurgy, Randburg, South Africa, August 15, 1967.
24. G.A. Walker, "Roasting and Cyanidation of Arsenopyrite Concentrates", Chemical Engineering and Mining Review, December 11, 1939, pp. 122-124.
25. L.E. Djinghenzian, "Theory and Practice of Roasting Sulfide Concentrates, with Special Reference



to Canadian Gold Ores and Concentrates”, Canadian Mining and Metallurgical Bulletin, June 1952, pp. 352-361.

26. N.A. Kolesnikov, V.F. Larin, A.P. Panteleeva, and IJ. Balchtina, “Fluidized Bed Roasting of Gold-Arsenic Concentrates Cor Maximum Removal of Arsenic”, Soviet Journal of Nonferrous Metals, Vol. 8, No. 6, June, 1967, pp. 54-57. Also, Tsvetnye Metally, Vol. 40, No. 6, June, 1967, p. 44 (Russ.).

27. N.A. Kolesnikov, I.I. Bakhtina, and G.D. Pervutinskii, “Improvements in the Roasting of Gold-Arsenic Concentrates”, Soviet Journal of Nonferrous Metals, Vol. 11, No. 12, 1970, pp. 79-81. Also, Tsvetnye Metally, Vol. 43, No. 12, December 1970, p. 73 (Russ.).

28. D.R. Stull and H. Prophet, JANAF Thermochemical Tables, Second Edition, NSRDS-NBS37, National Bureau of Standards, Washington, D.C., 1971.

29. C.E. Wicks and F.E. Block, “Thermodynamic Properties of 65 Elements - Their Oxides, Halides, Carbides and Nitrides”, USBM Bulletin 605, 1963.

30. A.D. Mah, “Thermodynamic Data for Arsenic Sulfide Reactions”, U.S. Bureau of Mines Report of Investigations 8671, 1982.

31. B.A. Strathdee and L.M. Pidgeon, “Thermal Decomposition and Vapor Pressure Measurements on Arsenopyrite and on Arsenical Ore”, The Canadian Mining and Metallurgical Bulletin, December 1961, pp: 883-887.

32. H. Hultgren, P.O. Desai, D.T. Hawkins, M. Gleisser, K. Kelly, and D.D. Wagman, Selected Values of the Thermodynamic Properties of the Elements, American Society for Metals, Metals Park, Ohio, 1973.

33. K.C. Mills, Thermodynamic Data for Inorganic Sulphides, Selenides and Tellurides, Butterworths, London, 1974.

34. P.B. Barton, Jr., “Thermochemical Study of the System Fe-As--S”, Geochimica et Cosmochimica Acta, Vol. 33, 1969, pp. 841-857.

35. J.R. Roberts, “The Treatment of Roaster Off-Gases at Campbell Red Lake Mines Limited”, presented at the Canadian Mineral Processors’ Meeting, Ottawa, Ontario, January 1976.

36. R.J. Lewis and R.L. Tatken (editors), Registry of Toxic Effects of Chemical Substances. Volume 1, U.S. Department of Health and Human Services, Washington, D.C., February, 1982, p. 189.

37. United States Environmental Protection Agency, “Proposed Rules”, Federal Register, Vol. 47, No. 114, Monday, June 1982, pp. 25682-25718.

38. J.O. Burckle, G.H. Marchant, and R.L. Meek, “Arsenic Emissions and Control- Gold Roasting

Operations”, Environment International, Vol. 6, 1981, pp. 443-451.

39. R.G. Behrens and G.M. Rosenblatt, “Vapor Pressure and Thermodynamics of Octahedral Arsenic Trioxide (Arsenolite)”, J. Chem. Thermodynamics, YoL 4, 1972, pp. 175-190.

40. D. Laguitton, “Arsenic Removal from Gold-Mine Waste Waters, Basic Chemistry of the Lime Addition Method”, CIM Bulletin, September 1976, pp. 105-109.

41. W.H. Lederer and R.J. Fenstenheim (editors), Arsenic, Yan Nostrand Reinhold Company, New York, 1983.

# PALLADIUM(II) COMPLEXES AS CATALYSTS FOR ORGANIC REACTIONS



Natalia V. Karninskaia  
and Nenad M. Kostić

Chemistry Department  
Iowa State University

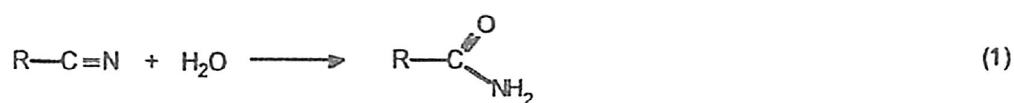
Ames, Iowa

[< Return to Index](#)

## INTRODUCTION

Palladium and platinum compounds are well-known stoichiometric reagents and catalysts for many organic interconversions. In our laboratory we work with the simple Pd(II) and Pt(II) aqua complexes (Chart I), which are easy to prepare from the available precursors and are stable at a variety of conditions. Liability of ligand exchange on Pd(II) and relatively low  $pK_2$  for the bound water in Pd(II) aqua complexes make these complexes especially valuable catalysts for hydrolytic reactions. We have studied several examples of such organic hydrolytic reactions, three of them are presented in this report.

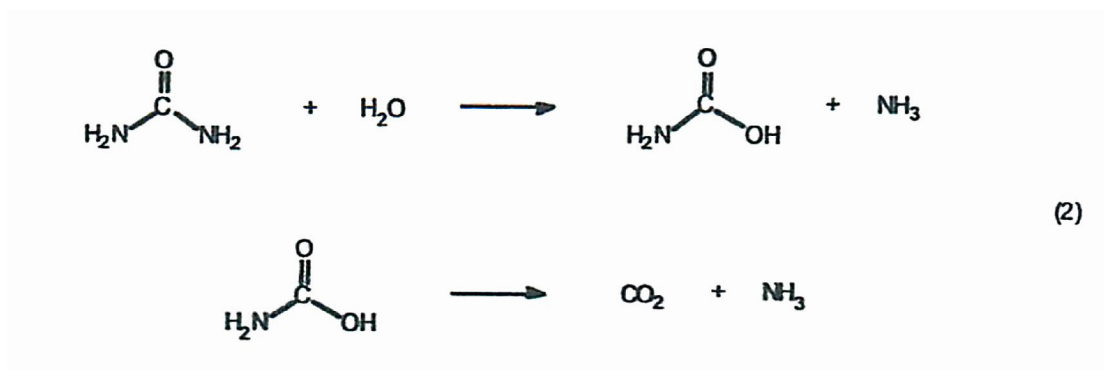
Hydration of nitriles and formation of corresponding carboxamides (eq 1) is an important reaction both in laboratory and in industry. This reaction is



catalyzed by various acids and bases, but many of these classical methods require harsh conditions and give low yields. The undesirable further hydrolysis of carboxamides into carboxylic acids cannot be avoided, because this reaction is faster than hydration, especially under basic conditions. Extreme acidity and basicity can, however, be avoided if transition-metal complexes are used. Such studies have been done with several transition metals, often under forcing conditions. Labile complexes served as catalysts. Inert complexes allowed reactive intermediates to be trapped and gave kinetic and stereochemical information about the mechanisms of hydration. The main advantage of transition-metal complexes over acids and bases is their selectivity. In the presence of these complexes, carboxamides are not converted to carboxylic acids. We report here on hydration of several nitriles catalyzed by palladium(II) aqua complexes. We examine the effects of the aqua ligands, ancillary ligands, solvent, and the pH value on the rate of hydration and present a general mechanism for this reaction. Since nitrile hydratases, which catalyze the reaction in eq 1 in vivo, are metalloenzymes, investigation of catalysis by transition-metal complexes may contribute to an understanding of these important but little-studied enzymes.<sup>1</sup>

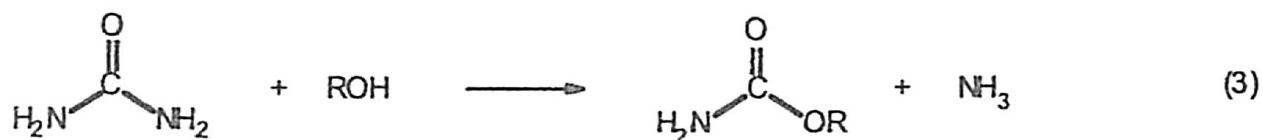
Many biological processes involve amide bond hydrolysis in proteins and peptides. The amide bond is extremely unreactive, the half-life for its hydrolysis in neutral solution is ca. 300 years. Transition-metal complexes hold great promise for the hydrolytic cleavage of biomolecules. Many of the previous studies have been done with esters and activated amides, however studies with regular (inactivated) amides, peptides, and proteins are becoming more frequent. These reactions are important in practice and interesting from the mechanistic point of view. Urea is the simplest example of an inactivated amide. Uncatalyzed hydrolysis of urea has not been reported. However, nickel(II)-containing enzyme urease catalyzes hydrolysis of urea into ammonia and carbamic acid. Carbamic acid then spontaneously decomposes into second molecule of ammonia and carbon dioxide (2).





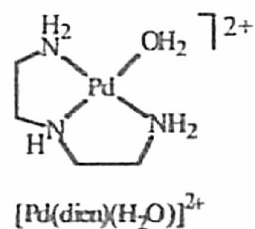
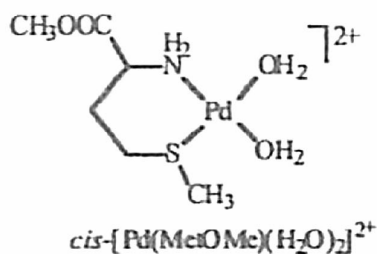
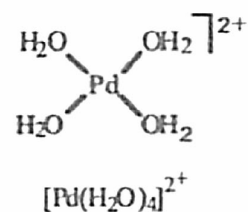
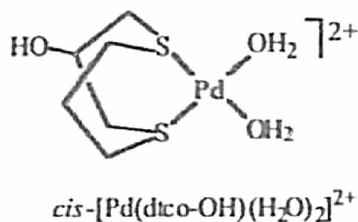
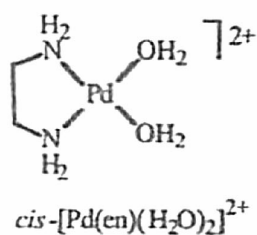
Here we present the first example of catalytic decomposition of urea by the simple palladium(II) aqua complexes. Since Pd(II) belongs to the same group as Ni(II) and has the same oxidation state, our mechanistic study provides some insights into the mechanism of enzymatic urea decomposition. The fact that carbamic acid is the common intermediate in both cases, also makes our reaction quite relevant to urease chemistry.<sup>2</sup>

The third example of organic reactions catalyzed by Pd(II) complexes is catalytic alcoholysis of urea in the presence of various alcohols (3). In a case of alkyl alcohols formed carbamic ester is more stable than carbamic acid, and carbon dioxide is not produced. If, however, aryl alcohols are used, the resulting ester is hydrolyzed to carbamic acid, which then decomposes into ammonia and carbon dioxide.<sup>3</sup>



Both reactions, hydrolysis and alcoholysis of urea catalyzed by Pd(II) aqua complexes, were studied quantitatively: binding of urea to the catalyst, formation of carbamic acid coordinated to palladium(II) via the nitrogen atom. conversion of this intermediate into carbamic ester or carbon dioxide and ammonia, direct alcoholysis of coordinated urea. We examine the effects of the aqua ligands on Pd(II), presence of inhibitors and other metal ions, and the pH value on the rate of hydration and present a general mechanism for these reactions.<sup>2-3</sup>

## Chart 1. The Complexes

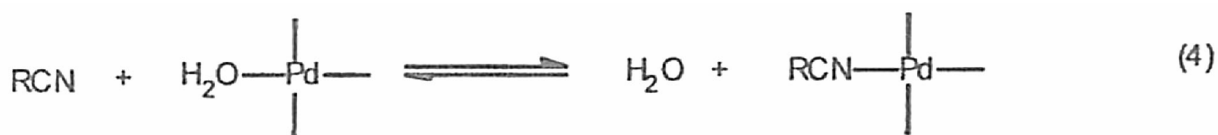


## HYDRATION OF NITRILES

### Detection of Nitrite Coordination to Palladium(II)

Carbon-13, nitrogen-15, proton NMR spectra, and visible absorbance experiments confirm the coordination and show that nitrile is a labile ligand to palladium(II).

The equilibrium in eq 4 was quantitatively studied by  $^1H$  NMR spectroscopy because of the sensitivity of this method.



The results for various nitriles and palladium(II) complexes are given in Table 1. Hydration of  $CH_3CN$  and  $CH_2ClCN$  at 293 K was slow enough not to interfere with the study of coordination. The corresponding three values of the equilibrium constant in Table 1 are accurate. Proton NMR spectra did not give evidence of binding of  $CH_2ClCN$  to  $[Pd(dien)(H_2O)]^{2+}$ , and  $CHCl_2CN$  underwent hydration too rapidly for the coordination to be studied. For these reasons, the last four values in Table 1 are estimates, obtained on the basis of known equilibrium constants.

**Table 1. Experimentally Determined and Estimated Equilibrium Constants for Displacement of an Aqua Ligand by a Nitrile Ligand (eq 4) at 293 K**

Entering Ligand	Complex	K, M <sup>-1</sup>	
		Determined	Estimated
CH <sub>3</sub> CN	cis-[Pd(en)(H <sub>2</sub> O) <sub>2</sub> ] <sup>2+</sup>	22 ± 2	
	[Pd(dien)(H <sub>2</sub> O)] <sup>2+</sup>	0.37 ± 0.04	
	[Pd(H <sub>2</sub> O) <sub>4</sub> ] <sup>2+</sup>	5.4	
CH <sub>2</sub> ClCN	cis-[Pd(en)(H <sub>2</sub> O) <sub>2</sub> ] <sup>2+</sup>	2.7 ± 0.3	
	[Pd(dien)(H <sub>2</sub> O)] <sup>2+</sup>		0.04
CHCl <sub>2</sub> CN	cis-[Pd(en)(H <sub>2</sub> O) <sub>2</sub> ] <sup>2+</sup>		0.3
	[Pd(dien)(H <sub>2</sub> O)] <sup>2+</sup>		0.004
	[Pd(H <sub>2</sub> O) <sub>4</sub> ] <sup>2+</sup>		0.05

### Dependence of the Hydration Rate on the Catalyst and the Substrate Concentrations

The reaction is of first order with respect to the catalyst. The results show that there is no saturation of the catalyst complex by the substrate under these conditions. Indeed, the equilibrium constant for nitrile coordination is low (see above).

### Dependence of the Hydration Rate on pH

Hydration of CHCl<sub>2</sub>CN catalyzed by the tridentate complex [Pd(dien)(H<sub>2</sub>O)]<sup>2+</sup> was independent of pH. The complex [Pd(dien)(CHCl<sub>2</sub>CN)]<sup>2+</sup> lacks aqua ligands; the water for hydration must come from the solvent. We assume that hydration involving the complex cis-[Pd(en)(CHCl<sub>2</sub>CN)]<sup>2+</sup>, which also lacks aqua ligands, will likewise be independent of pH.

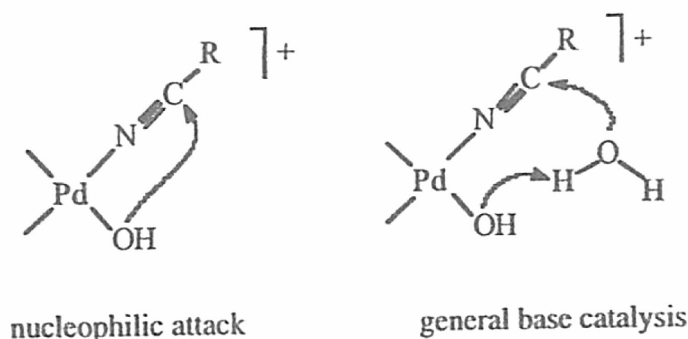
The dependence of the hydration rate on pH therefore comes from an acid base process involving an aqua ligand. Since the catalyst is [Pd(en)(H<sub>2</sub>O)<sub>2</sub>]<sup>2+</sup>, the complex responsible for the pH dependence is cis-[Pd(en)(CHCl<sub>2</sub>CN)(H<sub>2</sub>O)]<sup>2+</sup>; its acid-dissociation constant is K<sub>a</sub>. The experimental data were fitted to eq 5.

$$k_{\text{obs}} = \frac{k_{\text{H}_2\text{O}} [\text{H}^+] + K_{\text{aKOH}}}{K_{\text{a}} + [\text{H}^+]} \quad (5)$$

The fitted parameters are as follows:  $k_{\text{H}_2\text{O}} = (7.2 \pm 0.1) \times 10^{-4} \text{ min}^{-1}$ ,  $k_{\text{OH}} = (24 \pm 2) \times 10^{-4} \text{ min}^{-1}$ , and  $K_a = (8.0 \pm 0.1) \times 10^{-6} \text{ M}$ . The last value corresponds to  $\text{p}K_a = 5.1 \pm 0.1$  in  $\text{D}_2\text{O}$  as a solvent.

The hydroxo complexes may be somewhat better catalysts than their aqua precursors for two reasons, illustrated in Scheme 1. The hydroxo ligand is both a stronger nucleophile and a stronger general base than the aqua ligand. Kinetic experiments, however, cannot distinguish between those two mechanisms, i.e., between the internal and external nucleophilic attacks on the coordinated nitrile. Labeling experiments are inapplicable to these palladium(II) complexes, which are labile.

Scheme 1



The small increase in the rate of hydration in neutral and weakly basic solutions is not advantageous in practical catalysis, because with increasing pH value increases the rate of the undesirable hydrolysis of carboxamide into carboxylate. For this reason, we continued studying catalysis of hydration in acidic solutions.

### Dependence of the Hydration Rate on the Substrate Electrophilicity

Table 2 shows a marked increase in the rate of hydration as the electron-withdrawing ability of substituents increases in a series of similar nitriles. Table 1 shows a parallel decrease in the binding affinity of the nitrile for palladium(II). Evidently, reactivity is enhanced more by the electrophilicity of the nitrile carbon atom than by the substrate binding to the catalyst.

### Dependence of the Hydration Rate on the Ancillary Ligands Bound to Palladium(II)

Table 3 shows a considerable kinetic effect of the ligands that remain bound to palladium(II) during the catalytic reaction.

Because it contains the most nucleophilic aqua ligand, even though it has the least affinity for binding of the nitrile (Table 1), the complex  $[\text{Pd}(\text{H}_2\text{O})_4]^{2+}$  is more effective than the other complexes. For the aforementioned electronic reason, the bidentate ligands methionine ester (an S,N-donor), ethylenediamine (an N,N-donor), and a substituted 1,5-dithiacyclooctane (an S,S-donor) lessen the catalytic effectiveness of the palladium(II) atom.



**Table 2. Effect of Substituents on the Rate Constant for Hydration of Nitriles and Formation of Corresponding Carboxamides Catalyzed by 17 mM  $[Pd(H_2O)_4]^{2+}$**

Mole Ratio Catalyst : Substrate	Substrate	$k_{obs}, h^{-1}$ , at 313 K
1:10	CH <sub>3</sub> CN	0.0016 ± 0.0001
1:10	CH <sub>2</sub> ClCN	0.042 ± 0.003
1:10	CHCl <sub>2</sub> CN <sup>a</sup>	5.22 ± 0.16
1:1	4-CH <sub>3</sub> O-C <sub>6</sub> H <sub>4</sub> CN	0.010 ± 0.001
1:1	C <sub>6</sub> H <sub>5</sub> CN	0.023 ± 0.001
1:1	4-NO <sub>2</sub> -C <sub>6</sub> H <sub>4</sub> CN	0.35 ± 0.04

a) For disappearance of the nitrile.

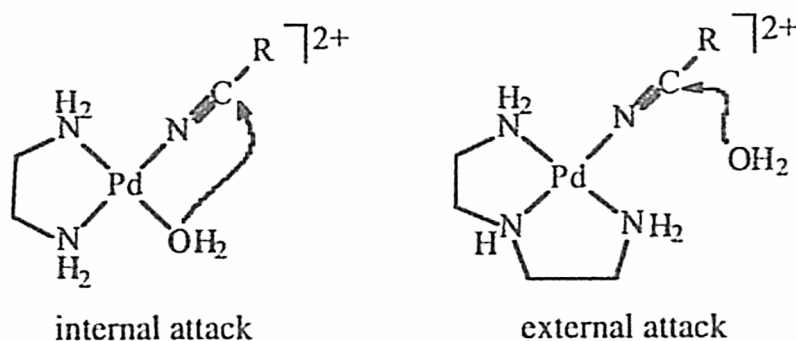
**Table 3. Rate Constant for Disappearance of CHCl<sub>2</sub>CN and Appearance of CHCl<sub>2</sub>C(O)NH<sub>2</sub> in Solutions that were Initially 170 mM in the Nitrile and 17 mM in the Palladium(II) Aqua Complex**

Catalyst	$k_{obs}, h^{-1}$ , at 313 K
$[Pd(H_2O)_4]^{2+}$	5.22 ± 0.16 <sup>a</sup>
<i>cis</i> -[Pd(MetOMe)(H <sub>2</sub> O) <sub>2</sub> ] <sup>2+</sup>	1.05 ± 0.01
<i>cis</i> -[Pd(en)(H <sub>2</sub> O) <sub>2</sub> ] <sup>2+</sup>	0.39 ± 0.02
<i>cis</i> -[Pd(dtco-OH)(H <sub>2</sub> O) <sub>2</sub> ] <sup>2+</sup>	0.05 ± 0.01
[Pd(dien)(H <sub>2</sub> O)] <sup>2+</sup>	0.020 ± 0.002

a) For disappearance of the nitrile.

That the diethylenetriamine (dien) complex is only about 20 times less reactive than the ethylenediamine (en) complex can be explained with reference to Scheme 2.

Scheme 2

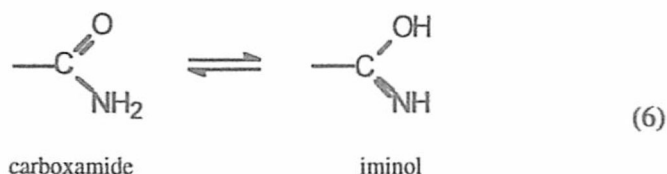


## Lack of Affinity between Carboxamides and Palladium(II)

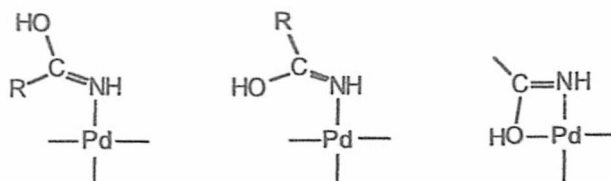
Carboxamides can coordinate to transition metals via the oxygen or the nitrogen atom. Various experiments showed that acetamide and dichloroacetamide do not detectably bind to  $[\text{Pd}(\text{H}_2\text{O})_4]^{2+}$  under the conditions used for the hydration reactions, even when the amide was present in a tenfold or 50-fold molar excess over the complex. This finding rules out inhibition of nitrile hydration by coordination of the product, carboxamide, to the catalyst. Without the inhibition, the catalysts are more efficient.

## The Observed Intermediate in the Reaction Catalyzed by $[\text{Pd}(\text{H}_2\text{O})_4]^{2+}$

In the reactions catalyzed by  $[\text{Pd}(\text{H}_2\text{O})_4]^{2+}$  an intermediate was observed at 6.68 ppm. The resonance that grows over time at 6.68 ppm, 0.40 ppm upfield from that of  $\text{CHCl}_2\text{CN}$  and 0.42 ppm downfield from that of  $\text{CHCl}_2\text{C}(\text{O})\text{NH}_2$ , cannot be due to either coordinated nitrile or coordinated carboxamide. The near equidistance of the middle resonance from the resonances of  $\text{CHCl}_2\text{CN}$  (0.40 ppm) and of  $\text{CHCl}_2\text{C}(\text{O})\text{NH}_2$  (0.42 ppm) suggests that the middle resonance is due to an intermediate in the conversion of the nitrile to the carboxamide, a species with partial characteristics of both. Iminol, the minor tautomer of carboxamide (eq 6), satisfies this requirement. It resembles both the nitrile and a carboxamide in having both a multiple carbon-nitrogen bond and a carbon oxygen bond. Iminols can be stabilized by transition metals,



and both unidentate and bidentate modes of coordination have been examined crystallographically. Therefore, there are good precedents for possible iminol intermediates in the hydration reaction, which are shown below. The two unidentate ligands are geometrical syn and anti isomers; the third intermediate, containing bidentate iminol, cannot show geometrical isomerism. Corresponding iminates are unlikely, because deprotonation is suppressed in acidic solutions used in our study.



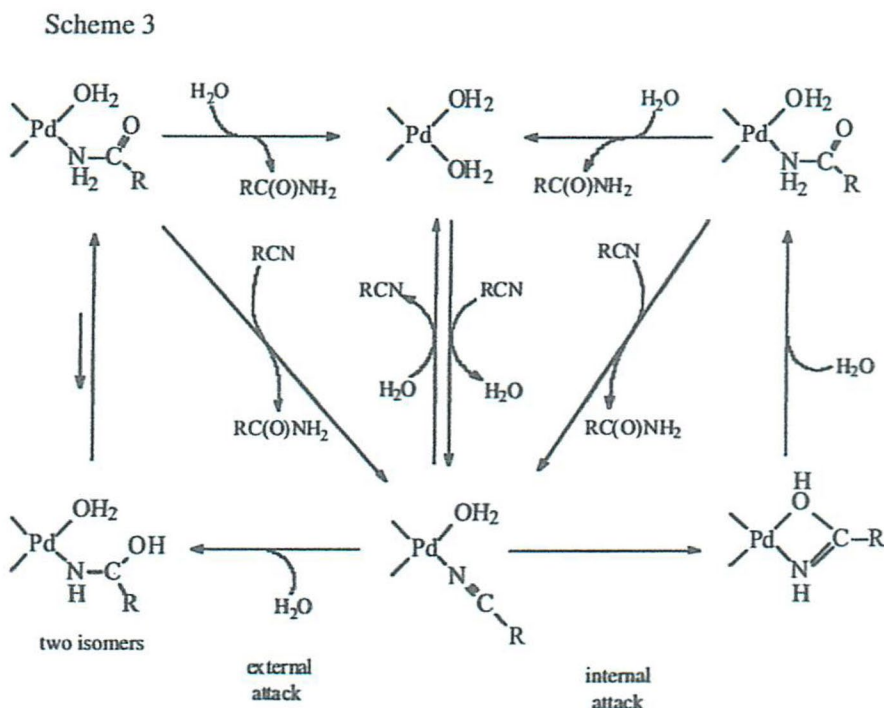
## Chemical Mechanism and the Iminol Intermediate

Although either unidentate or bidentate iminol intermediate (see formulas above) can result from either mechanism of hydration, the unidentate iminol may be more likely in the external attack, whereas the bidentate iminol may be more likely in the internal attack. As simulations with program KINSIM showed both mechanisms occurred.

Chemical shifts give a clue about the mode of iminol coordination. When the hydration is studied in aqueous (D<sub>2</sub>O) solution, the intermediate gives only the resonance at 6.68 ppm. This fact argues for the bidentate iminol complex, which cannot exist as geometric isomers. Monodentate iminol intermediate was not observed.

## Overall Mechanism. and Turnover in Hydration

The experimental facts discussed above are integrated in the mechanism in Scheme 3.



## Kinetics and Mechanism of Urea Hydrolysis

Carbon-13 NMR Spectroscopy in Kinetics. It is well known that quantitative analysis with <sup>13</sup>C NMR spectroscopy is difficult to perform due to differential relaxation and Nuclear Overhauser Effects (NOE). Both of these factors affect carbon signal intensity, such that carbon concentrations are not accurately obtained from the spectrum. Addition of Cr(acac)<sub>3</sub> or Fe(acac)<sub>3</sub> (relaxing agents) to the solution shortens long relaxation times of carbons and suppresses NOE. Thus, in the presence of a relaxing agent we were able to study kinetics of urea decomposition by carbon-13 NMR.

## Binding of Urea to $cis$ -[Pd(en)(H<sub>2</sub>O)]<sub>2</sub><sup>+</sup>Complex

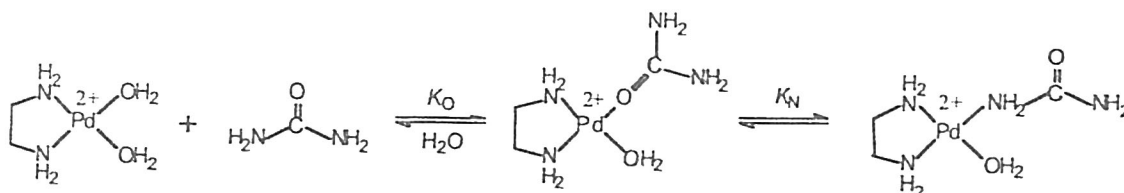
There are many possible modes of urea binding. Among those two are the most common: O-bound (I) urea and N-bound (II) urea.



When urea decomposition is catalyzed by  $cis$ -[Pd(dtco-OH)(H<sub>2</sub>O)<sub>2</sub>]<sup>2+</sup> complex we observe the increase in the concentration of N-bound isomer overtime. At the same time the concentration of the O-bound isomer, present almost from the start of the reaction, decreases. Therefore, it is reasonable to assume that O-bound urea isomerizes into thermodynamically more stable N-bound urea.

Urea binding occurs as shown in Scheme 4 with parameters  $K_O$  (binding through oxygen) and  $K_N$  (isomerization to N-bound urea complex).

Scheme 4



All calculated parameters shown in Table 4. In the presence of 1.5 M H<sub>2</sub>O these binding constants become somewhat lower due to competition between water and urea for coordination. This effect, however, is not very pronounced.

**Table 4. Equilibrium Constants for Urea Binding to [Pd(en)(H<sub>2</sub>O)<sub>2</sub>]<sup>2+</sup> Complex in Acetone-d<sub>6</sub> at 313 K**

Equilibrium Constants	No H <sub>2</sub> O Added	1.5 M H <sub>2</sub> O
$K_O$	23	20
$K_N$	0.060	0.050
$K = K_O \times K_N$	1.3	0.95



## Different Pd(II) Complexes Promote Decomposition of Urea

Five Pd(II) aqua complexes shown in Chart 1 were compared in terms of reactivity toward urea decomposition. The results are shown in Table 5. All complexes with monodentate and bidentate ligands ( $[\text{Pd}(\text{H}_2\text{O})_4]^{2+}$ ,  $\text{cis-}[\text{Pd}(\text{en})(\text{H}_2\text{O})_2]^{2+}$ ,  $\text{cis-}[\text{Pd}(\text{OMeMet})(\text{H}_2\text{O})_2]^{2+}$ , and  $\text{cis-}[\text{Pd}(\text{dtco-OH})(\text{H}_2\text{O})_2]^{2+}$ ) show very similar re-activity. We have chosen  $\text{cis-}[\text{Pd}(\text{en})(\text{H}_2\text{O})_2]^{2+}$  complex for our kinetic investigations.

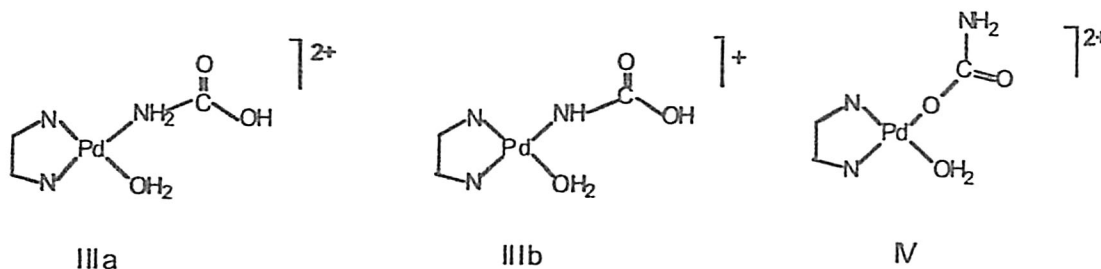
**Table 5. Initial Rate of  $\text{CO}_2$  Formation in the Decomposition of Urea Catalyzed by Various Palladium(II) Complexes in Acetone- $\text{d}_6$  at 313 K**

Complex	$v_i^{\text{CO}_2} \times 10^5, \text{Mmin}^{-1}$
$[\text{Pd}(\text{H}_2\text{O})_4]^{2+}$	$6.67 \pm 0.69$
$[\text{Pd}(\text{en})(\text{H}_2\text{O})_2]^{2+}$	$13.3 \pm 1.1$
$[\text{Pd}(\text{OMeMet})(\text{H}_2\text{O})_2]^{2+}$	$7.87 \pm 0.55$
$[\text{Pd}(\text{dtco-OH})(\text{H}_2\text{O})_2]^{2+}$	$16.5 \pm 1.0$
$[\text{Pd}(\text{dien})(\text{H}_2\text{O})]^{2+}$	$< 1.4 \times 10^{-3}$

Complex with tridentate ligand  $[\text{Pd}(\text{dien})(\text{H}_2\text{O})]^{2+}$  is not reactive to an appreciable extent due to the extremely low binding of urea and absence of internal water delivery or general base catalysis.

### Observed Intermediate in the Decomposition

Decomposition of urea catalyzed by Pd(II) aqua complexes involves formation of an intermediate. This species was studied by  $^{13}\text{C}$  and  $^{15}\text{N}$  NMR spectroscopy. The chemical shifts suggest either carbamic acid itself (IIIa) or its deprotonated form bound through N to Pd(II) (IIIb).



### Products and Overall Stoichiometry of the Reaction

The ultimate products of the hydrolytic urea decomposition are ammonia and carbon dioxide. Overall stoichiometry of the reaction was confirmed by initial rate measurements. Initial rate of  $\text{CO}_2$  formation was obtained from  $^{13}\text{C}$  NMR spectroscopy. It is equal to  $(1.33 \pm 0.1) \times 10^4 \text{ M min}^{-1}$ . Initial rate of overall ammonia production (including ammonium ion and ammonia), found from  $^{15}\text{N}$  NMR spectroscopy is  $(2.48 \pm 0.17) \times 10^4 \text{ Mmin}^{-1}$ . This finding demonstrates stoichiometry of urea decomposition as one equivalent of  $\text{CO}_2$  produced per two equivalents of ammonia as it should be from the overall scheme.

## Independence on Water Concentration

Initial rate of CO<sub>i</sub> formation does not depend on water concentration in the range 0.15M – 7.9M and it is equal to  $(1.33 \pm 0.10) \times 10^4$  Mmin<sup>-1</sup>. Water independence suggests that no external water is involved in the rate limiting step in urea decomposition.

## Kinetic Effects of Base

Decrease in the initial rate of CO<sub>2</sub> production with increasing base concentration was observed. This is consistent with either or both the decomposition of carbamic acid intermediate and dimerization of Pd(II) catalysts, forming inactive  $\mu$ -OH bridged complexes. We concluded that mostly deprotonated form of carbamate intermediate IIIb rather than dinuclear Pd(II) complexes is responsible for the slow carbon dioxide formation at high base concentration.

## Inhibitors of the Urea Decomposition

Thiourea and the product of the reaction ammonia inhibit production of CO<sub>2</sub> from urea due to their binding to Pd(II).

## Kinetic Effects of Acid

As Table 6 shows, an increase in the solution acidity inhibits coordination of urea to palladium(II) but favors the O-bound over the N-bound isomer in the diminishing fraction of urea that is coordinated. The initial rate of CO<sub>2</sub> formation decreases as the concentration of acid increases.

*Table 6. Effects of Acid on the Extent of Urea Coordination, the Mode of Coordination, and the Initial Rate of CO<sub>2</sub> Formation. Initial Concentrations of Urea and [Pd(en)(H<sub>2</sub>O)<sub>2</sub>]<sup>2+</sup> Complex were 0.30 M Each, the Temperature was 313 K, and the Solvent was Acetone-d<sub>6</sub>.*

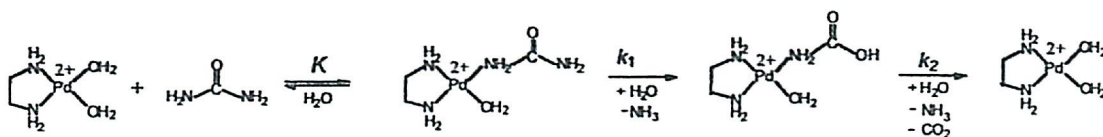
Added [DClO <sub>4</sub> ], M	[bound]/[free] urea	[O-bound]/[N-bound] urea	v <sub>i</sub> <sup>CO<sub>2</sub></sup> x 10 <sup>4</sup> , Mmin <sup>-1</sup>
0.000	3.10	8.70	1.330 ± 0.070
0.027	2.20	8.70	1.020 ± 0.090
0.080	1.10	14.1	0.800 ± 0.070
0.107	0.700	21.4	0.640 ± 0.050
0.133	0.500	22.4	0.600 ± 0.050

## Mechanism of Urea Decomposition

Concentration of the intermediate in Scheme 5 was fitted to eq 7, and rate constants k<sub>1</sub> and k<sub>2</sub> were obtained from this fitting.

$$[\text{Pd-NH}_2\text{COOH}] = \frac{k_1 K [\text{Pd(en)(H}_2\text{O)}_2^{2+}]_0 [\text{NH}_2\text{C(O)NH}_2]_0}{k_2 - k_1} \left[ \exp(-k_1 t) - \exp(-k_2 t) \right] \quad (7)$$

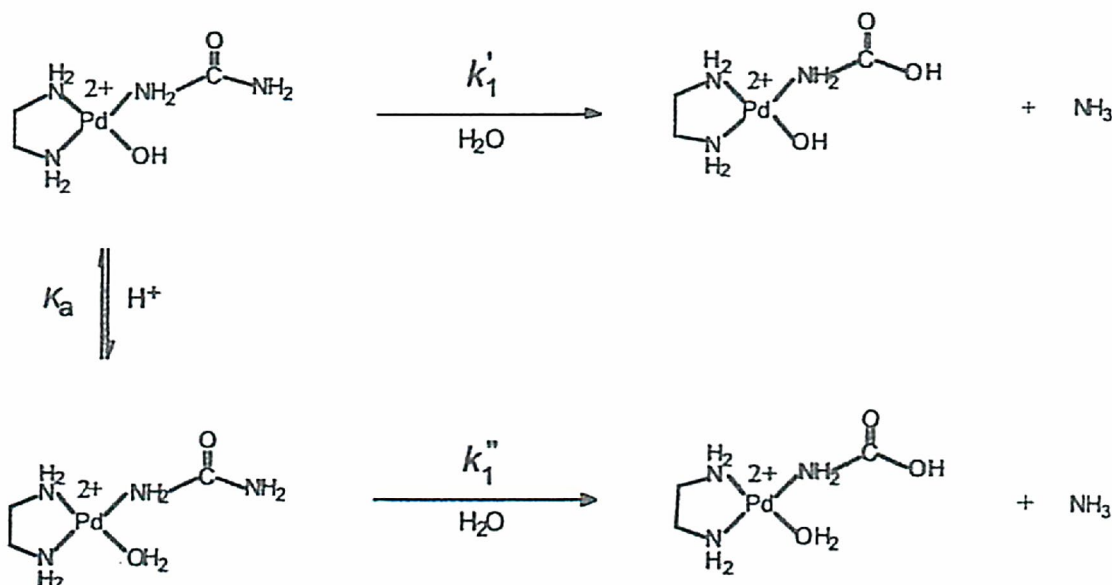
Scheme 5



The rate constant  $k_1$  corresponds to the nucleophilic attack at the carbon atom of N-bound urea. The experimental results were fitted to eq 8, derived from Scheme 6.

$$k_1 = \frac{k_1' K_a}{[\text{H}^+]} + k_1'' \quad (8)$$

Scheme 6



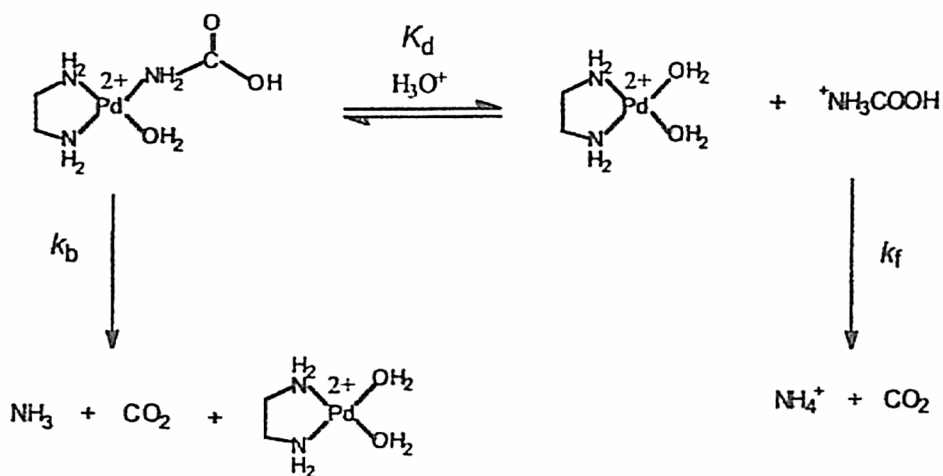
The equilibrium constant  $K_a$  could not be determined experimentally because the complex  $\text{cis-}[\text{Pd(en)}(\text{NH}_2\text{C(O)NH}_2)(\text{H}_2\text{O})]^{2+}$  is reactive and present in a very low concentration. Fortunately, this constant could be estimated on the basis of known  $\text{p}K_a$  values for various Pd(II) aqua complexes. With a reasonable estimate of  $K_a = 1 \times 10^{-6}$  M, the fitting yielded the rate constant for the aqua complex,  $k_1'' = 0.3 \text{ min}^{-1}$  and the one for the hydroxo complex,  $k_1' = 460 \text{ min}^{-1}$ . That the hydroxo complex is more reactive than the "parent" aqua complex is consistent with both internal attack and general base catalysis.

The composite rate constant  $k_2$  represents the disappearance of the carbamic acid intermediate by two pathways: direct decomposition when bound to Pd(m or when free; the corresponding rate constants are  $k_f$  and  $k_b$  shown in Scheme 7.

The later reaction is extremely fast:  $k_f = 6.0 \times 10^{10} \text{ min}^{-1}$ . Fitting the experimental data to eq 9, derived from Scheme 7, yielded  $K_d = 9.0 \times 10^{-14} \text{ M}^{-1}$  and  $k_b = 8.9 \times 10^{-4} \text{ min}^{-1}$ .

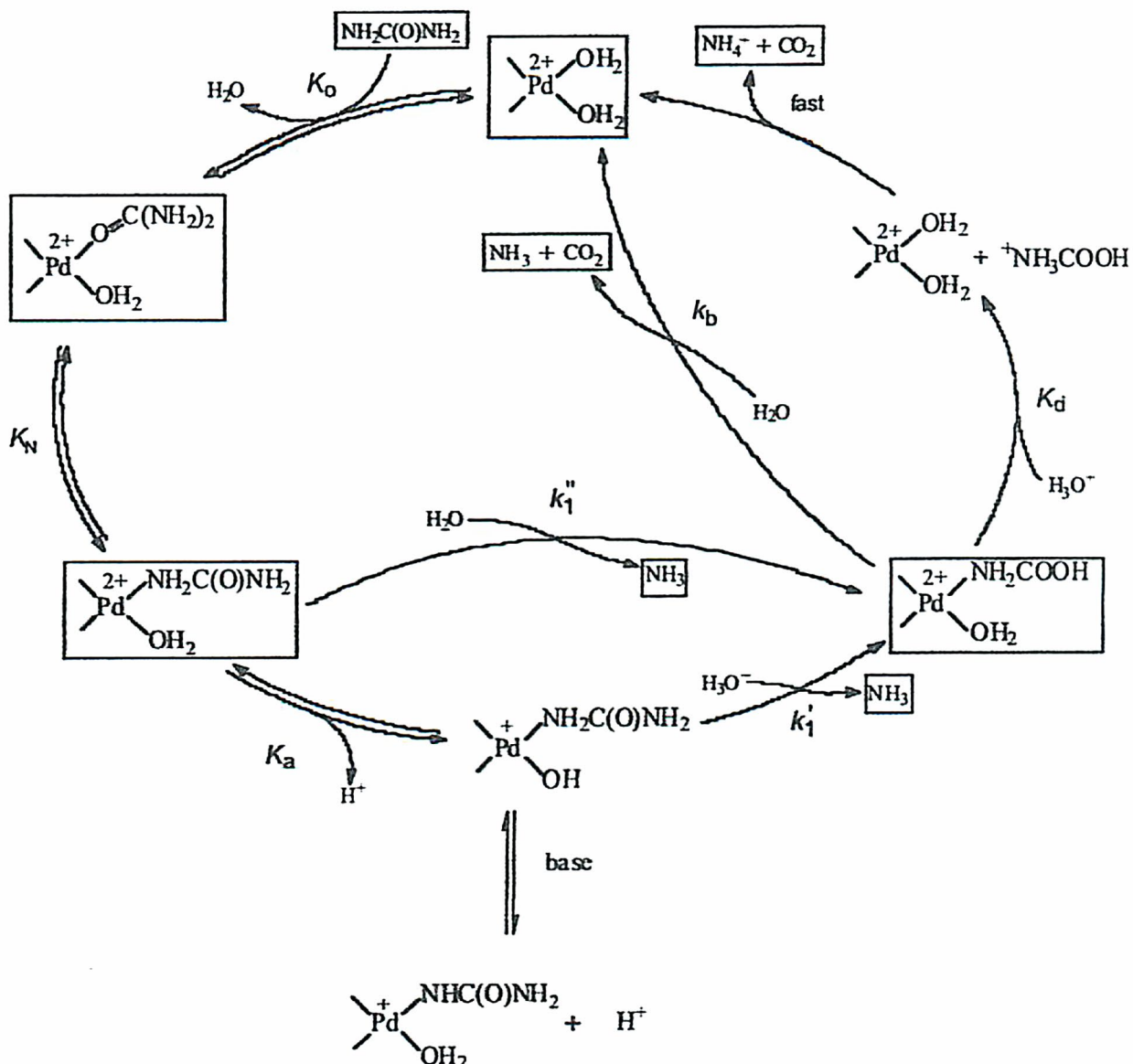
$$k_2 = \frac{k_f K_d [H^+]}{[Pd(en)(H_2O)_2^{2+}]} + k_b \quad (9)$$

Scheme 7





The overall Mechanism and Catalytic Turnover. All steps discussed so far are integrated in Scheme 8. The observed species are shown in boxes.



This mechanism, however, does not fully account for the kinetic results. The overall rate of the reaction (i.e., the initial rate of  $\text{CO}_2$  formation) is greater than the maximal rate of decomposition of carbamic acid, calculated from the known values of  $k_1$  and  $k_2$  and the maximal concentration of the carbamic acid intermediate. Some carbon dioxide is formed by a pathway that does not involve N-bound carbamic acid. Although the palladium(II) complex containing O-bound urea is clearly evident in the NMR spectra, there are no precedents for nucleophilic attack by water at the carbon atom in it and formation of O-bound carbamate anion. There are precedents for decomposition of O-bound carbamate anion into  $\text{CO}_2$  and  $\text{NH}_3$ , but this reaction is much slower than decomposition of N-bound carbamic acid. We, however, hesitate to implicate O-bound carbamate anion as a possible intermediate in the second pathway for urea decomposition until conversion of O-bound urea into O-bound carbamate anion is demonstrated.

## Catalytic turnover

Since ammonia poisons the palladium(II) catalyst and inhibits decomposition of urea, sequestration of ammonia is expected to promote decomposition. Indeed, Table 7 shows that this reaction is enhanced in the presence of certain metal cations

*Table 7. Effects of 1.0 M Added Metal Cation on the Half-life of Urea Decomposition. Initial Concentrations of Urea and  $[Pd(en)(H_2O)_2]^{2+}$  were 0.3 M and 0.075 M respectively, the Temperature was 333 K, and the Solvent was Acetone- $d_6$ .*

Cation	$\beta_1$	$\beta_2$	$t_{1/2}$ , h
Ag <sup>+</sup>	$2.0 \times 10^3$	$1.4 \times 10^7$	4.10
Cd <sup>2+</sup>	$3.2 \times 10^2$	$2.9 \times 10^4$	18.4
Ni <sup>2+</sup>	$4.7 \times 10^2$	$6.1 \times 10^4$	>26.7
Hg <sup>2+</sup>	$6.0 \times 10^8$	$3.0 \times 10^{16}$	<2.30
Zn <sup>2+</sup>	$1.5 \times 10^2$	$2.7 \times 10^4$	26.7

Stabilities of ammonia complexes follow the order of the binding constants  $Hg^{2+} > Ag^+ > Ni^{2+} > Cd^{2+} > Zn^{2+}$ . The order of half-lives for the reaction is remarkably similar:  $Hg^{2+} \ll Ag^+ < Cd^{2+} < Zn^{2+} < Ni^{2+}$ . The only qualitative discrepancy is the Ni(II) ion, whose activating effect is less than expected from its affinity for ammonia. Carbon-13 NMR spectra show Ni(II) to be the only cation out of these five that bind urea to a detectable extent under the conditions of our experiment.

As Table 8 shows, when ammonia is sequestered by complexation to the Ag(I) cation, the hydrolysis occurs with a turnover - one equivalent of  $[Pd(en)(H_2O)_2]^{2+}$  effects complete hydrolysis of four equivalents of urea. When the concentration of the Ag(I) cation is raised, this reaction becomes rather fast - its half-life is less than 4 h.

## Alcoholysis of Urea Catalyzed by $[Pd(en)(H_2O)_2]^{2+}$ Complex

Binding of Urea to Pd(II) in the Presence of Various Alcohols. As Table 9 shows, presence of different alcohols in similar concentrations does not affect urea coordination. In pure methanol overall binding of urea to Pd(II) is lower due to the competition with the solvent.

*Table 8. Effects of Ag<sup>+</sup> Ion Concentration on the Half-life of Urea Decomposition. Initial Concentration of Urea was 0.3 M, the Temperature was 333 K, and the Solvent was Acetone- $d_6$ .*

$[Ag^+]$ , M	$[Pd(en)(H_2O)_2]^{2+}$ , M	$t_{1/2}$ , h
0.1	0.075	16.5
0.5	0.075	4.60
1.0	0.075	4.10
1.0	0.150	2.50
2.0	0.075	3.30

**Table 9. Equilibrium Constants for Urea Binding to  $[Pd(en)(H_2O)_2]^{2+}$  Complex in the Presence of Various Alcohols in Acetone- $d_6$  at 313 K**

Alcohol	$K_0, M^{-1}$	$K \equiv K_0 \times K_N, M^{-1}$
none	23	1.3
CH <sub>3</sub> OH (3.6M)	30.6	0.63
CH <sub>3</sub> OH (pure, 22.6M)	18.0	0.23
CH <sub>3</sub> CH <sub>2</sub> OH (1.5M)	31.3	0.49
CFH <sub>2</sub> CH <sub>2</sub> OH (1.5M)	34.0	1.91
CF <sub>3</sub> CH <sub>2</sub> OH (1.5M)	41.9	2.3
CH <sub>3</sub> CH <sub>2</sub> CH <sub>2</sub> OH (1.5M)	28.3	0.41
CH <sub>3</sub> CH(OH)CH <sub>3</sub> (1.5M)	25.6	0.40
CH <sub>3</sub> CH(OH)CH <sub>2</sub> CH <sub>3</sub> (1.5M)	26.2	0.44
HOCH <sub>2</sub> CH <sub>2</sub> OH (0.9M)	36.0	0.83
HOCH <sub>2</sub> CH <sub>2</sub> CH <sub>2</sub> OH (0.9M)	32.4	0.92
HOCH <sub>2</sub> CH(OH)CH <sub>2</sub> OH (0.9M)	38.7	0.77

### Determination of the Reaction Rate Law

First order with respect to the concentration of MeOH was observed at low (< 1.0M) concentrations of methanol.

### Dependence on Water Concentration

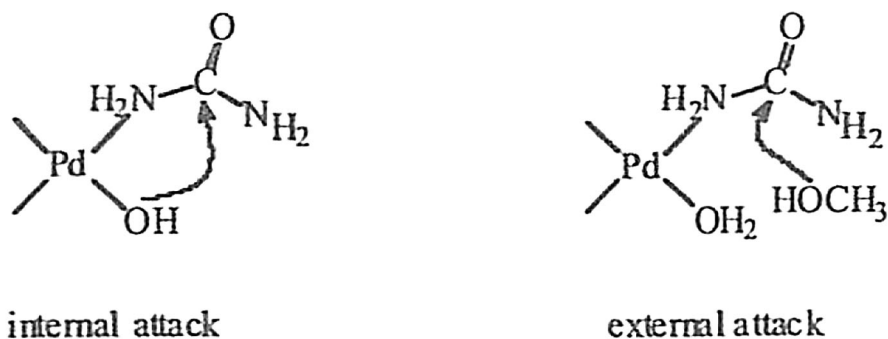
Initial rate of carbamate methyl ester formation slightly increases upon water concentration increases in the range 0.6 M-11.1M.

### Reaction Mechanism

Kinetics and the mechanism of urea methanolysis were studied by <sup>13</sup>CNMR spectroscopy similarly to the urea hydrolysis studies. Due to the low stability of palladium(II) complexes in acetone and methanol, we were unable to dry the reaction mixtures completely. Therefore hydrolysis of N-bound urea by the present water resulted in the formation of palladium(II) bound carbamic acid intermediate IIIa. In pure methanol formation of carbon dioxide was suppressed and intermediate IIIa was entirely converted into carbamate ester NH<sub>2</sub>COOMe.

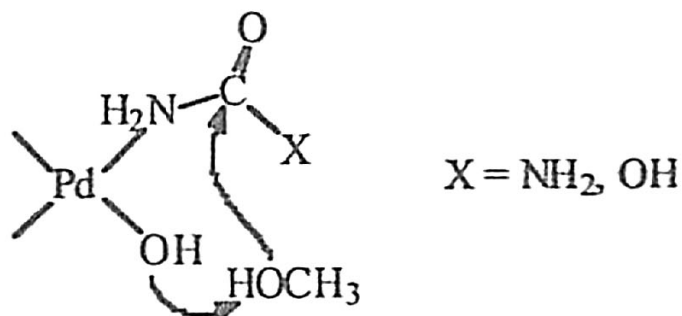
The rate constant for the formation of intermediate IIIa in MeOH is independent on the concentration of water in the range 0.6-11.1 M and is equal to  $0.5 \pm 0.2 \text{ min}^{-1}$ . This independence suggests intramolecular attack of bound water or hydroxide at N-bound urea as in Scheme 9. The fact that the overall methanolysis depends on the concentration of methanol, indicates intermolecular attack of free MeOH at bound urea (Scheme 9).

## Scheme 9



The rate constant for the disappearance of intermediate IIa  $k_{car}$ , and the over all initial rate of carbamate methylester formation grow as the concentration of water increases in the range 0.6-7.4 M. Presence of water affects methanolysis due to the general base catalysis. shown in Scheme 10.

## Scheme 10

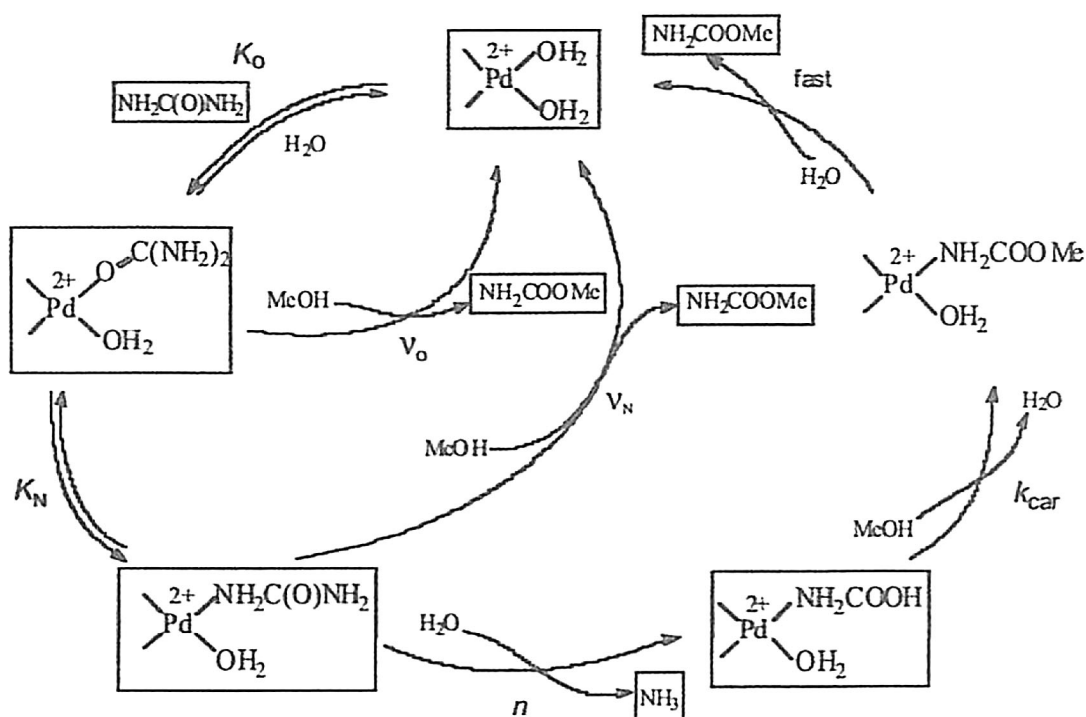


The rate constant for the disappearance of intermediate IIIa  $k_{car}$  and the over all initial rate of carbamate methylester formation decrease as the concentration of added acid increases. The observed rate constant  $k_{car}$  is a composite rate constant for the reactions of  $[\text{Pd}(\text{en})(\text{NH}_2\text{C}(\text{O})\text{NH}_2)(\text{H}_2\text{O})]^{2+}$  and  $[\text{Pd}(\text{en})(\text{NH}_2\text{C}(\text{O})\text{NH}_2)(\text{OH})]^+$  complexes. Experimental data were fitted to eq 8, derived from a scheme analogous to Scheme 6. The individual rate constants for aqua- and hydroxo-complexes are  $(1.37 \pm 0.31) \times 10^{-3} \text{ min}^{-1}$  and  $47.7 \pm 3.1 \text{ min}^{-1}$  respectively. The  $3.4 \times 10^4$  times enhancement in  $[\text{Pd}(\text{en})(\text{NH}_2\text{C}(\text{O})\text{NH}_2)(\text{OH})]^+$  complex suggests general base catalysis by bound hydroxide.

The overall mechanism for methanolysis reaction is presented on Scheme 11.



Scheme 11



### Alcoholysis Reactions with Alcohols other than Methanol

Almost in all cases the ultimate products were the carbamate ester of the respective alcohol and ammonia. The  $^{13}\text{C}$  NMR chemical shifts of various carbamate esters and the respective observed rate constants for the ester formation are shown in Tables 10, 11, and 12.

**Table 10. Carbon-13 Chemical Shifts and the Respective Observed Rate Constants for the Formation of Carbamate Esters  $\text{NH}_2\text{COOR}$  ( $R = \text{alkyl}$ ) in Acetone- $\text{d}_6$  at 313 K.**

R	Chemical Shift, ppm	$k_{\text{obs}} \times 10^4, \text{min}^{-1}$
$\text{CH}_3-$	158.38	$5.12 \pm 0.29$
$\text{CH}_3\text{CH}_2-$	158.51	$1.46 \pm 0.12$
$\text{CH}_3\text{CH}_2\text{CH}_2-$	158.47	$1.68 \pm 0.12$
$\text{CH}_3(\text{CH}_3)\text{CH}-$	157.94	$0.62 \pm 0.07$
$\text{CH}_3\text{CH}_2(\text{CH}_3)\text{CH}-$	158.53	$0.93 \pm 0.13$
$(\text{CH}_3)_3\text{C}-$	157.56	$0.23 \pm 0.01$
$(\text{CH}_3)_2\text{CHCH}_2\text{CH}_2-$	158.47	$2.3 \pm 0.16$

As results in Table 10 show, carbamate ester formation is affected by the bulkiness of the attacking alcohol. Thus, methanol and primary alcohols generally are more reactive than secondary and

tertiary alcohols. Reaction is not affected by the size of the attacking alcohol - ethanol, propanol, and isoamylalcohol give similar rate constants for urea alcoholysis.

**Table 11. Carbon-13 Chemical Shifts and the Respective Observed Rate Constants for the Formation of Carbamate Esters  $NH_2COOR$  ( $R = \text{fluoroalkyl}$ ) in Acetone- $d_6$  at 313 K.**

R	Chemical Shift, ppm	pKa	$k_{obs} \times 10^4, \text{min}^{-1}$
$CH_3CH_2-$	158.51	15.93	$1.46 \pm 0.18$
$CFH_2CH_2-$	157.87	$\approx 14.3$	$1.08 \pm 0.06$
$CF_3CH_2-$	158.12	12.39	$0.18 \pm 0.01$

Alcoholysis of palladium(II)-bound urea is strongly affected by the nucleophilicity of the attacking alcohol, as shown in Table 11. Fluoro substituents in ethanol derivatives decrease nucleophilicity of the hydroxyl oxygen atom as reflected by the decreasing  $pK_a$  values, and the nucleophilic attack of an alcohol is slowed down. Tertiary butanol has  $pK_a$  of  $> 19$  and is very nucleophilic. High nucleophilicity of this alcohol, however, does not offset the steric bulkiness, and the alcoholysis is slow.

We also studied diol alcoholysis, hoping to see an intramolecular reaction between coordinated urea and coordinated diol within the coordination sphere of palladium(II). However, there are not any indications at the intramolecular attack of a coordinated alcohol. The higher reactivity of primary diols in Table 12 relative to the monoalcohols in Table 10 is attributed to the presence of two primary hydroxyl groups per diol molecule. Thus, the effective concentration of a hydroxyl group in a diol is twice as high as in a monoalcohol. Lower diols are somewhat less reactive due to the reduced nucleophilicity of the hydroxyl oxygen atom. For instance,  $pK_a$  of ethylene glycol is 13.27, lower than that one for ethanol. In reactions with asymmetrical diols containing primary and secondary hydroxyl groups the primary ester is always formed. The rate of the ester formation is similar to the rate of an analogous primary monoalcohol. *Cis*-1,2-cyclohexanediol does not react to an appreciable extent, probably, due to the steric bulk and frigidness of hydroxyl groups. Glycerol gives two products - the primary alcohol ester and the secondary alcohol ester. Due to the low nucleophilicity of glycerol ( $pK_a = 14.4$ ) the rates of their formation are relatively low. The primary ester is being formed approximately 50 % faster than the secondary one (Table 12). Thus, per hydroxyl group the reactivities of primary and secondary hydroxyl groups in glycerol are similar.

**Table 12. Carbon-13 Chemical Shifts, Number of Carbon Atoms between Hydroxyl Groups (Linkage) in a Parent Alcohol, and the Respective Observed Rate Constants for the Formation of Carbamic Esters  $NH_2COOR$  ( $R = \text{hydroxyalkyl}$ ) in Acetone- $d_6$  at 313 K.**

R	Chemical Shift, ppm	Linkage, n	$k_{obs} \times 10^4, \text{min}^{-1}$
HOCH <sub>2</sub> CH <sub>2</sub> -	158.52	2	2.01 ± 0.13
HOCH <sub>2</sub> (CH <sub>3</sub> )CH-	158.35	2	0.97 ± 0.06
<i>cis</i> -1,2cyclohexanediol	none	2	< 9 × 10 <sup>-3</sup>
HOCH <sub>2</sub> CH <sub>2</sub> CH <sub>2</sub> -	158.62	3	3.22 ± 0.10
HOCH <sub>2</sub> CH <sub>2</sub> CH <sub>2</sub> CH <sub>2</sub> -	158.62	4	3.11 ± 0.12
HOCH(CH <sub>3</sub> )CH <sub>2</sub> CH <sub>2</sub> CH <sub>2</sub> -	157.92	4	2.22 ± 0.20
HOCH <sub>2</sub> CH <sub>2</sub> CH <sub>2</sub> CH <sub>2</sub> CH <sub>2</sub> -	158.50	5	2.62 ± 0.20
HOCH <sub>2</sub> CH <sub>2</sub> CH <sub>2</sub> CH <sub>2</sub> CH <sub>2</sub> CH <sub>2</sub> -	158.50	6	4.08 ± 0.10
HOCH <sub>2</sub> (OH)CHCH <sub>2</sub> -	158.67	1	0.61 ± 0.04
(HOCH <sub>2</sub> ) <sub>2</sub> CH-	158.05	1	0.46 ± 0.02

Despite their low nucleophilicity phenol derivatives form esters upon also hydrolysis similarly to alkyl alcohols. The phenyl esters in our system, however, are unstable toward hydrolysis, and are hydrolyzed to carbamic acid and a parent alcohol. Formation and disappearance of two esters was followed by <sup>13</sup>C NMR spectroscopy and the resulted rate constants are shown in Table 13. As expected, less nucleophilic *p*-nitrophenol is slower in nucleophilic attack at electrophilic carbon of palladium(II)-bound urea or carbamic acid than more nucleophilic *p*-methoxyphenol. Also carbamate *p*-nitrophenol ester decomposes faster due to better stabilization of the leaving group by the highly electronegative nitro group.

The phenyl ester hydrolysis was studied in some details with a commercially available carbamate phenyl ester. In the absence of palladium complex in acidic wet acetone (0.1M HClO<sub>4</sub>) at 318 K carbamate phenyl ester is stable and does not hydrolyze even after prolonged incubation. However, upon addition of 0.3 M *cis*-[Pd(en)(H<sub>2</sub>O)<sub>2</sub>]<sup>2+</sup> the ester hydrolyzed into phenol and carbamic acid with an estimated rate constant of 4 × 10<sup>-3</sup> min<sup>-1</sup>. Carbamic acid was not detected due to its fast decomposition to ammonia and carbon dioxide. Final products phenol and carbon dioxide were observed by <sup>13</sup>C NMR spectroscopy. The observed rate constant for phenol carbamate decomposition is similar to rate constants of N-bound carbamic acid disappearance, discussed in the previous section. Thus, palladium(II) also catalyzes the decomposition of carbamate phenyl esters, which will be addressed elsewhere.

**Table 13. Carbon-13 Chemical Shifts and the Respective Observed Rate Constants for the Formation and the Disappearance of Carbamic Esters  $NH_2COOR$  ( $R = \text{phenyl derivative}$ ) in Acetone- $d_6$  at 313 K.**

R	Chemical Shift, ppm	pKa	$k_f \times 10^3, \text{min}^{-1}$	$k_d \times 10^3, \text{min}^{-1}$
pCH <sub>3</sub> O-C <sub>6</sub> H <sub>4</sub> -	158.56	10.20	5.89 ± 1.63	5.18 ± 0.29
pNO <sub>2</sub> -C <sub>6</sub> H <sub>4</sub> -	158.52	7.16	4.71 ± 0.82	16.3 ± 0.9

## CONCLUSION

The uncatalyzed hydration of nitriles has a half-life longer than ca.  $1 \times 10^6$  h. Palladium(II) aqua complexes accelerate these reactions approximately 10<sup>6</sup>-fold under these conditions. Since the vinyl group resembles the CH<sub>2</sub>Cl and CHCl<sub>2</sub> groups in its electron-withdrawing ability, the results of this study may be relevant to hydration of acrylonitrile. Acrylamide, the product of this last reaction, is an important industrial chemical.

We have shown the first examples of catalytic decomposition of urea by hydrolysis and alcoholysis. These reactions are relatively fast (10<sup>5</sup>-fold enhancement relative to the uncatalyzed decomposition of urea to cyanate and ammonia) and clean.

We are now working on Pd(II) and Pt(II)-catalyzed hydrolysis of peptide bonds in tryptophan-containing dipeptides.

### References

- (1) Natalia V. Kaminskaia and Nenad M. Kosti. "Nitrile Hydration Catalyzed by Palladium(II) Complexes", *J. Chem. Soc., Dalton Trans.*, 1996, pp3677- 3686; and all the references cited therein.
- (2) Natalia V. Kaminskaia and Nenad M. Kosti. "Kinetics and Mechanism of Urea Hydrolysis Catalyzed by Palladium(II) Complexes", submitted for publication to *Inorg. Chem.*; and all the references cited therein.
- (3) Natalia V. Kaminskaia and Nenad M. Kosti. "Kinetics and Mechanism of Urea Alcoholysis Catalyzed by Palladium(II) Complexes", manuscript in preparation, and all the references cited therein.





# THE USE OF DESIGN OF EXPERIMENTATION SOFTWARE IN APPLIED COPPER GOLD ORE FLOTATION TESTING

**Dr. Corby G. Anderson, PE**

Director, Kroll Institute for Extractive Metallurgy  
Mining Engineering Department  
Colorado School of Mines  
Golden, Colorado 80401  
E-Mail: [cganders@mines.edu](mailto:cganders@mines.edu)

**Mr. Todd S. Fayram, QP**

Thornton Building  
65 East Broadway Street  
Suite 301  
Butte, Montana 59701  
E-Mail: [fayramtodd@msn.com](mailto:fayramtodd@msn.com)

**Dr. Larry G. Twidwell**

Emeritus Professor  
Center for Advanced Mineral and  
Metallurgical Processing  
Department of Metallurgical and  
Materials Engineering  
Montana Technological University  
Butte, Montana  
E-Mail: [ltwidwell@mtech.edu](mailto:ltwidwell@mtech.edu)

[< Return to Index](#)

## ABSTRACT

The successful application of flotation is now 100 years old. However, in a practical sense, it remains predominantly an art rather than a quantifiable science. Moreover, the laboratory testing, interpretation and application of the technology can still be tedious, time consuming and costly. This paper outlines the use of statistical design of experimentation for rapid optimization of gold bearing copper ore flotation testing with limited sample utilization. This results in less costly required testing, a more thorough understanding of the results and the ability to simultaneously optimize several variables and outcomes at once.

## INTRODUCTION

While flotation technology is now over 100 years old, the testing, interpretation and application of lab results can be tedious, costly and time consuming requiring extensive sample collection and preparation. In addition, applied flotation remains more of an art than a quantifiable science. This paper will elucidate the application of STAT-EASE Design-Expert software<sup>(1)</sup> to minimize required laboratory flotation testing while rapidly optimizing multiple results and outcomes in a statistically valid manner. The STAT-EASE program is based on proven design of experiment fundamentals. In this paper, the real world application of this methodology to a gold bearing copper ore will be illustrated.

## APPLICATION TO A COPPER AND GOLD ORE

Based on previous work along with current legal issues concerning limiting cyanide use in Montana, flotation with gravity concentration was the process chosen to develop the Elkhorn copper gold ore deposit. A review of previous scoping level test work revealed significant results on optimal collector and frother usage, grind time, and float time were missing on Elkhorn ore deposits such as Mt. Hagen.

Because of client budget constraints and a limited quantity of representative core samples material available, STAT-EASE statistical software was used to minimize the number of flotation experiments required to identify a statistical representative experimental set. Design of Experimentation is not new but with the advent of advanced computer programming, it has become more robust and approachable<sup>(2-13)</sup>. This commercially licensed program based on fundamentals of design of experiments provides highly efficient:

1. Two-level factorial screening studies so that the vital factors which affect a process can be identified.
2. Response surface methods to find ideal process settings and achieve optimal performance.
3. Mixture design techniques to discover optimal formulations.

Among other features, the program offers rotatable 3D plots for visualization of response surfaces. Again, the key feature is the ability to set up statistically valid design of experiment matrices which allow a minimum amount of experimentation to take place. This saves time and money allowing robust flotation testing and optimization to occur with a minimal amount of ore sample used.

## ELKHORN MT. HAGEN ORE COMPOSITE DEVELOPMENT

The Mt. Hagen ore composite was collected from different drill holes going across the deposit from north to south and top to bottom. No special considerations were given to the sample other than ensuring that the sample was taken from an ore run and the appropriate interval assigned. Approximately twelve inches of sample were taken from the appropriate interval and recorded. No special considerations were made for oxide, sulfide, or waste.

Upon arrival at the Center for Advanced Mineral and Metallurgical Processing (CAMP) laboratory, all samples were crushed to minus 3/8 inches and thoroughly mixed. A sample for assaying was split from the material using a Jones Splitter. This composite was assayed for gold, silver, and copper. The gold assays were completed using metallic screen fraction analysis at 100 mesh to identify any coarse gold. Multi-element ICP and X-ray diffraction analysis were also completed. Table 1 identifies the composite ore average analysis.

**TABLE 1**  
**Elkhorn Goldfields – Mt. Hagen Ore**  
**Weighted Average Composite**

COMPOSITE		23-Sep			
WEIGHTED AVERAGE					
		AU, OZ/TN	CU, %		
COMPOSITE ASSAY		0.204	0.40		
HOLE	WEIGHT	AU GRADE	CU GRADE	AU WEIGHT	CU WEIGHT
CEG04-12	21.2	0.180	0.55	3.825	11.58
CEG04-18	9.6	0.151	0.02	1.452	0.23
CEG04-11	25.3	0.260	0.39	6.589	9.82
CEG04-10	10.5	0.133	0.40	1.394	4.15
CEG04-24	50.3	0.210	0.41	10.544	20.85
		-	-	-	-
		-	-	-	-
		-	-	-	-
		-	-	-	-
<b>TOTAL</b>	116.9	0.204	0.40	23.80	46.63

## ELKHORN MT HAGEN ORE FLOTATION TESTING

Flotation testing was guided and completed using STAT-EASE diagnostic software. The software requires the development of a statistically valid design of the experiment matrix using several variables and outcomes. In the case of the Mt. Hagen deposit testing, the variables used were grind time, pH, flotation time, and the addition or not of sodium sulfide. In addition, the testing was used to simultaneously identify four outcomes: gold and copper grade and recovery.

The grind time variable was developed to review the effects of grinding and liberation at a base size of 150 mesh. A shorter grind time would add capacity and lower costs. A longer grind time will better liberate the ore and typically improve recovery. Based on previous testing, a twenty-five minute grind time gave an 80% passing 150 mesh ore size. The grinding pulp density was 50% solids by weight in a laboratory ball mill.

Sodium sulfide was used as a sulfidizing agent variable to promote flotation of oxidized copper and gold bearing minerals. Testing was completed to identify a response based on use or no use.

A variable pH of 8.5 or 10.5 was chosen to both promote and depress pyrite and pyrrhotite. At pH 8.5, pyrite and pyrrhotite tend to be promoted. At pH 10.5, both pyrite and pyrrhotite are effectively depressed. This difference in pH was used to assist in identifying the source of the gold and how to best optimize the gold recovery.

Flotation testing was completed with a Denver Laboratory flotation machine. The density of the flotation pulp was a constant 40% solids by weight. Each ore charge for the testing was 1,000 grams. Variable float times were used to optimize the float machine size requirements.

The collector chosen for this project was Cytec Aerofloat 3477. It was used at a constant dosage. This collector is a common dithiophosphate based collector. It was chosen because of its selectivity towards gold and copper and its positive results in previous testing of other Elkhorn ore deposits.

The frother chosen for the testing was pine oil. It was also used at a constant dosage. Pine oil was chosen in other Elkhorn ore deposit flotation testing because it minimized effects of specific minerals with the deposit.

With the development of the pertinent variables and measurable outcomes, several choices of matrix sizes and sample numbers can be developed. Accordingly, a higher number of tests can improve the statistical reliability of the data being developed. In the case of Mt. Hagen ore testing, four variables with four measurable outcomes were identified. The total number of samples and the size of the matrix required two to the power of four or sixteen total possible tests. The user of STAT-EASE can select a total, half, or quarter of this testing matrix to identify a statistically valid outcome.

For this real world project, there were significant restraints on both budget and sample quantity. A one half STAT-EASE matrix was chosen containing eight tests that would statistically validate the

testing of the sixteen total possible combinations. STAT-EASE software also can add midpoints into the data testing. Although this adds to the size of the sample matrix, midpoint testing adds extra results which can improve the outcome. In the Mt. Hagen ore testing two replicate mid-point tests were conducted based on the STAT-EASE testing matrix. Thus, a total of 10 tests were utilized as follows:

**TABLE 2**  
**STAT-EASE One Quarter Design of Experiment Matrix**

<u>TEST</u>	<u>GRIND TIME, MIN</u>	<u>SULFIDE DOSAGE, GRAMS</u>	<u>pH</u>	<u>FLOAT TIME</u>
1	30	1.0	8.5	15
2	20	0.0	8.5	15
3	25	0.5	9.5	17.5
4	30	1.0	10.5	20
5	30	0.0	10.5	15
6	25	0.5	9.5	17.5
7	20	1.0	10.5	15
8	20	0.0	10.5	20
9	20	1.0	8.5	20
10	30	0.0	8.5	20

This represents the eight tests determined by the software along with two midpoint replicate tests (i.e., test numbers 3 and 6 above).

## RESULTS

Upon completing the initial ten diagnostic flotation tests based on the above STAT-EASE matrix, the test results were illustrated in Table 3 and Table 4.

**TABLE 3**  
**Elkhorn Goldfields – Mt. Hagen**  
**STAT-EASE Matrix Assay Results**

Sample #	ASSAYS					
	CONCENTRATE			TAILS		
	Au (oz/t)	Ag (oz/t)	Cu (%)	Au (oz/t)	Ag (oz/t)	Cu (%)
1	0.608	0.18	0.87	0.056	0.14	0.026
2	0.474	0.38	0.66	0.182	0.14	0.035
3	0.606	0.58	0.61	0.052	0.14	0.024
4	0.592	0.48	0.73	0.068	0.24	0.026
5	0.524	0.54	0.71	0.068	0.24	0.027
6	0.452	0.32	0.46	0.064	0.14	0.019
7	0.618	1.40	0.69	0.062	0.18	0.020
8	0.918	1.34	1.25	0.124	0.08	0.051
9	0.508	0.36	0.60	0.088	0.10	0.059
10	0.416	0.50	0.46	0.102	0.12	0.026



**TABLE 4**  
**Elkhorn Goldfields – Mt. Hagen**  
**STAT-EASE Matrix Recovery Results**

Sample #	RECOVERIES TO CONCENTRATE		
	Au (%)	Ag (%)	Cu (%)
1	80.8%	33.32%	92.9%
2	45.1%	46.12%	85.6%
3	78.7%	56.82%	89.0%
4	74.2%	39.83%	90.3%
5	75.3%	47.13%	91.2%
6	81.4%	58.54%	93.7%
7	77.2%	72.52%	92.1%
8	47.5%	67.21%	75.0%
9	69.9%	59.20%	80.4%
10	68.5%	68.96%	90.4%

The above recovery data was entered into the STAT-EASE statistical software and modeled to optimize the gold recovery flotation requirements for the MT. Hagen deposit. STAT-EASE gives several options to transform the data into a statistical probability plot that allows for the best statistical presentation of each outcome. Figure 1 is an example of the half normal plot for gold recovery of the Mt. Hagen deposit.

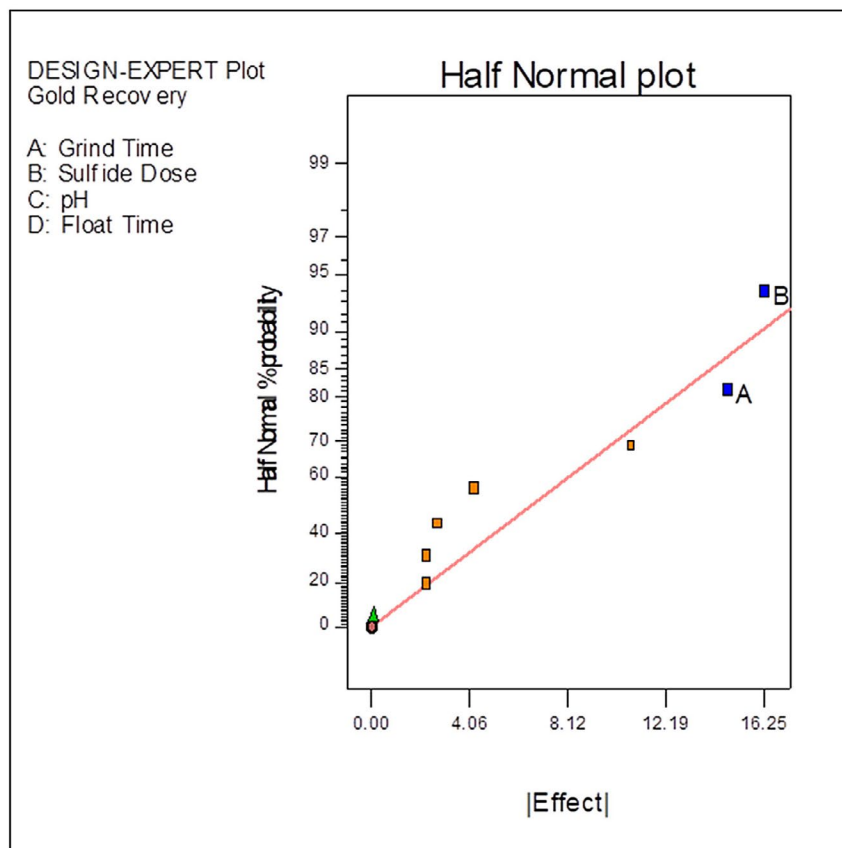


**Figure 1 - Example STAT-EASE Half Normal Plot For Gold Recovery**

Upon finding a graphical transformation to fit the variables with the outcomes, STATEASE allows you to add and remove effects generated from the variables to statistically optimize the data. Based on the reviewing of the statistical outcome of gold recovery, the probability that the gold recovery would be maximized using this data was 98.7%. A review was completed on all the outcomes (gold and copper recovery and gold and copper grade) and all outcomes were found to have probabilities over 90%. Based on this data no further testing was completed on the Mt. Hagen deposit. In reviewing the STAT-EASE variable data, plots such as Figure 2 and Figure 3 can be created.

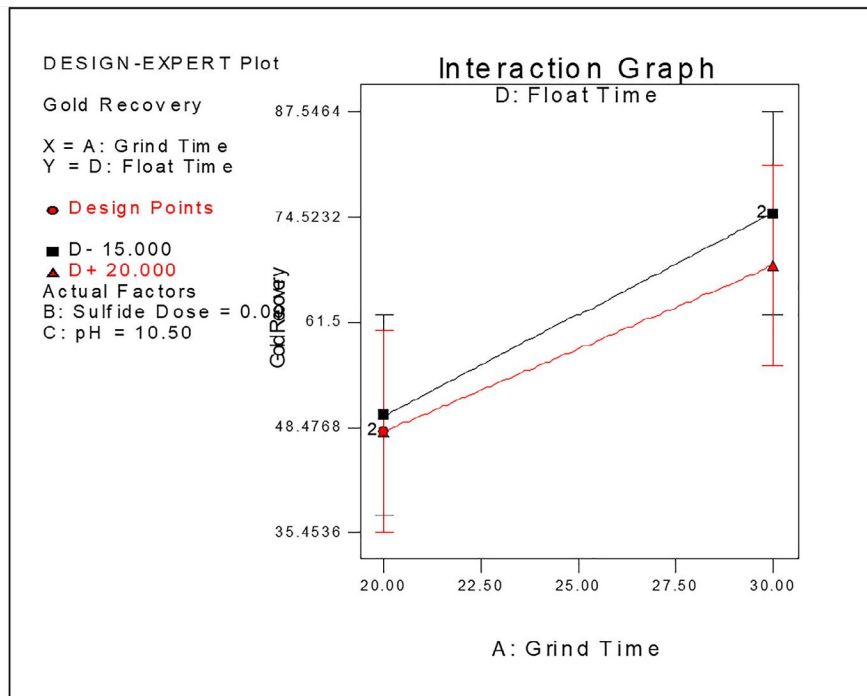


Figure 2 - Variable Interaction Graph for Gold Recovery

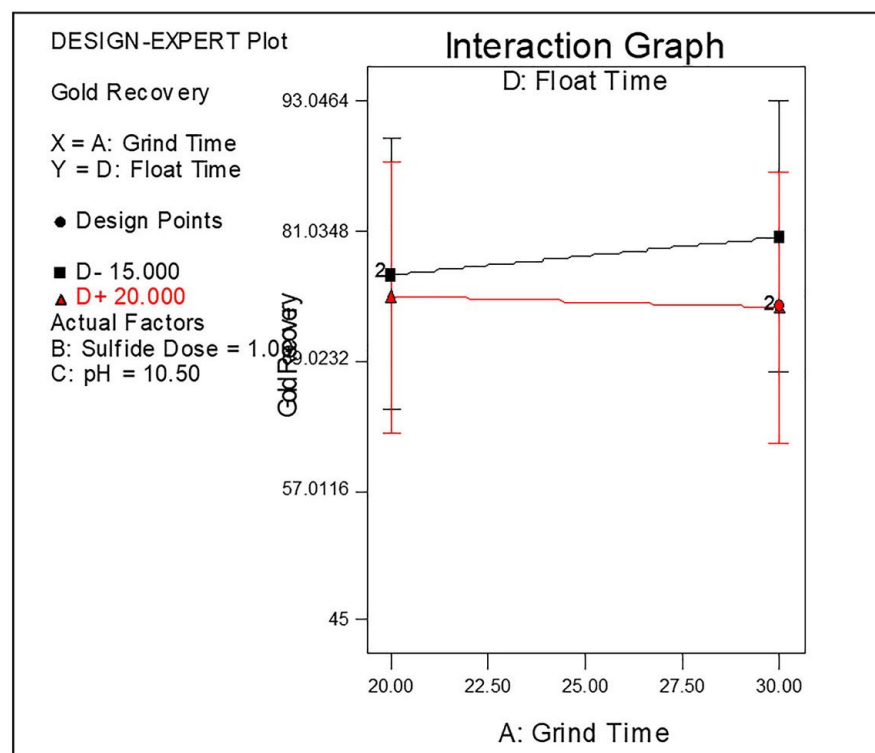


Figure 3 - Variable Interaction Graph for Gold Recovery

The above noted interaction graphs plot grind time against recovery with float time, pH, and sulfide dose as variables. As noted on the first graph, the sulfide dose is zero and on the second graph the sulfide dose is 1.00. Based on a review of the graph, the expected gold recovery would be identified as shown in Table 5.

**TABLE 5**  
**Statistical Model Predicted Gold Recoveries**

<b>VARIABLE</b>	<b>GRIND TIME, MINS</b>	<b>SULFIDE DOSE, GRAMS</b>	<b>RECOVERY, %</b>
GRIND TIME	20.00	0.00	48.5
GRIND TIME	20.00	1.00	78.0
GRIND TIME	30.00	0.00	74.5
GRIND TIME	30.00	1.00	78.0

By reviewing the above data, sulfide dose is extremely important for low grind times in that recovery is improved approximately 30%. Sulfide dose is not very important for higher grind times and recovery is only improved approximately 3.5%. In the case of a small ball mill with low grind times, sulfide dose optimizes recovery. Sulfide dose would not be important in the case where excess grinding capacity exists. All the variables can be manipulated together using various graphing techniques to optimize the specific flotation requirements for the specific orebody. In the case of the Mt. Hagen deposit, Table 6 identifies the rougher flotation variables that would be expected to maximize the recoveries in Mt. Hagen ore.

**TABLE 6**  
**Mt. Hagen Optimal Rougher Flotation Parameters**

<b>FACTOR</b>	<b>PARAMETER</b>
GRIND TIME	30 MINS
FLOAT TIME	15 TO 17.5 MINS
pH	10.5
SULFIDE ADDITION	YES

In summary, in real world situations where limited representative testing material is available or cost and time are significant issues, proper design of experimentation using STAT-EASE can identify statistically valid subsets and allow for rapid optimization and design.

## SUMMARY

This paper has illustrated the successful use of statistically valid design of experiments using STAT-EASE software. This methodology provides a low cost and rapid process for real world laboratory flotation testing, optimization, application and flow sheet development, particularly when minimal financial resources, time and representative samples are a constraint.

## REFERENCES

1. STAT-EASE Design-Expert Reference Manual, STAT-EASE Corporation, Minneapolis, Minnesota, 2002
2. Neter, J., Applied Linear Statistical Models: Regression, Analysis of Variance, and Experimental Designs, Published 1990, Irwin, Homewood, Illinois
3. Box, G.E.P., Box on Quality and Discovery: with Design, Control, and Robustness, Published 2000, Wiley, New York
4. Montgomery, D. C, Design and Analysis of Experiments, 5th Ed., ISBN: 0-471-31649-0, Published 2001, John Wiley and Sons
5. Lorenzen, T. J. and Anderson, V. L., Design of Experiments: A No-Name Approach, ISBN: 0-8247-9077-4, Published 1993, M. Dekker, New York
6. Kempthorne, O., The Design and Analysis of Experiments, Published 1975, Robert E. Krieger Publishing Co., Huntington, New York
7. Hinkelmann, K. and Kempthorne, O. (Editor), Design and Analysis of Experiments: Introduction to Experimental Design, ISBN: 0471551783, Published March 1994, John Wiley & Sons
8. Anderson, M. J. and Whitcomb, P. J., DOE Simplified: Practical Tools for Effective Experimentation, ISBN: J-56327-225-3, Published May 2000, Productivity, Inc.
9. Box, G.E.P., and Draper, N.R. Empirical Model Building and Response Surfaces ISBN: 0-471-81033-9, Published January 1987, Wiley-Interscience
10. Cochran, W.G., Experimental Designs, Published 1957, Wiley, New York

11. Wu, C.J.F. and Hamada, M. Experiments: Planning, Analysis, and Parameter Design Optimization, ISBN: 0-471-25511-4, Published 2000, Wiley, New York
12. Cornell, J., Experiments with Mixtures: Designs, Models, and the Analysis of Mixture Data, 2nd Ed., ISBN: 0-471-52221-X, Published April 1990, John Wiley and Sons
13. Pazman, A. Foundations of Optimum Experimental Design, Published 1986, D. Reidel, Boston



# FIRE ASSAY TIN COLLECTION

A PRACTICAL TOOL FOR  
ASSAYING COMPLEX  
REFINERY SWEEPS



John Whitney, Chemist  
Dana Evans, Chief Assayer

Gannon & Scott, Inc.  
Cranston, RI

[< Return to Index](#)

## ABSTRACT

Iridium, rhodium, and ruthenium melted with excess tin are soluble in HCl – H<sub>2</sub>O<sub>2</sub> or HCl – HNO<sub>3</sub> and are conveniently determined by AA or ICP. The same is true for platinum, palladium, gold and silver. Methods of determining the precious metals after tin collection supplement traditional lead collection methods and allow the refinery assay laboratory to determine iridium, rhodium and ruthenium and to determine the other precious metals in their presence. Recoveries of .5 to 100 mg of each precious metal carried through tin collection, dissolution, and measurement are evaluated. Each step in the process is described.

## INTRODUCTION

Samples are fused with fire assay tin flux. Tin buttons are recovered and melted in graphite crucibles. Molten tin/precious metal alloy is poured into water to make homogeneous shot. Tin and precious metal are dissolved together. Any residue of precious metal (Ir and Ru) is separated on a microfiber filter. Filtrate and washings are diluted to 500 mL. Filter and residue are decomposed by sodium peroxide, sodium carbonate fusion. Determinations are done by AA or ICP. Calibration curves are established using matched matrix standards and blank.

## COLLECT PRECIOUS METALS IN A 20G TIN BUTTON

Mix a one or two gram sample with 147 grams of tin fusion flux. Transfer to a 40 gram assay crucible and fuse. Starting at 750°C. (1400°F), raise temperature over 40 minutes to 1100°C (2000°F). Hold at 1100° for 20 minutes. Remove crucibles from assay furnace. Allow tin button and slag to solidify and cool. Break crucible and slag away from tin button. Clean the button thoroughly. The button should weigh 20 ± 2 g. Fuse a blank flux charge (147 g tin flux) with each set of samples to provide tin for matched matrix standards and blanks.

## Tin fusion flux

SnO<sub>2</sub> - 30 g

Flour - 30 g

Anhydrous Borax - 20 g

Silica - 7 g

Na<sub>2</sub>CO<sub>3</sub> - 60 g

## RE-MELT AND SHOT THE TIN BUTTON

Re-melt each tin button in a covered 33cc graphite fusion crucible. The graphite crucible (Aesar 14750) is placed inside a 30 g assay crucible and covered with a 3 inch scorifier. The assembly is placed in an assay furnace at 900° C for 10-15 minutes then removed and set on a refractory block. The molten tin is immediately poured into 2 gallons of water at least 12" deep. The tin shot is recovered and transferred to a 1000 mL beaker.

Re-melting and shotting are required because precious metals in the shotted tin are more homogeneously distributed and easier to dissolve than precious metal/tin phases that have segregated during slow solidification of the tin button.

## DISSOLVE TIN / PRECIOUS METAL SHOT

Dissolve tin with 150 mL of HCl (conc.). Warm to 80° C. Add 50 ml of water, add a stir bar and stir over a magnetic stirrer. From a pipet, slowly and cautiously add 15 ml of HNO<sub>3</sub> (conc.). CAUTION: THIS IS AN EXOTHERMIC (POTENTIALLY VIOLENT) REACTION as 20 grams of Sn<sup>+2</sup> are oxidized to Sn<sup>+4</sup>, aqua regia forms, and precious metals dissolve. Heat near boiling for 5 to 10 minutes. When the reaction is complete, there will be color change. Precious metals will dissolve and the presence of aqua regia is apparent.

Remove from heat, add 50 mL of water and allow solids to settle.

## RECOVER INSOLUBLES AND PREPARE STOCK SOLUTIONS OF SOLUBLES

Decant most of the solution into a 500 mL volumetric flask. Filter insolubles, (a heavy fine residue), on a 21mm 934 AH Whatman filter fitted to a 25 ml Coors #60148 porcelain, perforated, gooch crucible. The filter is supported over a vacuum filter flask. Use gentle vacuum assist. Transfer insolubles to filter with 10% HCl. Combine filtrate and washings with the decanted solution in a 500 mL volumetric flask. Dilute the stock solution of the soluble fraction to 500 mL with 10% HCl. The stock solution is 40 g/L tin and 30% HCl.

## DETERMINE IRIDIUM, RHODIUM, AND RUTHENIUM FROM THE AQUA REGIA INSOLUBLE

Prepare a 400 mL beaker containing 100 mL of water to receive each crucible. Fuse each filter and a blank filter in a zirconium crucible with 2 g of sodium peroxide and 1 g of sodium carbonate. Heat over a Meker burner until salts melt and the filter dissolves. Continue heating until crucible and molten salts are cherry red. Allow fusion to cool until salts solidify, then plunge into the water in the beaker. When the salt disintegrates, lift, rinse and remove the crucible. Add 50 mL of HCl (conc) to the beaker. Transfer sample solutions to 250 mL volumetric flasks and the blank to a 200 mL volumetric flask.

Samples (250 mL flasks) are 16 g/L NaCl, 20% HCl and are ready for ICP.

The stock blank solution (200 mL flask) is 20 g/L NaCl and 25% HCl.

Prepare an ICP matrix blank by diluting 80 mL of the stock blank to 100 mL with water.

Prepare an ICP standard (30 mg/L) Ir, Rh, or Ru by adding 3 mg of Ir, Rh, and Ru to 80 mL of stock blank solution and diluting to 100 mL with water.

## ANALYZE STOCK SOLUTION OF SOLUBLE PRECIOUS METALS

The matrix of stock solutions of samples and blank (all 500 mL) is 40 g/L tin, 30% HCl. We determine Au, Pt, Pd, Ag and Rh by AA. To determine up to 50 mg of Au, Pt, or Pd, 15 mg Ag or 20 mg Rh transfer a 50 mL aliquot to a 100 mL volumetric flask, add 10 mL of 10% La in 50% HCl and dilute to 100 mL with 10% HCl. The matrix is 20 g/L tin, 1% La and 25% HCl.

To prepare a midrange calibration standard, transfer to a 100 mL volumetric flask; 50 mL stock blank solution, 10 mL of 10% La in 50% HCl, 3 mg Au, Pt, Pd; 1 mg Ag and Rh. Dilute to 100 mL with 10% HCl. This midrange or reslope standard is 30 mg/L Au, Pt, Pd; 10 mg/L Ag and Rh, 20 g/L Tin, 1% La, and 26% HCl. Prepare low standard, high standard and blank as needed.

To determine up to 40 mg Ag, 50 mg Rh, and 125 mg Au, Pt, Pd, transfer 20 mL aliquots of samples and 20 mL aliquots of blank to 100 mL volumetric flasks. Add 10 mL of 10% La and 20 mL HCl (1+1). Prepare blank, mid range standard and additional standards as needed. Dilute to 100 mL with 10% HCl. This matrix is 8 g/L tin, 1% La, 25% HCl.

## DETERMINE IR AND RU BY ICP

To determine up to 50 mg Ir or Ru, transfer a 25 mL aliquot of the stock solution to a 100 mL volumetric flask. Add 15 mL of 50% HCl and dilute to 100 mL with 10% HCl. The matrix is 10 g/l tin, 20% HCl.

Matrix Blank: 25 mL stock blank, 15 mL of 50% HCl, dilute to 100 mL with 10% HCl.

High Standard (30 mg/L Ir, Ru): 25 ml stock blank, 3 mg Ir, 3 mg Ru, 12 mL of 50% HCl. Dilute to 100 mL with 10% HCl.

### Recoveries of 20 mg of Each Precious Metal

<u>Test Set</u>	<u>Rh</u>	<u>Au</u>	<u>Ag</u>
#1	19.64	19.65	18.86
	19.86	19.74	18.78
#2	<u>Ru</u>	<u>Pd</u>	<u>Ag</u>
	18.97	19.36	19.40
	19.89	19.48	19.12
#3	<u>Ir</u>	<u>Pt</u>	<u>Au</u>
	18.70	18.44	18.52
	19.34	18.75	18.88

Aliquots of standard solutions, 1 mg/mL or 10 mg/mL were pipetted on to tin flux contained in a plastic sandwich bag and mixed by kneading. Test samples and flux were placed in 40 g assay crucibles, dried, and assayed.

AA measurements were done in a matrix 10 g/L tin, 1% La, 25% HCl.

ICP measurements – 10 g/L tin, 25% HCl.

### Recoveries of 2-100 mg of Each Precious Metal

	<u>Ir</u>	<u>Rh</u>	<u>Ru</u>	<u>Au</u>	<u>Pt</u>	<u>Pd</u>
4138	5.00	50.00	2.00	50.00		2.00
	5.83	49.25	2.15	49.15		2.02
4139	2.00		50.00		2.00	50.00
	2.11		48.85		1.66	47.05
4140	50.00	2.00		2.00	50.00	
	50.05	1.91		1.69	51.99	

**Table 1**

	<u>Total Ir</u>	<u>Rh</u>	<u>Total Ru</u>	<u>Au</u>	<u>Pt</u>	<u>Pd</u>	<u>Insoluble from microfiber filter</u>
4586		5.00 4.68	50.00 46.62			50.00 48.44	0.8 mg Ru
4588	50.00 46.51		5.00 4.99	5.00 4.89	50.00 47.99	5.00 5.08	0.16 mg Ir
4589	5.00 5.05	50.00 48.85		50.00 48.98	5.00 4.88		0 mg Rh
4648	5.00 5.56	50.00 48.90		50.00 49.28	5.00 5.16		0 mg Rh

**Table 2** Insoluble precious metals were captured on a microfiber filter, determined and added to soluble precious metals.



	<u>Total Ir</u>	<u>Rh</u>	<u>Total Ru</u>	<u>Au</u>	<u>Pt</u>	<u>Pd</u>	Insoluble from microfiber filter
4696		<u>5.00</u> 4.86	<u>50.00</u> 47.04	<u>5.00</u> 5.06		<u>100.00</u> 98.10	0.38 mg Ru
4697	<u>50.00</u> 50.64		<u>5.00</u> 4.87		<u>50.00</u> 49.56	<u>100.00</u> 96.55	0 mg
4898			<u>100.00</u> 93.86			<u>100.00</u> 96.82	4.46 mg Ru
5200	<u>100.00</u> 96.16					<u>100.00</u> 100.00	6.16 mg Ir

**Table 3 Slags fused with sweeps flux (litharge based) with 100 mg Pd added. Pd bead melted together with tin button.**

## CONCLUSIONS

The optimum range for determining Ir, Rh, Ru, and Ag is 2–50 mg, up to 100 mg for Pt, Pd, and Au.

More sophisticated measurements of iridium concentrations would have produced better recovery data. Overall, however, results show that an assay laboratory with just a moderate investment in equipment and expertise can determine Ir, Rh and Ru, and can determine Au, Pt, Pd, and Ag in the presence of significant amounts of Ir, Rh, and Ru.

### Improving Sensitivity

Sensitivity can be improved by collecting the precious metals in a palladium bead via lead collection and cupellation, melting the palladium bead or replicate palladium beads with tin, dissolving tin and precious metals and performing determinations in final dilutions of 250 ml.

<u>Ir</u>	<u>Rh</u>	<u>Ru</u>	<u>Pd</u>	<u>Tin</u>
<u>1.00</u> 1.14	<u>1.00</u> 0.95	<u>1.00</u> 1.14	100 mg	5 g
<u>2.00</u> 2.37	<u>2.00</u> 1.83	<u>2.00</u> 1.85	100 mg	5 g

### Tin Melts of Assay Beads from Lead Collection and Cupellation

<u>Form</u>	<u>Wgt</u>	<u>Ir</u>	<u>Rh</u>	<u>Ru</u>	<u>Au</u>	<u>Pt</u>	<u>Pd</u>	<u>Ag</u>	<u>Tin</u>
Coherent	101 mg		<u>20.00</u> 19.78		<u>20.00</u> 19.60			<u>20.00</u> 17.28	19.5
Coherent	121 mg			<u>20.00</u> 18.86			<u>20.00</u> 19.34	<u>20.00</u> 16.84	19.5
Spherical *	252 mg	<u>20.00</u> 17.74			<u>20.00</u> 19.03	<u>20.00</u> 19.23	<u>100</u> 97.7		19.5

Assay beads that are flat, encrusted, or leaded can be melted with tin, shotted and analyzed by AA, ICP, or X-ray for estimates of precious metals concentrations. Palladium (100 mg) can be added as a collector to assure a coherent bead and to minimize losses to the cupel.

## **X-ray Analysis of Tin/Precious Metals Alloys**

Previous presentations have described melting assay beads from cupellation with tin in graphite crucibles. The molten tin alloy (usually 5 g) is poured into water. The shot is transferred to a spex cap and pressed for an X-ray specimen.

Tin collection buttons can be melted and shotted. Part of the shot is pressed in a spec cap and analyzed by X-ray. The information is used to devise an analytical scheme and to prepare calibration standards. The pressed tin alloy is broken out of the spec cap, combined with the rest of the sample, dissolved, and analyzed by AA and ICP.

## **REFERENCES**

1. Whitney, J.B. Tin Metal and Nickel Sulfide Are Compared As Fire Assay Collectors of Precious Metals From Platinum Refinery Concentrates. Precious Metals IPMI Proceedings 1986.
2. Testani, T.J., Whitney, J.B., and Worthington, M.A. Instrumental Analysis of Tin Buttons From Fire Assay Collection. Unpublished – 1983.
3. Whitney, J.B. Fire Assay Collections and Precious Metals Determinations – Streamlined and Evaluated, IPMI 25th Conference Proceedings 2001.
4. Whitney, J.B. Crucible Fusion Assays of Refinery Sweeps, Metallics, and Solutions, IPMI 27th Conference Proceedings, 2003.
5. Beamish, F.E. and VanLoon, J.C. Analysis of Noble Metals – Overview and Selected Methods, Academic Press, New York, NY. 1977

# PLATINUM GROUP METALS:

HIGHLY SELECTIVE SEPARATIONS  
BY MRT™ (MOLECULAR  
RECOGNITION TECHNOLOGY™)

– REVIEW OF INDIVIDUAL SEPARATIONS  
OF PALLADIUM, PLATINUM, RHODIUM,  
IRIDIUM AND RUTHENIUM FROM  
INDUSTRIAL FEEDSTOCKS AND  
COMPARISON WITH CLASSICAL  
PGM SEPARATION PROCESSES

S.R. Izatt<sup>1,2\*</sup>, R.M. Izatt<sup>1</sup>, R.L. Bruening<sup>1</sup>, K.E. Krakowiak<sup>1</sup>, L. Navarro<sub>1</sub>

<sup>1</sup>IBC Advanced Technologies, Inc., American Fork, Utah

<sup>2</sup>SeptraMet, Ltd., American Fork, Utah

\*Email: [sizatt@ibcmrt.com](mailto:sizatt@ibcmrt.com)

*< Return to Index*

**Keywords:**

highly selective industrial separations, platinum group metals, PGM, palladium, platinum, rhodium, iridium, ruthenium, SuperLig®, Molecular Recognition Technology™, MRT™

**ABSTRACT**

A disruptive, green chemistry, green engineering separation process, SuperLig® Molecular Recognition Technology™ (MRT™), is reviewed with industrial examples that achieve a circular economy and metal sustainability for individual platinum group metals (PGM: palladium, platinum, rhodium, iridium, ruthenium.) Highly selective single pass recovery yields and high product purities (99.95–99.99%) of individual PGM at the industrial scale from primary and secondary sources are obtained. Implementation of MRT™ processes at industrial scale is described for major PGM refineries processing primary ore and spent secondary PGM sources such as catalytic converters and e-waste. Significant process and operational advantages of MRT™ systems over solvent extraction (SX), ion exchange (IX) and precipitation (Classical PGM Separation Processes) for industrial PGM separations and recovery are discussed. A commercial comparison of MRT™ and Classical PGM Separation Processes shows that MRT™ has significantly lower capital expenditures (CAPEX) and operating expenditures (OPEX). Projected increasing demand for Pt, Ir and Ru as catalysts in the

emerging green hydrogen energy economy as well as these and other PGM in additional catalytic and other applications mandates the increased use of green energy processing to conserve the supply of these valuable resources in a circular economy.

## 1. Introduction

### 1.1. Platinum Group Metals (PGM: Palladium, Platinum, Rhodium, Iridium, Ruthenium) Refining

The industrial-scale adoption of SuperLig® Molecular Recognition Technology™ (MRT™) in the mid-1990s by a top secondary platinum group metals (PGM) refiner, Tanaka Kikinzoku Kogyo

K.K. [1-3] and a top primary PGM refiner, Impala Platinum Limited [1,4,5] marked the first disruptive innovation in PGM refining since the early widespread use of solvent extraction (SX), ion exchange (IX) and precipitation (Classical PGM Separation Processes) in the mid-20th century. The development of Classical PGM Separation Processes occurred in a period (mid-twentieth century) when much less attention was paid to clean chemistry operations and environmental issues associated with PGM mining and refining. Since that time, recovery of PGM from feeds derived from primary mined ore has become increasingly difficult as the grade of PGM has decreased, the need for mining at increasing depths has increased, the concentration of impurities has increased, socio-political issues have emerged, energy and water costs have increased, and the demand for greener, safer and more economic processing has accelerated [5-9].

Recovery of PGM from secondary sources has likewise become increasingly challenging as new feeds containing different mixtures of PGM (e.g., Pt, Ir and Ru as catalysts in fuel cell processes) become more common; feed concentrations of PGM trend lower; feed matrices become more complex; and environmental, safety, health and economic concerns intensify. PGM refining from feedstock derived from both primary mined ore and spent secondary sources such as catalytic converters and e-waste has traditionally involved use of Classical PGM Separation Processes. Despite the increasing complexities associated with PGM refining, these processes have remained essentially unchanged, with only incremental improvements that leave them with appreciable energy use; high capital expenditures (CAPEX) and operating expenditures (OPEX); low selectivity for individual PGM; low single pass PGM recovery rates; high in-process PGM inventories resulting in high metal financing costs and delayed sale of PGM; appreciable PGM loss during processing; complex flowsheets; extensive use of organic solvents and organic extractants; appreciable carbon footprint; and extensive waste generation with resulting widespread negative environmental consequences [10-14].

Sustainability in PGM refining can best be accomplished by successfully meeting the increasing challenges described above and avoiding problems associated with the use of Classical PGM Separation Processes. In order to do so, technology for PGM separations must incorporate green chemistry and green engineering for the efficient separation and recovery at high yield of individual PGM from primary and secondary sources while producing minimal waste, achieving a circular



economy and ensuring metal sustainability. Anastas and Zimmerman [15] made a similar observation in comparing present day industrial processes with those of the past: *“If the mining methods, manufacturing methods, distribution methods, and use profiles were developed before there was an awareness of sustainability consequences, there is no reason to believe that they were optimized, or even adequate for today’s circumstances, Einstein is often quoted as saying ‘Problems cannot be solved at the same level of awareness that created them.’ With our current level of awareness of what is acceptable for an enterprise to maintain its license to operate, comes a need for a new level of investment.”*

MRT™ processes, as will be explained in detail in this paper, are based on green chemistry and green engineering principles and provide an industrially proven and widely used green alternative to Classical PGM Separation Processes for industrial PGM processing. MRT™ systems have been used world-wide for nearly three decades for highly selective industrial separations and high-yield recovery of individual PGM from primary and spent secondary sources [1,16a,16b,17-19]. MRT™ systems have been recognized by others for their innovative use at major global enterprises for the successful recovery and separation of individual PGM with low costs, reduced processing time, innovative use of green technology, achievement of high purification levels, achievement of high selectivity and process scalability, minimal waste generation, and minimal carbon footprint [5,20-22].

## **1.2 Topics Covered in This Review**

This paper presents an account by an industrial team of the commercial success of their green chemistry metal separations technology. This technology grew out of successful original academic research on establishing host-guest molecular recognition principles over a half-century period [16b]. IBC Advanced Technologies, Inc. (IBC) markets the MRT™ and the SuperLig® products mentioned in this review.

The increasing importance of PGM to the global economy, PGM supply and demand dynamics, and the essential role played by separations science and technology in providing a sustainable PGM future will be examined. The separation and recovery of individual PGM using MRT™ processes will be reviewed. Principles of molecular recognition, green chemistry, and green engineering that are important in the design of PGM-selective MRT™ processes will be presented. Flowsheets will be given, and examples will be presented demonstrating the attainment of very high single pass recovery rates and product purities (99.95–99.99%) of individual PGM at the industrial scale from primary and secondary sources. The role of MRT™ processes in the separation and purification of iridium, platinum, and ruthenium in the emerging hydrogen economy will be evaluated. A commercial comparison of MRT™ and Classical PGM Separation Processes in industrial PGM separations and recovery will be used to illustrate the significant economic and process advantages of MRT™ systems in industrial operations.

## **2. Importance of Separations Science and Technology in the Achievement of PGM Sustainability in a Circular Economy**

## 2.1. Critical Importance of PGM in 21st Century Commerce

With the exception of osmium, all PGM have been designated as critical raw materials by the United States (US) [9,23] and the European Union (EU) [24,25] because these metals are essential to the economies of these nations but have supply chains associated with high risk [5]. The essential role of PGM in modern industrial, military, domestic, and other applications is due to their unique physical and chemical properties including their proven ability to catalyze (accelerate or make possible) chemical reactions, high electrical and thermal conductivity, multiple oxidation states, high corrosion resistance, high conductivity, unique optical qualities, and high melting points, among others [21,26]. It is seldom possible to substitute other metals for PGM in their applications without significant loss of function and, often, PGM are the best substitutes for other PGM in a particular application [9,23,27a].

PGM are used in a wide range of applications including in substance mixtures such as alloys or in compounds that resemble alloys. The number and type of applications for PGM are increasing rapidly following the rapid growth of existing and new technologies such as hydrogen-related applications, that require unique PGM properties for maximum function [27b]. However, at present, catalytic converters remain by far the largest single PGM application. For example, 90% of gross demand for Rh in 2020-2021 was in the autocatalyst sector [27b]. A sampling of the wide range of PGM applications that stem from their unmatched chemical and physical properties is given in Table 1.

Table 1. Some Important Applications of Platinum Group Metals in Several Sectors [22a,23,28].

<u>Sector</u>	<u>Application</u>
Aerospace (Non-defense)	Jet engines (casting, coatings)
Energy	Catalytic converters Fuel cells Land-based turbines Petroleum catalysts
Telecommunications and electronics	Capacitors Electric equipment Electronic equipment Flat panel displays Hard-disk drives Mobile phones
Transportation (non-aerospace)	Catalytic converters Automotive components Fuel cells
Other	Chemical catalysts Dental applications Glass applications Integrated circuits Jewelry Lighting Medical applications Metallurgical applications Plating solutions Refractory crucibles Touch screen technology

Hagelüken [29] observed in 2014 that more than 80% of global mine production of PGM had occurred in the preceding three decades confirming the observed rapid increase in demand for PGM use in society. The recent increase in the rate of mining primary PGM ore to meet this demand parallels the upsurge in new applications of these metals and provides a compelling reason for achieving sustainability in a circular economy for individual PGM to prevent their irretrievable depletion. PGM are among the rarest metals in the Earth's crust as seen in Figure 1 and are extremely difficult to separate from each other compounding the sustainability issue [30].

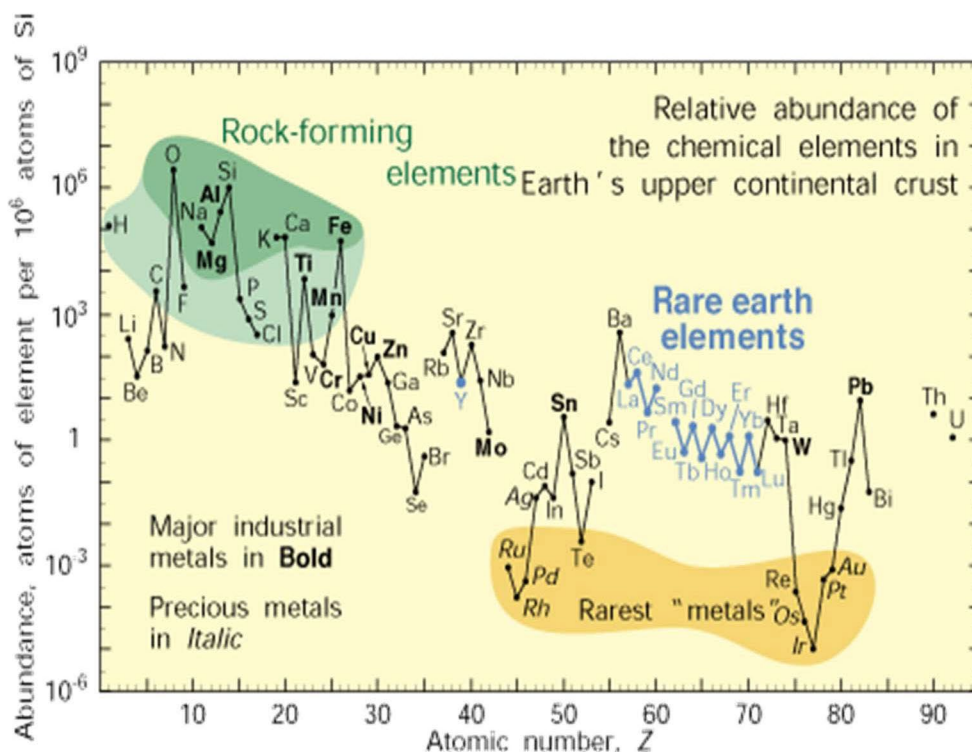


Figure 1. Abundance (expressed as atoms of element per 106 atoms of Si) of the Chemical Elements in Earth's Upper Continental Crust as a Function of Atomic Number. Platinum group elements are shown as six of the nine rarest elements present in Earth's crust.

Reproduced with permission from U.S. Geological Survey, Department of the Interior.

<http://pubs.usgs.gov/fs/2002/fs087-02/> (accessed May 3, 2023).

PGM are found together in nature with Pt and Pd being the most abundant. Due to the lanthanide contraction, the three lighter PGM (Ru, Rh, Pd) have densities nearly half those of the three heavier PGM (Os, Ir, Pt), but have very similar chemical properties. The PGM are characterized by multiple oxidation states, high affinity for "soft" anions such as chloride ion providing a variety of chloro anions, and a few hydrated simple cations. Selectivity in the MRT™ process is based on the ability to use supramolecular chemistry principles to design host SuperLig® materials that will have high affinity for specific guest PGM species. The variety of PGM chemistry provides the opportunity to produce SuperLig® materials that are highly selective for specific PGM species. A striking example of the high

selectivity of the MRT™ process is found by comparing the simple MRT™ flowsheet (Figure 6) with the traditional complex flowsheet in the refining of Ir as described in Section 7.2.

## 2.2 PGM Supply-demand Issues

Significant risks to the economies of the EU, US, and many other nations are associated with the supply-side of PGM. These risks begin with the geographical sourcing of these metals. Over 90% of global mined PGM production is located in only three countries, South Africa, Zimbabwe, and Russia, presenting the potential for supply disruption [24,28,31,32a].

Globally, in 2021, approximately 21% of Pt, 33% of Pd, and 32% of Rh supply came from metals recycled from spent secondary products, largely from spent automotive catalytic converters [27b]. In a separate European Union Horizon 2020 project, a flowsheet processed approximately 1.3 kg of spent milled autocatalyst and produced 1.2 g Pd, 0.8 g Pt, and 0.1g Rh in nitrate form with a 92- 99% purity [32b]. The overall recoveries from feedstock to product were calculated as 46% Pd, 32% Pt, and 27% Rh, respectively.

Iridium and Ru are also recycled, but at much lower rates. The gap between supply and demand for Pt, Pd, and Rh is widening giving further emphasis to the need for more effective and increased recycling of these critical metals to meet demand [28]. For example, Nasser and Fortier [9] observe that *“Demand (for PGM) continued to modestly outpace new supply during 2020, widening the deficit to nearly 400,000 oz.”*

Gordon, et al. [33] have studied the occurrence of PGM in the lithosphere and conclude that it is unlikely that significant new platinum resources will be found on Earth, further emphasizing the need for more effective recycling. The potential supply of PGM from spent secondary sources is large. In addition to the major secondary source, catalytic converters, many chemical wastes produced globally contain PGM, particularly Pt and Pd, at low concentrations of part-per-million (ppm) or less. These wastes include spent forms of petrochemical catalysts, chemical catalysts, plating bath solutions, and electrical and electronic products among others (Table 1.)

Karim and Ting [11] observe that recovery of PGM from spent automotive catalytic converters not only conserves natural primary ore to meet future demand but also supports sustainable development by minimizing waste disposal, limiting power consumption, and reducing environmental pollution. For example, these authors point out that 1 kg of Pt is obtained from processing 150 metric tons of primary ore at 1,000 meters depth with generation of 400 metric tons of waste, whereas the same amount of Pt can be recovered from recycling two metric tons of spent catalytic converters with much smaller waste generation [11].

The attractiveness of using urban mining as a means of augmenting the global PGM supply has been pointed out by Izatt and Hagelüken [34a]: *“Considering the high environmental impact of primary production of precious metals arising from low ore concentrations, difficult mining conditions, high energy and water use, high chemical consumption, large waste generation, and other factors,*

recovery of metals from EoL [end-of-life] products is appealing.” However, Zupanc, et al. [34b] caution that use of environmentally damaging processes in recycling “seems somewhat counterintuitive and calls for application of sustainable approaches in recovery of sparsely available noble metals in the pursuit of ‘Urban Mining.’” These authors further indicate that highly oxidative and acidic conditions coupled with use of toxic oxidants like aqua regia and Cl<sub>2</sub> produce large amounts of toxic and/or corrosive waste. Their conclusion is apt: [34b] *This goes against objectives of sustainable development, which seem somewhat counterintuitive when recycling, a principle of circular economy and green chemistry, is at aim.*”

### 3. SuperLig® Molecular Recognition Technology™ (MRT™) Systems

A SuperLig® resin consists of a ligand, pre-designed using supramolecular chemistry principles to have high target metal selectivity, covalently bound by a tether to silica gel or other solid support [10,16b]. The SuperLig® resin is used in solid bead form in a packed column. The steps in the operation of the MRT™ process are given in Table 2.

Table 2. Steps in the Operation of the MRT™ Process for Single Pass Separations from Feedstock Containing Individual PGM in the Column Mode [10,16b].

<u>Step</u>	<u>Operation</u>
Loading	Target PGM is selectively extracted from the feed by the SuperLig® resin, which has previously been loaded at high capacity onto the column.
Pre-elution wash	Remaining feed solution is washed from the column leaving only the target PGM bound to the SuperLig® resin.
Elution	All of the bound target PGM is completely eluted from the column with a small amount of eluent forming an eluate solution containing the concentrated target PGM at high purity. Bed volumes of 1-2 are typical in the elution step.
Post-elution wash	The remaining eluent solution is washed from the column and the cycle is repeated starting with the loading step.

The high selectivity of SuperLig® resins for target PGM and non-use of organic solvents allows the design of low-complexity operating systems that follow the steps in Table 2 and are defined by the flowsheets in Section 6 (see examples of systems in Section 7.) The chemistry involved functions at the molecular level in accordance with green chemistry and green engineering principles [10]. High target PGM selectivity and high target PGM–ligand binding constants make very high single pass separations at high column capacity levels possible, eliminating extensive and costly downstream processing. Classical PGM Separation Processes have low single pass recovery rates resulting in high in-process metal inventories due to the need for extensive re-work causing high metal financing costs and delay in selling the target PGM. Examples comparing recovery rates for MRT™ and Classical PGM Separation Processes are given in Section 7.3 involving Pd separation, in Section 7.2 involving Ir/Rh separation, and in Section 7.4 involving Pd separation. MRT™ systems are readily automated, have small space requirements, do not use highly deleterious chemicals, and, in the elution step,



produce pure, concentrated target PGM rapidly with short metal inventory times.

Selective and complete separation of the target PGM in the loading step ensures that traces of the target PGM do not pass to the raffinate which would require further separation steps downstream. High metal selectivity and binding strength enable high-capacity loading of the target PGM on the SuperLig® resin because competing metals either do not bind to the SuperLig® resin or are pushed off the column due to the higher binding strength of the target PGM to the SuperLig® resin. The result is complete separation of the target PGM from other PGM and base metals, which pass on to raffinate, where other SuperLig® resins can be used to selectively separate the remaining PGM. Selective recovery of each PGM in a comprehensive flowsheet avoids significant waste generation and conserves valuable resources.

Wash and elution steps are accomplished using mild chemicals such as water, dilute mineral acids, and others, that are designed to be as compatible as possible with the overall PGM refining flowsheet (examples are given in the flowsheets in Section 6.) In the elution step, all of the target PGM is completely eluted from the SuperLig® column. Enrichment of the PGM in the elution step makes possible the effective treatment of feedstock solutions containing low as well as high PGM concentrations. This flexibility allows for treatment of PGM-containing streams derived from secondary products that are currently discarded without recovery of the PGM they contain. An example is given in Section 7.5.

Binding and release of target metals by SuperLig® resins are rapid and the entire procedure can be incorporated into existing process flowsheets. The ability to efficiently separate, recover, and purify individual metals at any concentration level, in the presence of much higher concentrations of impurity metals, significantly reduces refining costs that are otherwise incurred through the use of Classical PGM Separation Processes that, to be efficient, use, depending on the process, organic solvents and/or harsh chemicals combined with heat and pressure to increase the concentrations of PGM in solution.

An important advance made by MRT™ systems is the significant reduction of platinosis risk. Platinosis is a disease caused by exposure to complex salts of platinum, mainly chloroplatinates. These salts are well-known respiratory sensitizing agents leading to work-related sensitization and allergies in the work environment, especially in the PGM refining process. Heederick, et al. [35] have discussed the history of platinosis and the on-going effort to arrive at a safe level of exposure to these salts. These authors also evaluated the quantitative exposure-response relationship between occupational chloroplatinate exposure and sensitization using routinely collected health surveillance data and chloroplatinate exposure data. Their results suggest an occupational exposure limit of 200 ng/m<sup>3</sup> for chloroplatinates [35]. MRT™ platinum refining systems are closed and do not generate chloroplatinates, thereby minimizing worker exposure, and significantly reducing the risk of platinosis.

#### **4. Role of Thermodynamics and Kinetics in Designing Highly Metal-selective MRT™ Systems**

##### **4.1. Technical Comparison of MRT™, Ion Exchange, and Solvent Extraction Processes**

MRT™ systems have been incorrectly listed in the literature as IX processes.[36,37] MRT™ processes do not exchange ions as is done in IX systems. The extraction mechanism in MRT™ systems is based on selective molecular recognition of a target metal ion by a ligand bound to a solid support (SuperLig® resin) as is described in Section 3.

The important roles of thermodynamics and kinetics in creating efficient separation processes are explained in the following section where studies from Mintek (Figure 2) and the U.S. Department of Defense (Table 3) are given that show SuperLig® resins to be significantly more effective than IX, chelating IX or SX in comparable separation systems.

## 4.2. Thermodynamics and Kinetics

The efficiency of a metal separations process is directly related to the relative magnitudes of the apparent binding constants ( $K$ ) associated with the interaction of the target metal and impurity metals with various components of the separation system. For example, in an MRT™ system these components include the ligand component of the SuperLig® resin, the eluent, and the wash reagent. In SX and IX systems, extractant and resin molecules, respectively, are involved. Impurity metals are invariably present in metal separations and compete with the target metal for ligand binding sites that may be present. Therefore, the efficiency of the separation system is dependent on the difference in  $\log K$  values ( $\Delta \log K$ ) between the competing metals for various ligand binding sites. The magnitude of the  $\Delta \log K$  value is very important in determining separation efficiency since it determines metal selectivity. Decreasing  $\Delta \log K$  values result in progressively lower separation efficiencies and the need for an increased number of separation stages to obtain high target metal purity values. The increased number of separation stages is the cause of high inprocess metal inventories that must be re-worked resulting in high metal holding (inventory) cost and delay of PGM being sold to the market, which is a critical issue in commercial operations. Excessive waste generation must be managed as a result, at high cost, to avoid environmental, safety, health, and other problems.

The critical role of thermodynamics in metal separations can be summarized as follows:

- high  $\log K$  values are required for high efficiency in metal separations and recovery
- high  $\Delta \log K$  values for the target metal vs. impurity metals are required for high target metal selectivity
- high  $\log K$  and large  $\Delta \log K$  values for target metal vs. impurity metals eliminate multiple separation stages, avoid expensive downstream processing of impurities, and minimize generation of waste

Design for rapid kinetics of metal–ligand binding and release is essential for an industrial separation system. Rapid kinetics for MRT™ processes can optimize product production in several ways including:

- savings in operation time
- minimization of in-process PGM inventories

- reduction in space requirements
- reduction in labor requirements
- reduction in chemical usage
- increased ability to design simpler and more compact separation systems
- easier incorporation of separation systems into automated, in-line processing units

An example of rapid kinetics is given by the MRT™ Pd separation system, where Pd is loaded at 0.5 liter/minute/kg SuperLig® 2 and eluted at 0.25 liter/minute/kg SuperLig® 2. Demonstration of rapid kinetics for PGM separations is supported by the incorporation of MRT™ systems into industrial plant process flowsheets on a real-time basis, as illustrated in Section 7.4 for separation of Pd at the Boliden Rönnskär precious metals refinery.

MRT™ systems are designed to enhance both thermodynamic and kinetic properties specific to PGM processes. It is critical to understand that MRT™ systems are designed to not only selectively bind a target element, but also to completely release that target element in each cycle allowing for multi-cycle use and easy system automation.

The thermodynamic and kinetic properties of MRT™ systems result in orders of magnitude greater selectivity factors and apparent binding constants than those for either IX or SX systems.

Although not involving PGM, a study undertaken by Mintek (South Africa) directly compares the performance of SuperLig® 177, an SX extraction agent, and an IX system in Co purification by Cd removal. Results from this study are given in Figure 2 [1,38a,38b]. Direct comparisons such as these are typically made by companies before selection of MRT™ processes for their industrial PGM separations (see Section 7.)

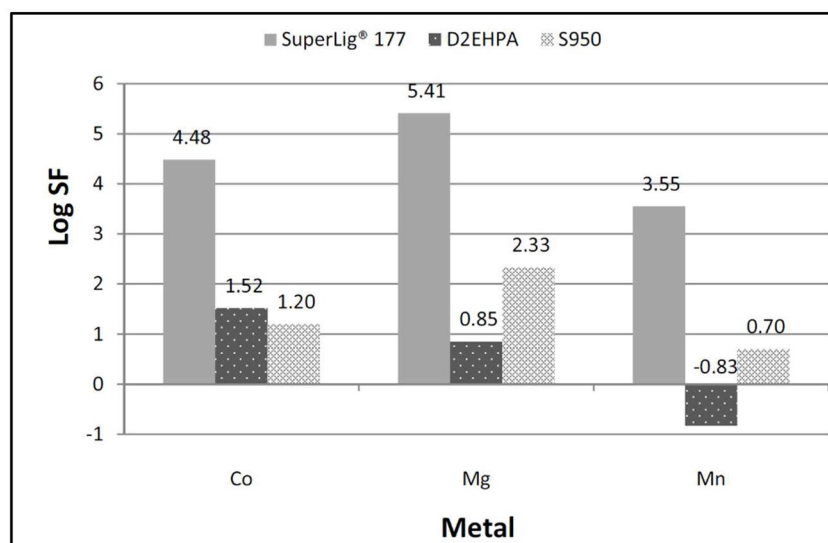


Figure 2. Plot of the Log of the Selectivity Factor (Log SF) Versus Metal for the Separation by SuperLig® 177, D2EHPA, and S950 of Cadmium from Cobalt, Magnesium, and Manganese, all Initially Present in a Co Electrolyte Feed Solution. Reproduced from [38b].

Cadmium is an important impurity in the refining of Co electrolyte solutions which also contain various other impurity metals including Mg and Mn. The selectivity factors (SF) in Figure 2 measure the relative abilities of SuperLig® 177, di-2-ethylhexyl phosphoric acid (D2EHPA), and the adsorption agent amino-methyl phosphoric acid resin (Purolite S950) to separate Cd (~6 mg/L) from a Co electrolyte feed solution containing 60 g/L Co and trace amounts of Mg and Mn. The differences in log SF values show that SuperLig® 177 is many orders of magnitude more effective than either SX or IX processes in separating Cd from Co and other impurity metals present in this electrolyte solution. In addition, the recovered Cd in the MRT™ system is available for reuse or safe disposal rather than being discarded into landfill or tailings ponds as is usually done with traditional processes.

The significantly larger apparent log K values for interaction of several metal ions with a SuperLig® resin compared to a sulfonate IX resin and a chelating IX resin containing iminodiacetic acid are shown in Table 3, as given in a U.S. Department of Defense report [39]. Important factors in the low selectivity of IX resins are the low resin-metal ion binding constant and the similar log K values for each charge type. In these resins, binding strength for metal ions increase in the order 1+ < 2+ < 3+.

Table 3. Apparent Log K Values Valid at pH 6 for the Interaction of Several Metal Ions with a SuperLig® resin, a Regular Ion Exchange Resin, and a Chelating Ion Exchange Resin [39].

<u>Metal Ion</u>	<u>SuperLig® Resin</u>	<u>Regular IX, Sulfonic acid group</u>	<u>Chelating IX, Imino-diacetic acid group</u>
Ni <sup>2+</sup>	17.0	<0.7	4.9
Cu <sup>2+</sup>	22.0	<0.7	7.3
Zn <sup>2+</sup>	14.4	<0.7	3.8
Cd <sup>2+</sup>	13.8	<0.7	3.0
Pb <sup>2+</sup>	14.4	<0.7	4.2
Ag <sup>+</sup>	13.8	<0.7	<0.7

Within a charge type, the variation in log K values is small as seen in Table 3. The presence of the iminodiacetic acid chelating group enhances the metal selectivity of the IX resin over the regular IX resin. However, the magnitude of the log K values is small compared to those with the SuperLig® resin.

## 5. Principles of Green Chemistry and Green Engineering Applied to Hydrometallurgical Separations of PGM using MRT™ Systems

Green chemistry has been defined as *“the design of chemical products and processes to reduce or eliminate use and generation of hazardous substances [15,40,41].* A cardinal principle of green chemistry is that it is better to prevent generation of waste than to clean it up after it is formed. Waste generation has become a defining feature of our civilization, especially in the past few decades [34a,42]. The United Nations Brundtland Commission’s report in 1987 characterized sustainable development as *“development that meets the needs of the present without compromising the ability of future generations to meet their own needs [43].* We [10,30] and others [12,22] have promoted

the desirability of developing technologies for the separation and recovery of metals from primary and secondary sources that conform to green chemistry and green engineering principles, produce minimal waste, and lead to a circular economy and metal sustainability. Significant obstacles to attainment of increased metal sustainability together with their consequences have been discussed by us [30].

In their analysis of chemical systems, Anastas and Eghbali [40] indicate that organic solvents account for most industrial waste in the chemical industry and that it is preferable to use systems that either minimize or do not require solvent use. This assessment is confirmed by Firmansyah, et al. [28] who point out that disposition of solvent wastes is one of the major issues in industry. Solvent wastes raise environmental and economic concerns and account for the vast majority of mass wasted in syntheses and processes in industry. Use of organic solvents in PGM separation processes increases the risk of workers' exposure and has led not only to serious accidents but to fires that destroy facilities and shut down production for extended periods of time. Anastas and Eghbali [40] suggest that *"the ideal solution would be to not use any solvent because the decision to include an auxiliary always implies efforts and energy to remove it from a designated system."*

Design of MRT™ systems is based on optimization of thermodynamic and kinetic parameters, as explained in Section 4.2. This optimization permits the principles of green engineering to be incorporated into these systems. Key aspects of green engineering are predictability of operation (thereby allowing the process to be automated and run efficiently in a semi-continuous mode), low energy and water usage, low environmental risks, and avoidance of high pressures and temperatures (thereby avoiding the need for extensive equipment infrastructure). Thermodynamic and kinetic optimization leads to MRT™ system predictability (i.e., the SuperLig® column will bind a known amount of target PGM and that target PGM can be completely eluted in a known volume) and operation over a range of temperatures at atmospheric pressure, without the need to employ large amounts of energy, extensive heating, or pressurization. Unlike many IX resins, SuperLig® resins do not need to be burned to recover PGM. In the MRT™ process, the target PGM is completely eluted from the SuperLig® resin in each cycle, thereby allowing for simple recovery of the target individual PGM, system predictability, and easy automation.

Systems that do not require intensive energy input are highly desirable in metal separations and recovery. O'Connor et al. [12] indicate the need in recycling for methods that can separate recovered metals from one another, so they can be easily reinserted in the manufacturing process. These authors discuss green engineering aspects of such separations and emphasize that separation processes need to be simple, economically feasible, have low energy requirements, and low environmental risks. Green chemistry and green engineering principles mandate that in the design of chemical processes, the introduction of new pollutants or the use of highly toxic and/or corrosive chemicals and/or heat and pressure should be avoided. The chemical industry has benefited greatly over the past three decades from the introduction of green chemistry practices [44]. Similar benefits are seen where green chemistry and green engineering principles have been introduced in various steps in metal lifecycles, including in PGM separations and recovery from primary ore and spent secondary sources [10,16a,17,45, 46a,46b,46c].



An important contribution of MRT™ systems has been the introduction of green chemistry and green engineering processes into the field of industrial PGM separations [16a,16b]. In Table 4, process properties of MRT™ systems are listed together with advances derived from use of these systems.

Table 4. Process Properties of MRT™ Systems with Advances Achieved from their Use. Compiled in part from information in earlier publications [16a,17,46c,49].

<u>Process Property</u>	<u>Advance</u>
High selectivity for individual PGM	<ul style="list-style-type: none"> <li>• Ensures very high single pass individual PGM separations in column loading step</li> <li>• Provides the flexibility to target specific, commercially important PGM, such as Rh, early in the flowsheet.</li> <li>• Ensures maximum column loading capacity</li> <li>• Minimizes retention on column of competing PGM and/or impurity metals</li> <li>• Dramatically reduces PGM in the processing pipeline, thus reducing metal financing costs, and releasing metal earlier for sale</li> <li>• Eliminates or markedly reduces need for downstream processing</li> <li>• Minimizes SuperLig® and reagent use while reducing equipment size</li> <li>• Minimizes MRT™ system footprint</li> </ul>
Rapid kinetics	<ul style="list-style-type: none"> <li>• Ensures rapid PGM binding to, and release from, the SuperLig® resin making incorporation into plant operation on a real time basis feasible</li> </ul>
High energy conservation	<ul style="list-style-type: none"> <li>• Minimizes energy consumption by operation over a range of temperatures at atmospheric pressure and by conservation of equipment, labor, chemicals and facilities used</li> </ul>
Simplified process design and operation	<ul style="list-style-type: none"> <li>• Ensures an uncomplicated operating system in a small compact working space</li> <li>• Results in simple flowsheets</li> <li>• Makes easy automation of the process feasible</li> </ul>
Efficient and rapid wash of SuperLig® column with mild wash solutions	<ul style="list-style-type: none"> <li>• Increases compatibility with refinery plant operations</li> <li>• Facilitates washing of residual feed from the column after loading and residual eluent after elution using mild reagents, e.g., H<sub>2</sub>O, dilute acids, and simple salts</li> <li>• Minimizes operational and environmental risks</li> <li>• Allows for recycling of wash solutions whenever possible</li> </ul>
Efficient and rapid elution of target PGM	<ul style="list-style-type: none"> <li>• Enhances the complete and efficient transport of all of the target PGM from the loaded column to the eluate using simple eluents, e.g., H<sub>2</sub>O, dilute acids, simple salts and metal complexing agents</li> <li>• Ensures that all of the PGM bound to the SuperLig® column is recovered in concentrated form in the elution step by use of a small volume (2-3 bed volumes) of eluent</li> <li>• Enables recovery at high yield of a concentrated PGM solution</li> <li>• Minimizes operational and environmental risks, ensures compatibility with refining plant requirements and provides eluent recycling whenever possible</li> </ul>

Recovery of target PGM in a concentrated eluate	<ul style="list-style-type: none"> <li>• Enhances conversion to final product by enrichment of PGM in the eluate</li> <li>• Makes possible the economic recovery of PGM when present at low levels in spent secondary products</li> </ul>
Minimal waste generation	<ul style="list-style-type: none"> <li>• Avoids major waste generation problems by non-use of organic solvents and hazardous chemicals</li> <li>• Adds no contaminants to process feed solution</li> <li>• Minimizes contentious interactions with public and community leaders over pollution and other environmental issues</li> <li>• Eases permitting issues</li> </ul>
Recovery rather than discard of impurity metals	<ul style="list-style-type: none"> <li>• Allows recovered impurity metals to be sold for value or sent for safe disposal thereby minimizing management, disposal, environmental and health issues</li> </ul>
Minimal carbon footprint	<ul style="list-style-type: none"> <li>• Allows for carbon minimization goals to be met</li> </ul>
Low cost	<ul style="list-style-type: none"> <li>• Results in increased market competitiveness</li> </ul>

The flowsheets and examples of industrial installations that follow describe the application of MRT™ systems to the commercial highly selective separation and high-yield recovery at high purity levels of individual PGM from a variety of primary and secondary sources.

## 6. Flowsheets for the Green Chemistry Separation of PGM from Industrial Feedstocks and Summary of Advances Achieved by use of MRT™ Processes

The flowsheets in Figure 3 – Figure 7 illustrate the simplicity of the MRT™ approach to the selective separation of individual target PGM from feed solutions containing other metals, often at concentrations much higher than that of the target PGM. A key advantage of MRT™-based flowsheet design is the flexibility to target specific, commercially important PGM, such as Rh, early in the flowsheet. This is shown in Figure 5, where Rh is selectively separated from an input stream containing Rh, Pd, Pt, Ru, Ir, Au, Ag, and base metals.

In each flowsheet, incoming HCl feed solutions containing the target PGM, and other metals are passed through the appropriate loaded SuperLig® column(s) for selective separation of the target PGM. No contaminants are added to the process stream in the MRT™ process. The ability to selectively separate an individual PGM efficiently is of critical importance since the need for multiple stages is eliminated, PGM processing loss is minimized, the use of hazardous/contaminating chemicals is avoided, and waste generation is minimized. Reagents for washing the SuperLig® column and eluting the SuperLig®-bound PGM are simple and compatible with the production of the final PGM product. End-of-life SuperLig® resins are devoid of PGM and easily handled in accordance with a specific company's policy on disposition of spent materials.

SuperLig® resins are capable of very high single pass recovery yields on an industrial scale. For example, the Boliden Rönnskär MRT™ system (Section 7.4) recovers palladium at 99.99% yield in a single step from a feed stream derived from the recycling of e-waste, spent catalytic converter

residues, and other materials. Factors that may influence the single pass recovery yield include the individual PGM being recovered, the relative concentration of the individual PGM and other constituents in the feed solution, and the dynamics of the SuperLig®-individual PGM interaction.

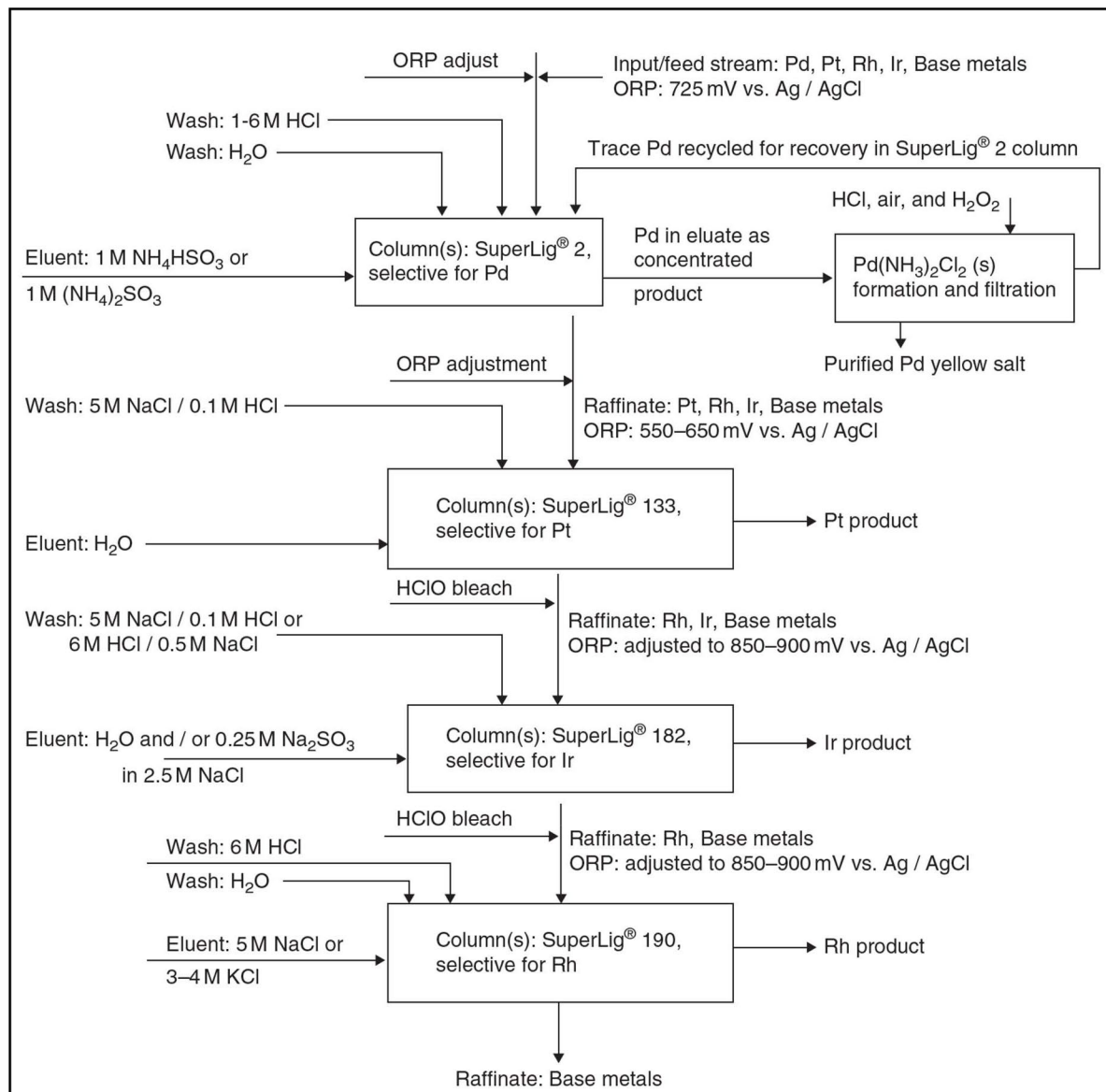


Figure 3. Individual, Sequential, Selective Separations of Palladium, Platinum, Iridium, and Rhodium from a Base Metal Matrix. ORP = oxidation-reduction potential. Adapted with permission from [47].

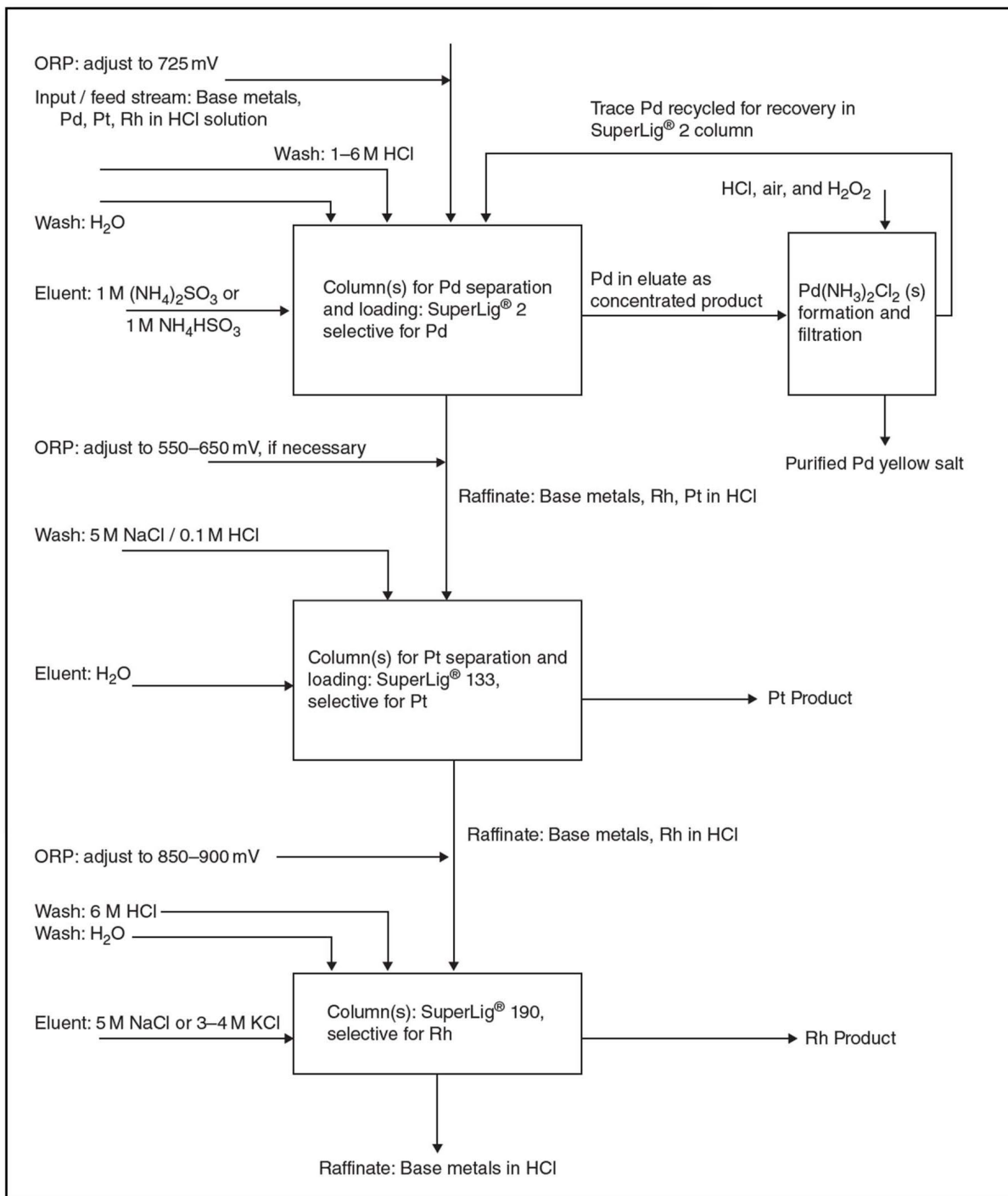


Figure 4. Individual, Sequential, Selective Separations of Palladium, Platinum, and Rhodium from a Feed Solution Containing these Metals and Base Metals in an HCl Solution.

ORP = oxidation-reduction potential.

Adapted with permission from [47].

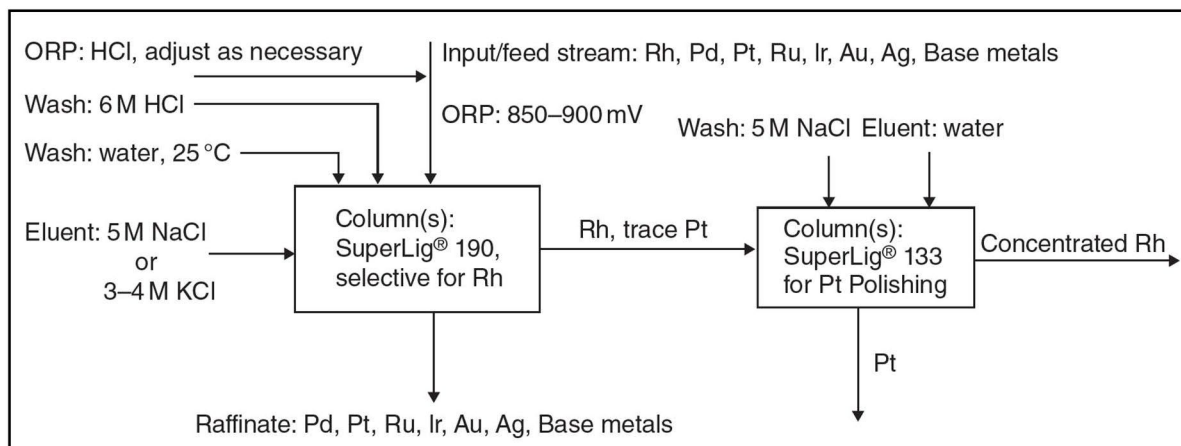


Figure 5. Flowsheet for the Selective Separation of Rhodium from Palladium, Platinum, Ruthenium, Iridium, Silver, Gold, and Base Metals. ORP = oxidation–reduction potential. Adapted with permission from [47].

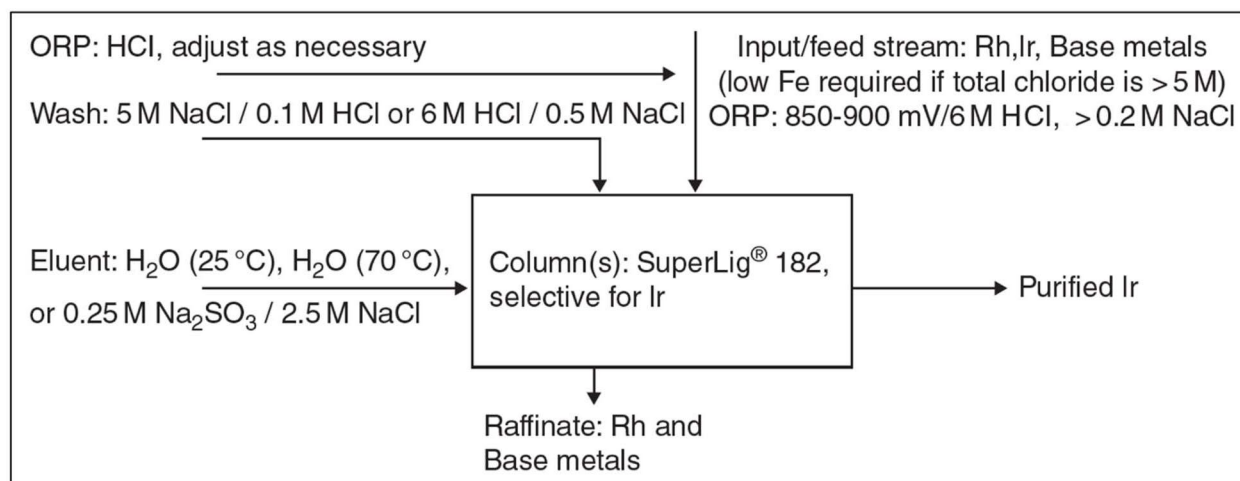


Figure 6. Flowsheet for the Selective Separation of Iridium from Rhodium and Base Metals. ORP = oxidation–reduction potential. Adapted with permission from [47].



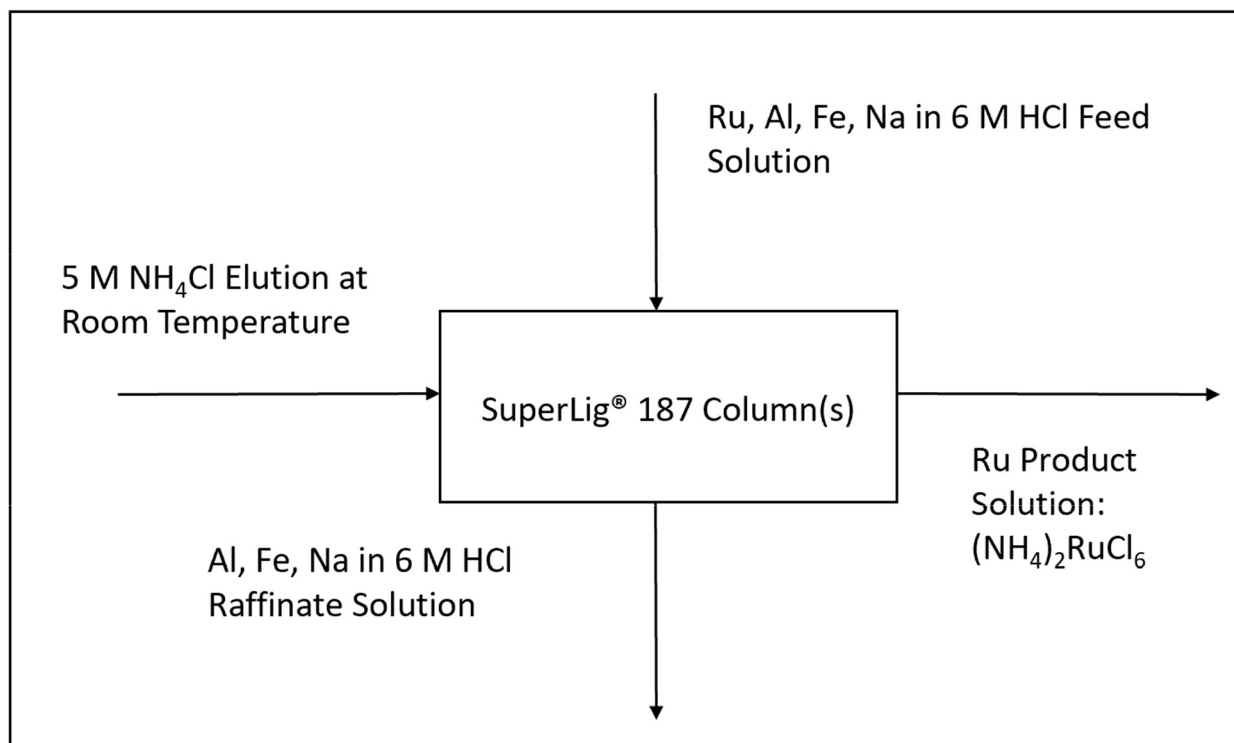


Figure 7. Flowsheet for the Selective Separation of Ruthenium from a Matrix of Aluminum, Iron, Sodium, and other Base Metals in 6 M HCl using the MRT™ Process.

Oxidation-reduction potential (ORP): 300–400 mV vs. Ag/AgCl electrode. Wash: HCl.

Reproduced with permission from [48].

Green chemistry advances provided by SuperLig® MRT™ systems are given in Table 5.

Table 5. Advances Offered by Green Chemistry MRT™ Systems to PGM Refining Operations. Compiled in part from information in earlier publications [16a,17,46c,49].

1.	Very high single pass individual PGM recovery yields
2.	Product purities of 99.95%-99.99%
3.	Flexibility to target specific, commercially important PGM, such as Rh, early in the flowsheet
4.	Significant reduction in the risk of platinosis and other negative health effects because the MRT™ system is self-contained, thereby greatly reducing worker exposure
5.	Rapid processing time for target PGM resulting in lower financing costs and earlier release of the target PGM for sale
6.	Reduction in processing losses resulting from very high single pass individual PGM recovery yields
7.	Lowered PGM refining expenses from the elimination and/or reduction of process chemical use, number of process steps, considerable associated infrastructure, and labor costs
8.	Lowered maintenance costs due to less infrastructure use and simplicity of equipment
9.	Reduced need for effluent control measures because no organic solvents or corrosive chemicals are used
10.	Ability to treat both dilute and concentrated feed streams of any solution volume
11.	Option of producing a salt product that may be sold or reduced to market-grade metal
12.	Capability for rapid and semi-continuous operation of the MRT™ process at high flow rates for both loading and elution
13.	Capability to recycle wash and elution solutions
14.	Competitive capital costs with simple, compact equipment requiring minimal space
15.	Reduction of PGM security risk by minimizing exposure with a self-contained system
16.	Multi-cycle use of SuperLig® resins
17.	Minimal waste generation and minimal carbon footprint
18.	Establishment of a circular economy for individual PGM leading to sustainability of these critical metals

## 7. Selected Industrial-Scale Examples of MRT™ PGM Separation Systems

A summary of MRT™ processes used for a variety of industrial PGM separations is given in Table 6. In each case, the appropriate flowsheet in Section 6 or a modification thereof is used for the separation of the indicated PGM.

Table 6. Separation, Recovery, and Purification of Individual Platinum Group Metals from Various Matrices using MRT™ Systems. Adapted from ref. 46a and 46c.

PGM	Separation, Recovery, Purification Event	Ref
Pt	Pt from spent catalytic converters and other feeds Pt from Pt/Cr/Co/Cu alloy scrap from a sputtering process	a,b c
Pd	Pd from spent catalytic converters and primary mine feed Pd from spent petrochemical catalysts Pd from dipping bath solutions Pd from plating baths Pd from spent secondary sources	a,b,d,e f,g h i,j k
Rh	Rh from spent catalytic converters and other feeds	a,b,d,e,l
Ir	Ir from primary mine feed matrix of Rh and base metals	m,n,o,p
Ru	Ru from alloy scrap	c

<sup>a</sup>[49]; <sup>b</sup>[50]; <sup>c</sup>[48]; <sup>d</sup>[1]; <sup>e</sup>[4]; <sup>f</sup>[51]; <sup>g</sup>[52]; <sup>h</sup>[53]; <sup>i</sup>[54]; <sup>j</sup>[46a]; <sup>k</sup>[46b], <sup>l</sup>[2]; <sup>m</sup>[16a]; <sup>n</sup>[47]; <sup>o</sup>[46c]; <sup>p</sup>[18]

Industrial examples selected from those listed in Table 6 are now presented to show in more detail the effectiveness and flexibility of the green chemistry MRT™ approach. Particularly challenging PGM separations are described that include the selective separation of Rh from complex secondary feed, the selective separation of Ir from Rh in primary mine feed, and the selective separation of Pd (a) from primary mine feed, (b) from various primary and secondary sources, including e-waste, at a copper smelter, and (c) from low-grade spent plating feed with a modular mobile unit deployed on-site, sent to be processed at a central refining location and returned to the on-site location for reuse in a circular fashion.

An important principle in scientific work is that results should be reproducible in the hands of others. The following examples involving PGM separations show this principle in the case of MRT™ processes by describing their adoption and use by multiple industrial companies. In each case, the MRT™ process was tested extensively in-house against existing technologies being used at the industrial site. The MRT™ process was chosen for its superior economic and process value to the companies. The MRT™ processes for Pd separation in the case of Impala and Rh separation in the case of Tanaka have been in use for nearly three decades.

### 7.1 Refining of Rhodium at Tanaka Kikinzoku Kogyo K.K. (TKK)

Since the mid-1990s, TKK has used the MRT™ process to extract and purify Rh from spent catalytic converter and other feeds [1-3,55]. High selectivity for Rh is obtained by use of SuperLig® 190 that recognizes Rh as a chloro anion making it highly selective for Rh over other metals present as cations. Platinum present at concentrations in excess of those of Rh can result in trace Pt impurity, present as an anion, in the concentrated Rh product. The trace Pt impurity is removed using another SuperLig® resin, resulting in pure Rh and Pt products.

The MRT™ Rh system installed at TKK is shown in Figure 8.



Figure 8. MRT™ Industrial Facility for Rhodium Separation and Recovery at Tanaka Kikinzoku Kogyo K.K. Reproduced with permission from [2].

## 7.2 Refining of Iridium at the Sibanye–Stillwater South Africa Precious Metals Refinery

The traditional flowsheet employed to separate Ir from Rh has been described by Le, et al. [56]. A large number of steps are involved in this very complex flowsheet including the use of harsh chemicals and organic solvents, high temperature (1,000 °C) ignition of precipitates, digestion and electrolytic refining, and repeated salt recrystallizations among others. Le, et al. [56] state that the separation of Ir from Rh is extremely difficult because of the similar chemical properties of the Rh and Ir chloro anions. Classical PGM Separation Processes are unable to distinguish between these anions with a high degree of selectivity resulting in complex separation flowsheets with multiple separation steps involved. The complexity of the traditional flowsheet and the need to improve the industrial Rh/Ir separation process is recognized by Le, et al. [56] as follows: “These processes are complicated and consume a large amount of energy and thus the development of a simple process to recover these metals from industrial wastes is necessary.”

The substantial difficulties in the traditional Rh/Ir separation flowsheet have been overcome by a simple, compact, and effective MRT™ process (see Figure 6) that has been used for the industrial scale refining of Ir by Sibanye–Stillwater’s South African Precious Metals Refinery since 2015 [18]. The MRT™ system operates by an entirely different mechanism than the traditional system and is highly selective for Ir over Rh.



Sequential steps in the MRT™ iridium separation operation are shown in Figure 9.

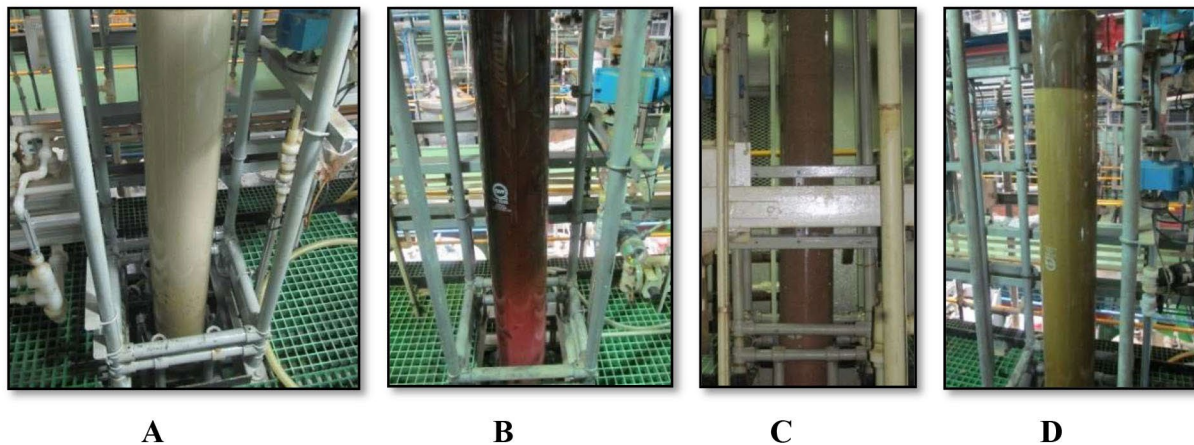


Figure 9. MRT™ Industrial Facility for Iridium Separation and Recovery at the Sibanye-Stillwater South Africa Precious Metal Refinery.

Frame A: unloaded SuperLig® 182 column; Frame B: 6M HCl wash displacing Rh to raffinate after Ir binding to SuperLig® 182; Frames C and D: SuperLig® 182 columns loaded with Ir. Reproduced with permission from [18].

The MRT™ process is fully automated using a supervisory control and data acquisition (SCADA) system. SCADA screens are shown in Figure 10.

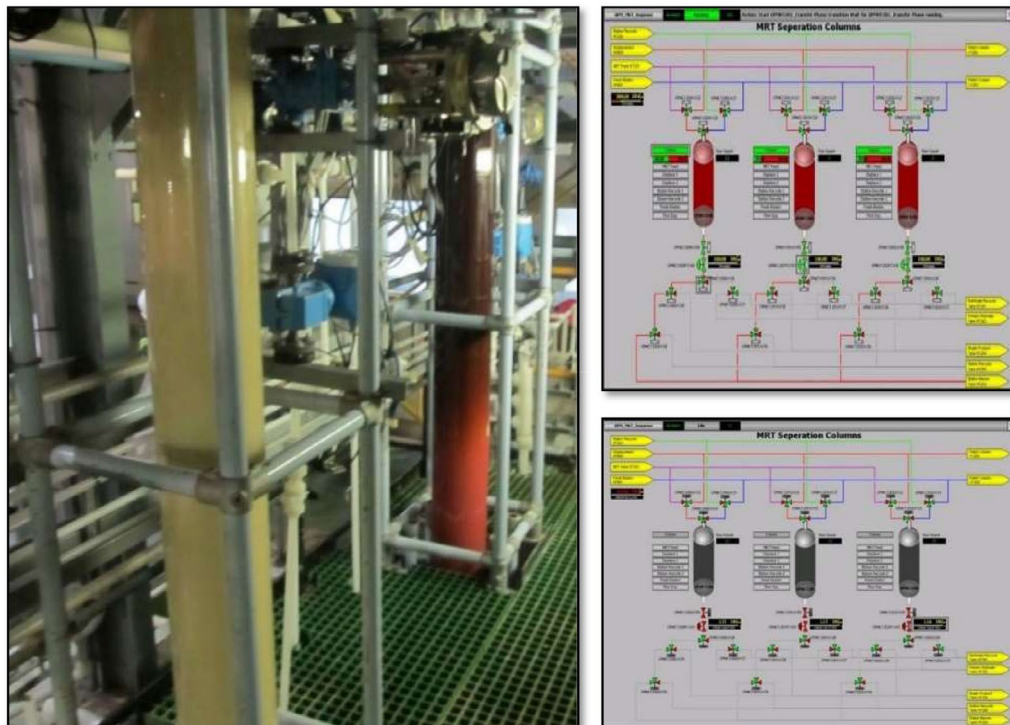


Figure 10. Fully Automated MRT™ Industrial Facility (left) with SCADA Screens (right) at the Sibanye-Stillwater South Africa Precious Metal Refinery.

Reproduced with permission from [18].



### 7.3 Refining of Palladium at Impala Platinum Limited

Impala has used the MRT™ process since the mid-1990s to refine large quantities of Pd at commercial scale [1,4,5]. In this process, Pd (~30 g/L) is selectively separated from a feed stream containing other PGM as well as base metals. The composition (g/L) of a typical feed stream is Au (<0.001), Pt (50–60), Pd (30–40), Rh (8–10), Ru (10–15), Ir (4–5), Fe (8–12), Cu (2–4), and Ni (4–7.) SuperLig® 2 is highly selective for Pd over the other metals present. Prior to implementing the MRT™ process, Impala used classical precipitation methods to refine PGM. Extensive comparative laboratory and pilot tests with MRT™, IX, and SX were made by Impala in the mid-1990s prior to the choice of the MRT™ process for the separation system. The MRT™ process was able to separate Pd in a single pass as a first step in the PGM processing eliminating the need to recover traces of Pd downstream. The classical methods were unable to make this single pass separation of Pd resulting in the requirement for multiple passes downstream.

MRT™ columns installed at the Impala Springs Refinery are shown in Figure 11.

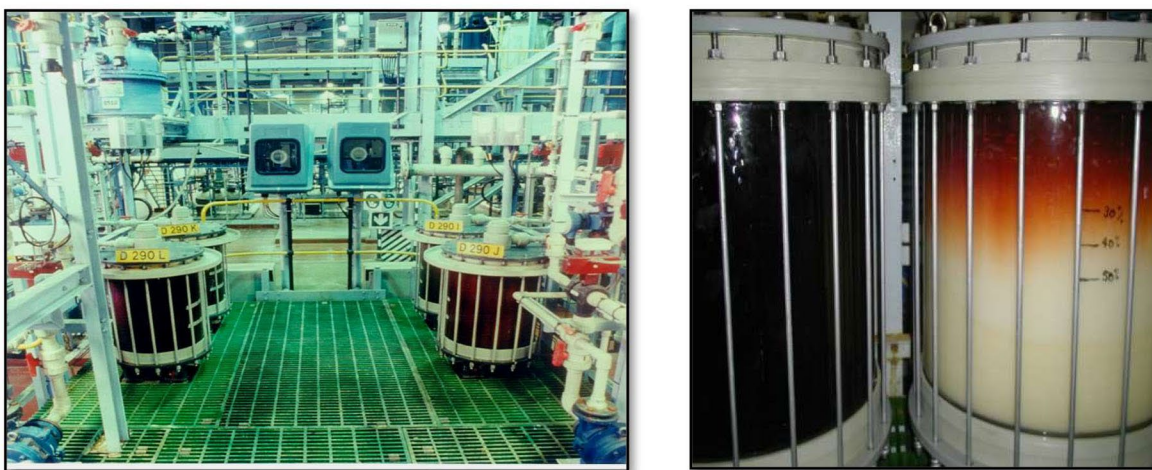


Figure 11. MRT™ Industrial Facility for Palladium Separation and Recovery at Impala Platinum Limited Springs Refinery (left.) On the right frame, in the close-up of the left column, the dark coloration is caused by the loaded Pd. The column on the right in the right frame is in the process of being loaded. It is evident that Pd is retained by SuperLig® 2 upon first contact. Reproduced with permission from [4].

### 7.4 Separation of Palladium from Primary and Spent Secondary Sources at the Boliden Rönnskär Copper Smelter

The MRT™ process is used for the highly selective separation of Pd from primary and spent secondary sources in the precious metals plant at the Boliden Rönnskär copper smelter in Sweden [46b]. Palladium is recycled from e-waste, spent catalytic converter residues, and other materials. The purity of the Pd product is around 99.95%. The recovery (feed product → solution) yield is in the order of 99.99%. Palladium separation is achieved in a single step ensuring no need for additional

steps for Pd recovery downstream.

The MRT™ installation at the Boliden Rönnskär copper smelter is shown in Figure 12 [46b].



Figure 12. MRT™ Industrial Facility for Palladium Separation and Recovery at the Boliden Rönnskär Precious Metals Refinery in Sweden. The column on the left is packed with SuperLig® 2 resin beads. The column on the right is loaded with Pd (dark coloration.) Reproduced with permission from [46b].

Advances made by use of the MRT™ system with their consequences are [46b]:

- highly selective, single step separation of Pd with 99.99% recovery yield eliminating expensive downstream processing
- non-use of organic solvents or harsh chemicals eliminating a host of process, environmental, and social problems associated with the use of these solvents
- minimal waste generation minimizing potential environmental and social concerns
- hundred-fold or more concentration of Pd in the elution step reducing equipment size and enabling the economic recovery of Pd from formerly inaccessible, low concentration level solutions
- rapid binding and release kinetics permitting inclusion in the plant process flow-sheet on a real time basis
- compact, simple separation systems conserving space, labor, time, chemicals, energy and infrastructure with significant reduction in CAPEX and OPEX values
- attainment of a circular economy in Pd making possible the achievement of Pd sustainability
- minimal use of fossil fuel-derived processes or chemicals insuring a minimal carbon footprint

## 7.5 On-Site Separation of Palladium from Industrial Plating Baths using a Modular Mobile Unit.

Plating baths are examples of the many applications of Pd in commerce. Typically, the Pd is present in the bath in colloidal form at low concentrations. The colloidal Pd is consumed during use through adsorption on parts, adsorption on rack coating, chemical breakdown, and drag-out. It is desirable to recover as much of this waste Pd as possible for reuse.

SepraMet, Ltd. has deployed an MRT™ unit to recover Pd from a colloidal tin (Sn)/palladium activator drag-out bath at a major North American plating on plastics (POP) line [46a,46c,54]. In operation, the modular MRT™ unit for Pd separation and recovery from plating baths using SuperLig® 277 is provided to a customer, loaded with spent Pd, and returned to SepraMet for Pd retrieval. The regenerated MRT™ unit can then be returned to the customer for reloading in a circular process that can be repeated indefinitely.

The modular MRT™ unit and a depiction of the circular process are shown in Figure 13.

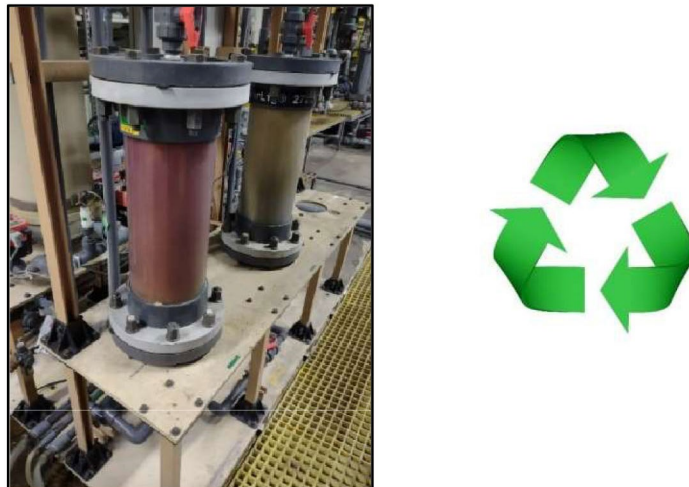


Figure 13. Industrial Installation of MRT™ Modular unit (left) for Separation and Recovery of Palladium from Plating Baths. The circular process is depicted on the right.

The MRT™ system replaced an IX process at the customer location that had proven inadequate for making the required separation. Limitations of the IX method included [46c]:

- applicability to only one of the two portions of the conventional POP operation
- not being applicable to the direct metallization lines
- not being selective for capture of Pd over Sn present in the plating bath leading to the requirement for an additional separation procedure to obtain pure Pd
- requirement of an additional destructive and energy-intensive smelting process to recover Pd
- inconsistency in the quantity of Pd recovered over time

The MRT™ system enables [46c]:

- recovery of Pd from both activator and accelerator sections of the conventional POP lines
- use on the activator section of direct metallization lines
- selective one-step separation of Pd with no retention of Sn
- production of a consistent yield of Pd
- recovery of both Pd(0) and Pd(II)
- constancy in the flow rates and contents of process tanks

Significant amounts of Pd previously going to waste are recovered using the MRT™ process.

Beneficial features of the MRT™ system include [46c]:

- high selectivity and high recovery yields for Pd present at low concentration levels
- no use of organic solvents or chemical separating agents
- operation over a range of temperatures at atmospheric pressure
- no use of energy-intensive processes such as thermal processing by burning or incineration
- a simple, closed system with zero emissions
- use of simple chemicals and dilute reagents that mostly can be recycled
- no customer liability
- no negative environmental consequences

Recovery of Pd conserves a valuable resource while minimizing drag-out costs, providing environmental benefits, and off-setting production costs. Palladium in these wastes would normally be discarded because recovery is not economical. A major economic and public relations benefit to the customer is the elimination of the need to dispose of the waste with attendant time, labor, space, public relations issues, and environmental costs [46c].

Modular MRT™ systems have the possibility of (1) significantly increasing the separation rates and recovery yields of PGM or other metals of value in global locations where recycling rates are very low [34a,57,58] and (2) enabling economic recovery of currently discarded metals when present at low levels in industrial processes including mining waste solutions and tailings, refining streams, waste streams, and processing streams derived from e-waste. Marketing of pure metal products recovered in the modular approach can offset recovery costs. Modular MRT™ separation processes offer promise for achieving sustainable, economic metal separation and recovery of valuable critical metals that are presently being discarded.

## **7.6 Selective Separation and Purification of Iridium, Platinum, and Ruthenium for Use in the Emerging Hydrogen Economy.**

There is much current interest in the use of hydrogen as an alternative energy source to fossil fuels to generate power for domestic heating and in the industrial and transport sectors [59a,59b,60-- 63]. The potential for this technology is enormous and includes, perhaps, revolutionizing the global energy economy toward a predicted hydrogen economy/society. An appealing feature of this technology is



the wide distribution and availability of hydrogen as a source element ensuring plentiful supply. A major challenge is retrieving hydrogen effectively and economically from water or other compounds in which it is found.

One promising method for hydrogen production from water is by a membrane electrode assembly (MEA) fuel cell process, which requires the use of high corrosion-resistant materials (Ir, Pt, and Ru) for the catalysis components of the apparatus [59a]. Iridium is an important component because it is the most corrosion-resistant metal known and has unique catalytic properties. However, in order to ensure sufficient Ir, a circular economy in which Ir is used, recycled, and reused is very important. In a White Paper [59b], Johnson Matthey expresses confidence *“that iridium supply can be made to support PEM electrolyser growth ambitions to 2030 and beyond if the supply chain works together to innovate, recycle and reuse this critical element.”*

As the hydrogen economy advances, several companies have begun manufacturing PGM-containing MEA assemblies. One of these, Isondo Precious Metals (IPM) in South Africa, recently started construction of a state-of-the-art industrial plant to manufacture MEAs for the global automotive, aeromotive, stationary power and hydrogen generation technology supply chains [64]. IPM selected the MRT™ process to recycle Ir, Pt and Ru from IPM's manufacturing operations as well as from spent MEAs [19]. The more efficient recycling of Ir, Pt and Ru using the MRT™ process promises to result in a circular economy for these individual PGM and make a major contribution to their sustainability.

## **8 Commercial Comparison of MRT™ and Classical PGM Separation Processes for Industrial PGM Separations**

High performance MRT™ PGM separation systems are commercially advantageous because the value of their performance far exceeds the associated costs when compared with Classical PGM Separation Processes. The positive benefit-cost ratio of MRT™ PGM separation systems is derived from simplification of PGM refining process flowsheets and minimization of whole-life or lifetime costs (which include financial as well as environmental and social costs.) The stability, durability and cost-effectiveness of SuperLig® resins have been proven by their industrial use in MRT™ PGM refining systems over several decades.

We have summarized and compared MRT™ and Classical PGM Separation Processes for industrial PGM separations as follows [16a]:

*One perceived advantage of less selective technologies, such as IX and SX, over MRT is the low price of the resins or reagents involved. However, this price is not indicative of the true costs incurred by these technologies. As compared to MRT, the negative externality costs associated with less selective technologies are paid for in more complex capital equipment systems; larger system footprints; limited or no resin reusability; extensive use of sub-optimal and/or hazardous and flammable chemicals, such as solvents, that introduce substantial risk into the process and require complicated operational and environmental protocols; higher energy costs; lack of system flexibility to target specific, commercially important metals early in the flowsheet; higher number of separation stages; increased volumes*



*of eluates, washes, and wastes; larger and more complex waste treatment systems; slower metal binding and release; incomplete and slow extraction and recovery of the target metal; complex pre- and post-treatment regimens; lower metal purities; lower metal recoveries; higher metal losses; and longer retention of valuable metals in the process, resulting in high metal inventories and working capital costs. Low selectivity means that traces of impurity metals follow target metals, and this translates into the creation of multiple side streams that then need to be processed, resulting in higher costs, greater environmental liabilities and increased worker exposure. All the above factors must be taken into account to determine the true cost effectiveness of a separations technology.*

Due to the proprietary interests involved, there is a lack of publicly available information for direct comparisons of CAPEX and OPEX for MRT™ and Classical PGM Separation Processes. However, compelling evidence that MRT™ PGM systems have lower CAPEX and OPEX is found in the increasing number of industrial installations of MRT™ PGM systems worldwide. Prior to installation of commercial MRT™ PGM systems, extensive comparison tests of MRT™ with Classical PGM Separation Processes are routinely made by companies for economic and process evaluation (see Section 7.)

The complexity of Classical PGM Separation Processes for individual PGM separations is illustrated by the industrial separation of Ir and Rh (see Section 7.2.) High energy, material, infrastructure, and labor costs result. Added to these costs are larger and more complex waste treatment systems; appreciable carbon footprint; and extended time periods for achieving effective separations resulting in long metal pipeline retention times and high metal financing costs.

Central to the cost-effectiveness of MRT™ separation systems are the much higher separation factors (SF) exhibited by MRT™ over those exhibited by SX and IX in comparable separation systems. One example is found in Figure 2, where a comparison is given of the relative effectiveness of MRT™, SX-based D2EHPA, and IX-based Purolite S950 in removing Cd from a Co electrolyte solution containing Mg and Mn impurities. This example does not involve PGM separations. However, the same comparative principles are applicable to the relative SF values for MRT™, SX and IX for other metals of interest, including PGM. The SF values in Figure 2 for the D2EHPA and Purolite S950 processes were several orders of magnitude lower than those for MRT™ suggesting that CAPEX and OPEX for these technologies would be much greater than those for MRT™ for Cd removal. Similar SF results would be expected for separations of individual PGM using MRT™ and Classical PGM Separation Processes.

Lower CAPEX and OPEX values for MRT™ processes result from the green engineering and green chemistry advances listed in Tables 4 and 5. Very high single pass recovery rates of individual PGM by MRT™ processes coupled with rapid processing times maximize the financial rate of return and minimize working capital needs due to low metal inventories. Green chemistry processes of the MRT™ type are desirable for 21st century individual PGM separations where increasingly stringent environmental and health standards must be achieved in concert with intensifying demands for economic efficiency as PGM applications continue to expand [30,46c].

## 9 Conclusions

The selective separation and recovery at industrial scale of individual PGM from primary and secondary sources using MRT™ processes has been reviewed. Very high single pass recovery yields and product purities (99.95–99.99%) are obtained leading to a circular economy for individual PGM and increased metal sustainability for these critical resources. Principles of molecular recognition, green chemistry, and green engineering that are important in designing PGM-selective MRT™ processes have been discussed and these processes have been contrasted with Classical PGM Separation Processes used in the PGM refining industry.

Major conclusions follow:

1. The industrial-scale adoption of MRT™ processes in the mid-1990s by a top secondary PGM refiner, Tanaka Kikinzoku Kogyo K.K. [1-3] and a top primary PGM refiner, Impala Platinum Limited [1,4,5] marked the first disruptive innovation in industrial scale PGM refining since the early widespread use of Classical PGM Separation Processes in the mid-20th century.
2. PGM are listed as critical metals in the US and EU because they are essential to the economies of these nations but have supply chains associated with high risk. Over 90% of global mined PGM production comes from just three countries: Russia, South Africa, and Zimbabwe, presenting the potential for supply disruption [1,24,28,31]. In addition, there is a constantly diminishing supply of mined PGM ore that becomes more expensive to mine with time. Limited prospects exist for new major global discoveries of mineable PGM ore [33].
3. The status of the PGM supply-demand balance is precarious with the gap widening [9,28,65]. Achievement of global sustainability requires enhancement of the PGM supply by increasing the sourcing of PGM from spent secondary sources through recycling.
4. Globally, in 2021, approximately 21% of Pt, 33% of Pd, and 32% of Rh supply came from metals recycled from spent secondary products, largely from spent automotive catalytic converters [27b]. There is a great need to increase the recycling rate of individual PGM from spent secondary sources, such as those in Table 1 at their end-of-life. For example, recycling of PGM from spent electronics is 5–10% [58]. Increasing recycling rates of PGM from these spent sources would access a large quantity of PGM that is currently not being recovered.
5. MRT™ processes exemplify the type of industrially proven selective separation technologies needed to meet increasingly stringent environmental standards and to more efficiently and cost effectively separate and recover individual PGM from primary mine feeds as well as from lowgrade levels present in many waste streams and spent products [10,12,37,66].
6. MRT™ systems are effective in performing selective industrial separations of individual PGM in a compact column-based operating mode from both primary and secondary sources. Green chemistry and green engineering advances of these systems are presented in Tables 4 and 5.

7. Highly selective single pass recovery rates and high product purities (99.95–99.99%) of individual PGM at the industrial scale from primary and secondary sources are obtained in MRT™ processes.
8. SuperLig® MRT™ systems have been adopted at industrial-scale by top secondary and primary PGM refiners including Tanaka Kikinzoku Kogyo K.K. [1–3,55], Sibanye–Stillwater [18], Boliden Rönnskär [46b], and Impala Platinum [1,4,5].
9. Recycling rates of individual PGM from spent products not normally recycled can be enhanced using MRT™ processes. An example is given of a modular unit (Figure 13) capable of performing separation and recovery processes at an industrial site of low-level Pd from plating bath waste streams. In a circular economy mode, the loaded unit is sent to a central site where the Pd is retrieved, the column is recharged, and then returned to the industrial site for reloading. Accessing spent secondary sources such as this could make a major contribution to individual PGM sustainability since it is estimated that less than half of the PGM mined is recovered by recycling [27a,63].
10. The expanding use of new PGM-containing products including catalysts necessitates more efficient and selective separation processes to perform the increasingly complex separations that will be needed for efficient, cost-effective recycling of individual PGM from these products. An example is given in Section 7.6 involving MEAs, essential to the emerging green hydrogen energy economy, which employs Ir, Ru and Pt as catalysts for water oxidation [19].
11. The demonstration with numerous examples shows that MRT™ systems have superior performance in PGM refining to Classical PGM Separation Processes which are profligate in their use of energy, time, and resources (Section 8.)

Adherence to green chemistry and green engineering principles in individual PGM separation and recovery operations is essential to the goal of achieving greater PGM sustainability in a circular economy [10,22,30]. The effectiveness of MRT™ systems in enhancing the recovery of individual PGM from a variety of primary and spent secondary sources in industrial settings has been shown, a major step toward greater PGM sustainability. This study points to a future where metal sustainability is the norm, resources are conserved, waste generation is minimal, and carbon generation is close to zero.

## AUTHOR CONTRIBUTIONS

Steven R. Izatt and Reed M. Izatt conceived the preparation of the paper. Ronald L. Bruening, Luis Navarro, and Krzysztof E. Krakowiak contributed to the experimental work and the process comparisons for the PGM systems described. Steven R. Izatt performed the business aspects of the study.

## CONFLICTS OF INTEREST

In accordance with our ethical obligation as researchers, we report that IBC Advanced Technologies, Inc. (IBC) markets Molecular Recognition Technology™ (MRT™) and the SuperLig® products mentioned in this review. The authors are owners and/or employees of IBC. We consider that the importance of individual PGM separations in the world today makes it important that the separations community be aware of these important technical advances made by IBC. We are objectively reporting our results together with reported results of others taken from the literature.

## REFERENCES

1. Izatt, S.R., Bruening, R.L., Izatt, N.E., 2012. Metals Separations and Recovery in the Mining Industry. *Journal of Metals*, 64, 1279–1284.
2. Ichiishi, S., Izatt, S.R., Bruening, R.L., Izatt, N.E., Bruening, M.L., Dale, J.B., 2000. A Commercial MRT Process for the Recovery and Purification of Rhodium from a Refinery Feedstream Containing Platinum Group Metals (PGMs) and Base Metal Contaminants, International Precious Metals Institute, 24th Annual Conference, Williamsburg, Virginia, June 11–14.
3. Ueda, T., Ichiishi, S., Okuda, A., Matsutani, K., 2016. Refining and Recycling Technologies for Precious Metals in Metal Sustainability: Global Challenges, Consequences, and Prospects; Izatt, R.M. (Ed.), Wiley, Oxford, U.K., pp 333–360.
4. Black, W.H., Izatt, S.R., Dale, J.B., Bruening, R.L., 2006. The Application of Molecular Recognition Technology (MRT) in the Palladium Refining Process at Impala and Other Selected Commercial Applications, International Precious Metals Institute, 30th Annual Conference, Las Vegas, Nevada, June 10–13.
5. Mooiman, M.B., Sole, K.C., Dinham, M., 2016. The Precious Metals Industry: Global Challenges, Responses, and Prospects in Metal Sustainability: Global Challenges, Consequences, and Prospects; Izatt, R.M. (Ed.), Wiley, Oxford, U.K., pp 361–396.
6. Krogscheepers, C., Gossel, S.J., 2015. Input Cost and International Demand Effects on the Production of Platinum Group Metals in South Africa. *Resources Policy*, 45, 193–201.
7. Makua, L., Langa, K., Saguru, C., Ndlovu, S., 2019. PGM Recovery from a Pregnant Leach Solution using Solvent Extraction and Cloud Point Extraction: A Preliminary Comparison, *Journal of the Southern African Institute of Mining and Metallurgy*, 119. DOI: <http://dx.doi.org/10.17159/2411-9717/17/484/2019>
8. Mudd, G., 2012. Key Trends in the Resource Sustainability of Platinum Group Elements, *Ore Geology Reviews*, 46, 106–117.

9. Nassar, N.T., Fortier, S.M., 2021. Methodology and Technical Input for the 2021 Review and Revision of the U./S, Critical Materials List: U.S. Geological Survey Open-File Report 2021-1045, 31 pp., <https://doi.org/10.3133/ofr20211045> (accessed May 3, 2023).
10. Izatt, R.M., Izatt, S.R., Izatt, N.E., Krakowiak, K.E., Bruening, R.L., Navarro, L., 2015. Industrial Applications of Molecular Recognition Technology to Green Chemistry Separations of Platinum Group Metals and Selective Removal of Metal Impurities from Process Streams, *Green Chemistry*, 17, 2236-2245.
11. Karim S., Ting, Y-P., 2021. Recycling Pathways for Platinum Group Metals from Spent Automotive Catalyst: A Review on Conventional Approaches and Bio-processes, *Resources Conservation and Recycling*, 170, 105588.
12. O'Connor, M.P., Zimmerman, J.B., Anastas P.T., Plata, D.L., 2016. A Strategy for Material Supply Chain Sustainability: Enabling a Circular Economy in the Electronics Industry through Green Engineering, *ACS Sustainable Chemistry & Engineering*, 4, 5879-5888.
13. Vereycken, W., Riaño, S., Van Gerven, T., Binnemans, K., 2021. Extraction Behaviour and Separation of Precious and Base Metals from Chloride, Bromide, and Iodide Media using Undiluted Halide Ionic Liquids. *ACS Sustainable Chemistry & Engineering*, 18, 16-34.
14. Kaya, M., 2016. Recovery of Metals and Nonmetals from Electronic Waste by Physical and Chemical Recycling Processes, *Waste Management*, 57, 64-90.
15. Anastas, P.T., Zimmerman, J.B., 2018. The United Nations Sustainability Goals: How can Sustainable Chemistry Contribute? *Current Opinion in Green and Sustainable Chemistry*, 13, 150-153.
16. (a) Izatt, S.R., et al., 2016. Selective Recovery of Platinum Group Metals and Rare Earth Metals from Complex Matrices using a Green Chemistry-Molecular Recognition Technology Approach in *Metal Sustainability: Global Challenges, Consequences, and Prospects*, Izatt, R.M., (Ed.), Wiley: Oxford, U.K., pp 317-332. (b) Izatt, N.E., Bruening, R.L., Krakowiak, K.E., Izatt, S.R., 2000. Contributions of Professor Reed M. Izatt to Molecular Recognition Technology: From Laboratory to Commercial Application. *Industrial & Engineering Chemistry Research*, 39, 3405-3411.
17. Izatt, S.R., Izatt, R.M., Bruening, R.L., Krakowiak, K.E. 2020. Selective Separation and Purification of Platinum Group Metals, Rare Earth Elements, and Cobalt from Primary and Secondary Sources Using a Green Chemistry SuperLig® Molecular Recognition Technology (MRT) Approach in *Critical and Rare Earth Elements: Recovery from Secondary Sources*; Abhilash and Akcil, A., (Eds.), CRC Press, New York, pp. 203-232.
18. Kwinana, P., Masinga, T., Izatt, S.R., Bruening, R.L., Kujanpää, J., Izatt, R.M. 2021. Industrial-scale Refining of Iridium at Sibanye-Stillwater's South African Precious Metals Refinery using SuperLig® Molecular Recognition Technology™ (MRT™), International Precious Metals Institute 45th Annual Conference, Reno, Nevada, October 6-9.



19. IBC Advanced Technologies, Inc., Press Release: IBC selected by Isondo Precious Metals to supply SuperLig® Molecular Recognition Technology (MRT) System for Platinum Group Metals and Gold Refining, July 19, 2021, <https://www.prnewswire.com/in/news-releases/ibc-selected-byisondo-precious-metals-to-supply-superlig-r-molecular-recognition-technology-mrt-system-forplatinum-group-metals-and-gold-production-818113969.html> (accessed May 4, 2023).
20. Ehrlich, H.V., Buslaeva, T.M., Maryutina, T.A., 2017. Trends in Sorption Recovery of Platinum Metals: A Critical Survey. *Russian Journal of Inorganic Chemistry*, 62, 1797-1818.
21. Zheng, H., Ding, Y., Wen, Q., Liu, B., Zhang, S. 2021. Separation and Purification of Platinum Group Metals from Aqueous Solution: Recent Developments and Industrial Applications, *Resources Conservation and Recycling*, 167, 105417.
22. Yakoumis, I., Panou, M., Moschovi, A.M., Pantias, D., 2021. Recovery of Platinum Group Metals from Spent Automotive Catalysts: A Review. *Cleaner Engineering and Technology*, 3, 100112.
23. Fortier, S.M., Nassar, N.T., Lederer, G.W., Brainard, J., Gambogi, J., McCullough, E.A., 2018. Draft Critical Mineral List—Summary of Methodology and Background Information—U.S. Geological Survey Technical Input Document in Response to Secretarial Order No. 3359: U.S. Geological Survey Open-File Report 2018–1021, 15 pp., <https://doi.org/10.3133/ofr20181021> (accessed May 4, 2023).
24. European Commission, Study on the Review of the List of Critical Raw Materials: Criticality Assessments, June 2017, B-1049, Brussels, Belgium, <http://hytechcycling.eu/wpcontent/uploads/Study-on-the-review-of-the-list-of-Critical-Raw-Materials.pdf> (accessed May 4, 2023).
25. European Commission, Study on the EU's list of Critical Raw Materials (2020), Factsheets on Critical Raw Materials, [https://lecho-circulaire.com/wpcontent/uploads/2020/09/CRM\\_2020\\_Factsheets\\_critical\\_Final.pdf](https://lecho-circulaire.com/wpcontent/uploads/2020/09/CRM_2020_Factsheets_critical_Final.pdf) (accessed May 4, 2023).
26. Axet M.R., Philippot, K., 2020. Catalysis with Colloidal Ruthenium Nanoparticles, *Chemical Reviews*, 120, 1085-1145.
27. (a) Rasmussen, K.D., Wenzel, H., Bangs, C., Petavratzi, E., Liu, G., 2019. Platinum Demand and Potential Bottlenecks in the Global Green Transition: A Dynamic Material Flow Analysis, *Environmental Science & Technology*, 53, 11541-11551; (b) Cowley, A. JM PGM Market Report, May 2022, <https://matthey.com/documents/161599/509428/PGM-market-report-May-2022.pdf/542bcada-f4aca673-5f95-ad1bbfca5106?t=1655877358676>, Accessed May 4, 2023
28. Firmansyah, M.L., Yoshida, W., Hanada, T., Goto, M., 2020. Application of Ionic Liquids in Solvent Extraction of Platinum Group Metals, *Solvent Extraction Research and Development*, 27, 1-24.
29. Hagelüken, C., 2014. Recycling of (Critical) Metals in *Critical Metals Handbook*; Gunn, G., (Ed.), Wiley, Oxford, U.K., pp 41-69.

30. Izatt, R.M., Izatt, S.R., Bruening, R.L., Izatt, N.E., Moyer, B.A., 2014. Challenges to Achievement of Metal Sustainability in Our High-Tech Society. *Chemical Society Reviews*, 43, 2451–2475.
31. Zientek, M.L., Loferski, P.J., Parks, H.L., Schulte, R.F.; Seal, R. R. II. Platinum-group Elements, Chap. N of Schulz, K.J., DeYoung, Jr. J.H., Seal, R.R. II, Bradley, D.C., (Eds.), *Critical Mineral Resources of the United States—Economic and Environmental Geology and Prospects for Future Supply*: U.S. Geological Survey Professional Paper 1802-N, 2017, pp N1–N91, <https://doi.org/10.3133/pp1802N> (accessed May 4, 2023).
32. (a) Jones, R.T., 2005. An Overview of Southern African PGM Smelting, An Overview of Southern African PGM Smelting, *Nickel and Cobalt 2005: Challenges in Extraction and Production*, 44th Annual Conference of Metallurgists, Calgary, Alberta, Canada, 21–24 August, pp.147–178; (b) Nicol, G., Goosey, E., Yildiz, D.S., Loving, E., Nguyen, V.T., Riaño, S., Yakoumis, I., Martinez, A.M., Siriwardana, A., Unzurrunzaga, A., et al., 2021. Platinum Group Metals Recovery using Secondary Raw Materials (PLATIRUS): Project Overview with a Focus on Processing Spent Autocatalyst, *Johnson Matthey Technology Review*, 65, 127–147.
33. Gordon, R.B., Bertram, M., Graedel, T.E., 2006. Metal Stocks and Sustainability, *Proceedings of the National Academy of Sciences USA*, 103, 1209–1214.
34. (a) Izatt, R.M., Hagelüken, C., 2016. Recycling and Sustainable Utilization of Precious and Specialty Metals in Metal Sustainability: Global Challenges, Consequences, and Prospects; Izatt, R.M., (Ed.), Wiley, Oxford, U.K., pp. 1–22; (b) Zupanc, A., Install, J. Jereb, M.; Repo, T. 2022. Sustainable and Selective Modern Methods of Noble Metal Recycling, *Angewandte Chemie International Edition*, 62, e202214453.
35. Heederik, D., Jacobs, J., Samadi, S., van Rooy, F., Portengen, L., Houba, H., 2015. Exposure- Response Analyses for Platinum Salt-exposed Workers and Sensitization: A Retrospective Cohort Study Among Newly Exposed Workers using Routinely Collected Surveillance Data. *Journal of Allergy and Clinical Immunology*, 137, 922–929.
36. Crundwell, F.K., Moats, M.S., Ramachandran, V., Robinson, T.G., Davenport, W.G. 2011. *Extractive Metallurgy of Nickel, Cobalt, and Platinum-Group Metals*, Elsevier: Amsterdam, pp. 520–527.
37. Ilyas, S., Kim, H., Srivastava, R.R., 2021. Integrated Recovery Processes for Precious Metals from Urban Mine Sources and Case Studies in Sustainable Urban Mining of Precious Metals, Ilyas, S., Kim, S.H., Srivastava, R.R., (Eds.), CRC Press, Boca Raton, Florida, pp 214–240.
38. (a) van Deventer, J., du Preez, R., Scott, S., Izatt, S.R., 2007. Cadmium Removal from Cobalt Electrolyte, *The Fourth Southern African Conference on Base Metals*, Symposium Series S47; Swakopmund, Namibia, July 23–27; (b) Izatt, S.R., Izatt, N.E., Bruening, R.L., 2011. Review of Selective Separations of Cobalt, Uranium, Zinc, Nickel, and Associated Contaminants from Various Process Streams, *The Southern African Institute of Mining and Metallurgy*, 6th Southern African Base Metals Conference, <https://www.saimm.co.za/Conferences/BM2011/221-Izatt.pdf> (accessed May 4, 2023).

39. Ford, K. H. U.S. Department of Defense, ESTCP Project: CP-9805, Demonstration of Removal, Separation, and Recovery of Heavy Metals from Industrial Waste Streams using Molecular Recognition Technology (MRT), January 2003. <https://apps.dtic.mil/sti/citations/ADA409943> (accessed May 5, 2023).
40. Anastas, P., Eghbali, N., 2010. Green Chemistry: Principles and Practice. *Chemical Society Reviews*, 39, 301-312.
41. Anastas, P.T., Zimmerman, J.B., 2003. Design Through the 12 Principles of Green Engineering, *Environmental Science & Technology*, 94A-101A, March 1.
42. Williams, I. D., 2016. Global Metal Reuse, and Formal and Informal Recycling from Electronic and Other High-tech Wastes in Global Challenges, Consequences, and Prospects, Izatt, R.M., (Ed), Wiley, Oxford, U.K., pp 33-51.
43. Brundtland Commission, *Our Common Future*, Oxford, U.K., 1987.
44. Ganesh, K.N., Zhang, D., Miller, S.J., Rossen, K., Chirik, P.J., Kozlowski, M.C., Zimmerman, J.B., Brooks, B.W., Savage, P.E., Allen, D.T., et al., 2021. Green Chemistry: A Framework for a Sustainable Future, *Environmental Science & Technology*, 55, 13, 8459-8463. <https://doi.org/10.1021/acs.est.1c03762> (accessed May 4, 2023).
45. Izatt, R.M., Izatt, S.R., Izatt, N.E., Krakowiak, K.E., Bruening, R.L., 2017. Green Chemistry Molecular Recognition Processes Applied to Metal Separations in Ore Beneficiation, Element Recycling, Metal Remediation, and Elemental Analysis in Beach, E.S., Kundu, S., (Eds.), *Handbook of Green Chemistry Volume 12 – Tools for Green Chemistry*, Anastas, P.T., (Ed.), (*Handbook of Green Chemistry Series*), Wiley-VCH: Weinheim, pp 189-240.
46. (a) Izatt, S.R., Bruening, R.L., Izatt, R.M., Kujanpää, J.K., 2017. Recovery from Low Grade Resources of Platinum Group Metals and Gold Using Molecular Recognition Technology (MRT), International Precious Metals Institute 41st Annual Conference, Orlando, Florida, June 10-13; (b) Izatt, S.R., Bruening, R.L., Izatt, R.M., 2022. Highly Selective Separation and Recovery at High Purity of Palladium at the Boliden Rönnskär Copper Smelter using Molecular Recognition Technology™ (MRT™), International Precious Metals Institute 46th Annual Conference, Orlando, Florida, June 11-14; (c) Izatt, S.R., Bruening, R.L., Izatt, N.E., Izatt, R.M. 2020. Precious Metal Separation and Recovery from Primary and Secondary Sources using SuperLig® Molecular Recognition Technology Processes. *The IPMI Journal*, 1, 51-81, [https://cdn.ymaws.com/www.ipmi.org/resource/collection/FC2EBE3B-5DF2-4E56-B592-11B446D5ACEF/IPMI\\_Journal\\_Vol\\_1\\_No\\_1\\_2020.pdf](https://cdn.ymaws.com/www.ipmi.org/resource/collection/FC2EBE3B-5DF2-4E56-B592-11B446D5ACEF/IPMI_Journal_Vol_1_No_1_2020.pdf) (accessed May 4, 2023).
47. Izatt, S.R., Bruening, R.L., Izatt, N.E., 2014. Green Chemistry Approach to Platinum Group Metals Refining, International Precious Metals Institute, 38th Annual Conference, Orlando, Florida, June 7-10.
48. Izatt, S.R., Dale, J.B., Bruening, R.L., 2007. *The Application of Molecular Recognition Technology*

(MRT) to Refining of Platinum and Ruthenium, International Precious Metals Institute, 31st Annual Conference, Miami, Florida, June 9-12.

49. Xiaotang, H., Xilong, W., Izatt, S.R., Bruening, R.L., 2016. Processing of Spent Automotive Catalysts Using SuperLig® Molecular Recognition Technology (MRT) Products, International Precious Metals Institute, 40th Annual Conference, Phoenix, Arizona, June 11-14.

50. Bruening, R.L., Dale, J.B., Izatt, R.M., Izatt, S.R., 1995. Use of SuperLig® Materials at Pilot or Industrial Scale to Recover at High Purity Rh, Pt, and Pd from Spent Catalyst, Spring 1995 National AIChE Meeting, Houston, Texas, March 29-23.

51. Izatt, N.E., Izatt, S.R., Bruening, R.L., Dale, J.B., 2010. Review of Applications of SuperLig® Molecular Recognition Technology Products for the Gold Industry, ALTA 2010 Gold Symposium, Perth, Australia, May 24-29.

52. Izatt, S.R., Mansur, D.M., 2006. Environmentally Friendly Recovery of Precious Metals from Spent Catalysts, International Precious Metals Institute Petroleum Seminar, Houston, Texas, November 13-14.

53. Ezawa, N., Izatt, S.R., Bruening, R.L., Izatt, N.E., Bruening, M.L., Dale, J.B., 2000. Extraction and Recovery of Precious Metals from Plating Solutions Using Molecular Recognition Technology. Transactions of the Institute of Metal Finishing, 78, Part 6, 238-242

54. Izatt, S.R., King, J. 2017. Palladium Recovery from Tin/Palladium Activator Drag-Out Using Molecular Recognition Technology, SUR/FIN Manufacturing & Technology Trade Show & Conference, Atlanta, Georgia, June 19-21.

55. Izatt, S.R., Izatt, N.E., Bruening, R.L., Dale, J.B., 2009. A Commercial Molecular Recognition Technology (MRT) Process for the Recovery and Purification of Rhodium from a Complex Refinery Feed Stream, International Precious Metals Institute, 33rd Annual Conference, Orlando, Florida, June 13-16.

56. Le, M.N., Lee, M.S., Senanayake, G., 2018. A Short Review of the Separation of Iridium and Rhodium from Hydrochloric Acid Solutions by Solvent Extraction. Journal of Solution Chemistry, 47, 1373-1394.

57. Kopacek, B., 2013. Mobile Hydrometallurgy to Recover Rare and Precious Metals from WEEE, 15th Workshop on International Stability, Technology, and Culture, The International Federation of Automatic Control, Prishtina, Kosovo, June 6-8, IFAC Proceedings Volumes (IFAC-PapersOnline) 15 (PART1), pp 5-9.

58. Reck, B.K., Graedel, T.E., 2012. Challenges in Metal Recycling, Science, 337, 690-694.

59. (a) Miller, H.A., Bouzek, K., Hnat, J., Loos, S., Bernäcker, C.I., Weissgärber, T., Röntzsch, L., Meier-

Haack, J., 2020. Green Hydrogen from Anion Exchange Membrane Water Electrolysis: A Review of Recent Developments in Critical Materials and Operating Conditions. *Sustainable Energy and Fuels*, 4, 2114–2133; (b) Johnson Matthey White Paper. Two Key Focus Areas will Ensure Iridium Availability does not Stall Electrolyser Growth. <https://matthey.com/documents/161599/0/JM+Iridium+White+Paper.pdf/db45aebe-8182-2fc1-548a-a3072a4e6423?t=1669022842596> (accessed May 5, 2023).

60. Mølmen, L., Eiler, K., Fast, L., Leisner, P., Pellicer, A., 2021. Recent Advances in Catalyst Materials for Proton Exchange Membrane Fuel Cells. *APL Materials*, 9, 040702.

61. Bezerra, L.S., Maia, G., 2020. Developing Efficient Catalysts for the OER and ORR using a Combination of Co, Ni, and Pt Oxides along with Graphene Nanoribbons and NiCo<sub>2</sub>O<sub>4</sub>. *Journal of Materials Chemistry A*, 6, 17691–17705.

62. Stephen, A.J., Rees, N.V., Mikheenko, I., Macaskie, L.E., 2019. Platinum and Palladium Bio-synthesized Nanoparticles as Sustainable Fuel Cell Catalysts. *Frontiers in Energy Research*, July 24. doi: 10.3389/fenrg.2019.00066, <https://www.frontiersin.org/articles/10.3389/fenrg.2019.00066/full> Accessed May 5, 2023.

63. Cowley, M., Johnson Matthey PGM Market Report, May 2021, <https://matthey.com/documents/161599/162993/JM-Pgm-Market-Report-May-2021.pdf/b954f429-7c60-f31e-9ebd-a47f0c87ea9d?t=1650968145902> Accessed May 5, 2023.

64. Isondo Precious Metals, Establishing a First of Its Kind Industrial-scale Manufacturing Plant for Electrolyser and Fuel Cell Components, <https://www.isondopm.com/> Accessed May 5, 2023.

65. Cowley, M., Johnson Matthey PGM Market Report, February 2021, <https://matthey.com/en/news/2021/pgm-market-report-february-2021> Accessed May 5, 2023).

66. Nguyen, V.T., Riaño, S., Aktan, E., Deferm, C., Fransaer, J., Binnemans, K., 2021. Solvometallurgical Recovery of Platinum Group Metals from Spent Automotive Catalysts, *ACS Sustainable Chemistry & Engineering*, 9, 337–350.



